Obtaining winter wheat parameters for LINTUL from a field experiment

Comparing old and young winter wheat varieties and evaluating the progress by breeding

Wiert Wiertsema

MSc thesis Plant Production Systems

February, 2015

WAGENINGEN UNIVERSITY
WAGENINGEN UR

Obtaining wheat parameters for LINTUL from a field experiment

Comparing old and young winter wheat varieties and evaluating the progress by breeding

Wiert Pauwel Wiertsema

MSc student Crop Sciences

Reg.nr.: 901229953130

MSc thesis Plant Production Systems

PPS-80439 and PPS-50403

February 2015

Supervisors: Ing. H.C.A. Rijk

Plant Production Systems Group

Dr. ir. P.A. Leffelaar

Plant Production Systems Group

Examinator: Prof. dr. ir. M.K. van Ittersum

WAGENINGEN UNIVERSITY

WAGENINGEN UR

Preface

In front of you is laying the final product of nine months work at the Plant Production Systems Group. A major part of this time I have been working in the field but most of the time I have been working behind my desk at the third floor at PPS while looking at one of the courtyards of Radix. During the process of working on this thesis, I learned a lot about crop modelling, doing measurements and observations, data analysis, literature research, etcetera. But above all I have learned the most from people that came across during this period.

I would like to thank my supervisors for their time and feedback during the whole period. All the small talks with the people from PPS at the coffee machine or during lunch time were pleasant distraction from the thesis, and often gave me new insights in the work I was doing. With some study mates from the 'koffie' whatsapp-group who were also working on their thesis we could share our thesis experiences and frustrations. Like the Dutch saying: "shared sorrow is half sorrow". The part of the work that I enjoy very much was the field work. Together with the men from Unifarm doing the crop samplings early in the morning and afterwards processing the samples at Radix Agros were fine moments. Finally, I would like to thank in particular Timo Sprangers, who worked for his BSc thesis in the same winter wheat trial and who cooperated during the measurements in the field.

Wiert Wiertsema

Summary

The farmers yields of winter wheat in the Netherlands are stagnating the last two decades around 8.5 Mg ha^{-1} (16% moisture). However, the yield of winter wheat at trial fields still increases. The reasons for the gap between experimental and farmers yields are badly understood. The aim of this study was to obtain new parameters for a model by which the potential yield of winter wheat in the Netherlands can be simulated. There was specific interest in the effect of breeding on the potential yield.

LINTUL1 was the model for which new parameters were obtained. A field trial was conducted in the season 2013-214 on river clay soil near Wageningen from which developmental and crop growth parameters were estimated. The trial included three nitrogen levels in order to be sure that (close to) the optimal amount of nitrogen was applied. Three varieties were used in the trial. Two recently introduced (Tabasco and Julius) and one older variety (Ritmo), to see the effects of breeding on crop characteristics. From March 5 2014 a meteorological station was located at the trial for location specific weather data.

Ten times during the growing season crop samplings were done to measure the distribution of dry matter over various plant organs. From these data, parameters like RUE, SLA, relative growth rate and allocation fractions were determined. From the final harvest the net grain yield, kernels m^{-2}, ears m^{-2}, thousand kernel weight and harvest index were determined.

The maximum yield obtained was 12.51 Mg ha^{-1} (with 15% moisture) from one experimental unit. The relative growth rate was found to be 0.0061 d^{-1}, RUE on average over the growing season was 3.20 g above ground dry matter per MJ PAR. The plant organs included in the model were grains, ears, stems, green leaves and dead leaves. Roots were not parameterized because no data were available on the dry matter of the roots.

The obtained temperature sums were distinct from earlier findings. The thermal sum of the period before anthesis was 680 ˚Cd and the thermal sum from anthesis till maturity was 1030 ˚Cd. However, the calculation of these thermal sums depended on several developmental parameters which could not be calculated based on the obtained dataset. Therefore, it is recommended to do research on the developmental parameters of recent varieties under current climatic conditions for winter wheat.

Not all parameters are calculated for all varieties and all nitrogen applications. Therefore, no extensive comparison between varieties is described in this report. Nevertheless it is recommended that parameters for these varieties and nitrogen applications are calculated.

For further improvement of the model it is suggested to make the RUE developmental stage dependent. Also the simulation of SLA was not exactly the same as the observed SLA and needs to be resumed. Some recommendations are done on the measurement of light interception and how the light extinction coefficient can be determined from these measurement.

Table of Contents

1. Introduction

The farmers yields of winter wheat in the Netherlands are stagnating the last two decades around 8.5 Mg ha^{-1} (16% moisture) (Centraal Bureau voor de Statistiek [CBS], 2014; Figure 1.1). The yield of winter wheat in variety trial fields however still increases. The reasons for this growing gap between the experimental yields and actual yields of farmers are badly understood. One of the reasons is that experimental fields don't have a field border effect with more traffic of machinery and spray and fertilizer tracks. It has also been suggested that farmers give higher priority to other (economically more important) crops and therefore apply less inputs than optimal and they do not seed, fertilize and spray at the optimal time. In addition, increased weight of machinery causes more soil compaction which also may reduce crop growth (Andersen *et al.*, 2013). These are all reasons that can explain why farmers do not achieve (close to) the theoretical maximum yields at this moment and don't keep pace with the yield increase in variety trials.

The aim of this research is to develop a tool to calculate the theoretical maximum yield for winter wheat in the Netherlands. If this theoretical maximum is known, then, the next step can be to identify causes for the difference between obtained yields by farmers and this theoretical maximum.

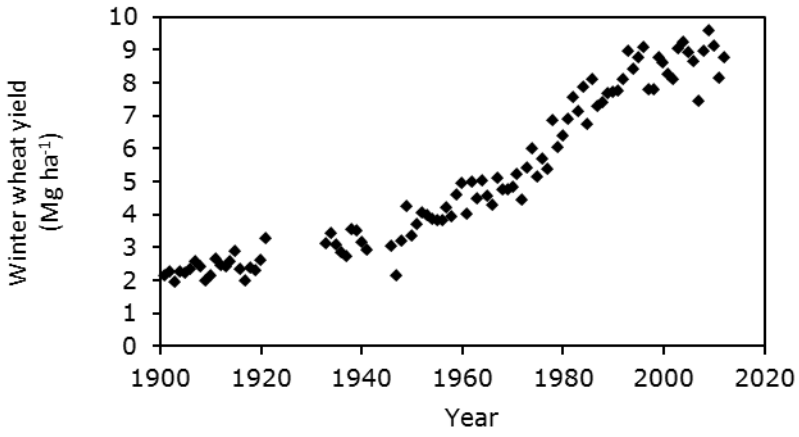

Figure 1.1. Average yields of winter wheat in the Netherlands from 1901 till 2012. No data was available for the periods 1922–1932 and 1942–1945. All the yields are converted into grain yields with 16% moisture. This corresponds with the fresh weight of the grains that are suitable for storage (Centraal Bureau voor de Statistiek, 2014).

1.1 Potential, water-limited, water- and nutrient limited and actual yield levels

Usually a distinction is made between four production levels: potential, water-limited, water- and nutrient-limited and actual (Van Ittersum *et al.,* 2013).

The potential production level (Figure 1.2) describes the theoretically maximum yield (Y_p) and is defined by climatic factors such as atmospheric CO_2 concentration, amount of incoming radiation and temperature (of the air and/or the soil temperature) and by crop characteristics such as

physiological (photosynthetic) characteristics, phenological characteristics (crop development), optical properties of leaves (reflection, transmission and absorption of radiation) and its geometric characteristics (leaf arrangement and ability to intercept radiation). These factors cannot be affected and are therefore *defining factors*. However, over the years these factors can change because of climate change and plant breeding.

The next production level describes the crop yield that is limited by inputs such as water and nutrients. These are the *limiting factors* and these can be managed by farmers. By far the most agricultural areas in the world are non-irrigated and therefore water limitation is likely to occur during some stages in the growing season. Shortages of nutrients are also implemented in some crop growth models, but to a lesser extent.

The actual production level describes the actual yield (Y_a) obtained by farmers. This yield is in addition to the water- and nutrient limited yield also reduced by weeds, pests, diseases and pollutants.

Using these three production levels, the yield gap (Y_g) may be defined as the difference between Y_p (irrigated crops) or Y_w (rain fed crops) and Y_a (Van Ittersum *et al.*, 2013).

Modelling at different production levels

In the previous section differences between production levels (Y_p, Y_w, Y_a) were clearly defined. Crop growth models can be developed for these different production levels. Crop growth models can be used in several ways *e.g.* research tool, teaching tool, decision support system, etc. As a research tool, models can be used to test hypotheses about relations between different factors. Models are useful to quantify complex processes. The following paragraph will introduce the modelling of the potential yield of winter wheat.

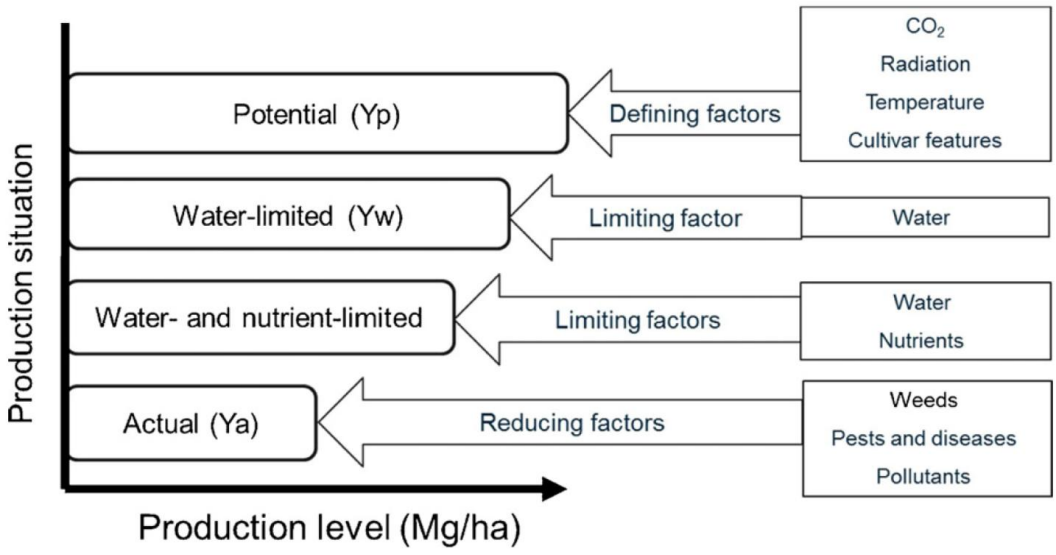

Figure 1.2. The relationships between the yield defining, limiting and reducing factors with the potential, water (and nutrient) limited and actual yield, respectively (Van Ittersum *et al.*, 2013).

1.2 Potential yield of winter wheat

Since the average actual yields of winter wheat in the Netherlands are stagnating (CBS, 2014), while the obtained yields at experimental sites still are increasing it is an interesting question how much the actual yields are below the theoretical potential yields. This can show how much the yields could rise, given the type of cultivar and climate.

The potential yield can roughly be estimated with the following equation:

$$Y = HI * RUE * \int_0^t PAR * (1 - e^{-k*LAI}) * dt \quad (1)$$

where Y is an estimation of the potential yield, HI is the harvest index and RUE is the radiation use efficiency. Both HI and RUE are considered constant over the growing season. PAR is the total amount of photosynthetic radiation that is absorbed by the crop during the season, k is an extinction coefficient of the light within a canopy and LAI is the leaf area index, and the integration is done from 0 (emergence) till t (maturity).

Based on crop data of the growing season 1983-1984 from Groot and Verberne (1991) (see Appendix I), combined with weather data of 2014, and using Equation 1, the potential yield of winter wheat was calculated as 14.7 Mg ha^{-1} (including 15% moisture). For this calculation a HI of 0.5, a RUE of 3 g DM MJ^{-1}, and an extinction coefficient of 0.6. The conversion to 15% moisture is done by dividing the dry matter yield with 0.85. It should be noted that this calculation is based on crop data from 1983-1984, with the variety Arminda. Nowadays higher yielding varieties are used, so it is expected that the potential yield using the current varieties will even be higher. This could be caused by a higher RUE or by the higher CO_2 concentration in the air (Het Lam, 2014) and maybe because of a changed k.

The 14.7 Mg ha^{-1} is far above the average actual yields of farmers in the Netherlands and it

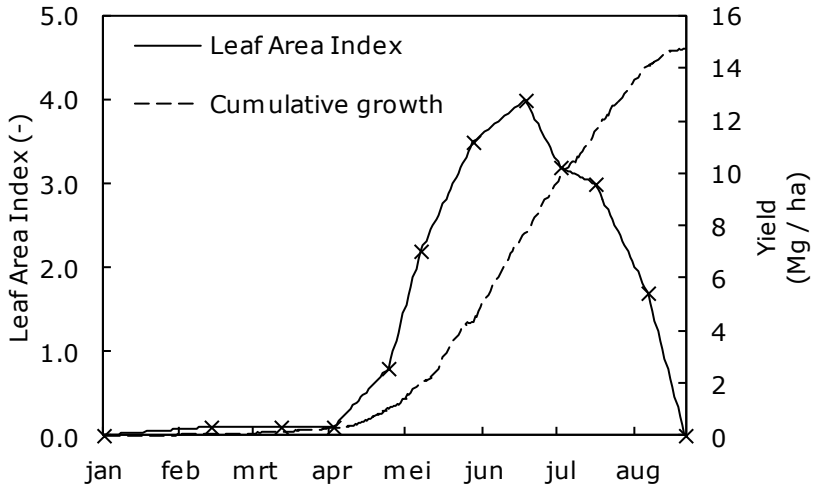

Figure 1.3. The full line shows the development of the leaf area index of a winter wheat crop in the growing season 1983-1984 (Groot & Verberne, 1991). The line between the data points is linearly interpolated. The dashed line shows the cumulative growth of the grain yield (15% moisture), which is calculated based on Equation 1 with data about the photosynthetic radiation from the growing season 2013-2014.

suggests that improvement of the yield should be possible. Disadvantage of Equation 1 is that it is a very simplified approach. It only gives insight in the yield and how this is realized, but the development of the crop is excluded from this model. Figure 1.3 shows the development of the yield based on Equation 1. According to this calculation, the grain filling starts together with the growth of the leaf area. This is not in accordance with reality. Equation 1 is actually a very basic model of the final yield, but it is not suitable to give more insight in crop development. Therefore, more sophisticated models are developed.

1.3 Crop modelling approaches

Two main approaches for crop modelling include: (i) models based on photosynthesis with a CO_2 uptake module and growth and maintenance respiration, conversion of CO_2 to assimilates and subsequently dry matter, etc., and (ii) models based on the light or radiation use efficiency. The amount of intercepted light is based on the leaf area index and this is utilized to produce dry matter using the experimental linear relationship found by (Monteith, 1977).

This second approach is the basis for the Light INTerception and UtiLization (LINTUL) models (Spitters & Schapendonk, 1990). LINTUL is a straightforward model that requires crop parameters and weather data as input. The model was developed for potato but it has been applied for many other crops including winter wheat (Het Lam, 2014).

All the production levels described in section 1.1 can be modelled with both approaches of modelling. However, the amount of data needed for the first approach for parameterization is larger than for the second approach. This research will make use of the LINTUL approach.

1.4 Changes in G × E in the last decades

As described in section 1.1, the potential yield of a crop is defined by prevailing climatic conditions and the genetic properties of a crop. The potential yield can be estimated with the first type of LINTUL models: LINTUL1 (Van Oijen and Leffelaar, 2008). Other types of LINTUL models can simulate the yield of a crop under water-limiting conditions (LINTUL2; Van Oijen and Leffelaar, 2011) or with limiting nutrients.

LINTUL1 for winter wheat, described by Het Lam (2014), is parameterized for the Netherlands. Most parameters are based on field experiments of the 1980s and 1990s. Therefore, the parameters are based on varieties that are not commonly used by farmers nowadays. In addition, changes in the climate might also affect the parameters. The following section describes how the genotype of winter wheat and the prevailing climate have changed over the last decades, and how this might affect the potential yield.

Changes in management are discussed shortly. While management is not affecting the potential yield, it does affect yields from trial fields from which the potential yield is estimated. Therefore, changes in management can have effect on potential crop growth models.

Genetic change

The first proof that genetics have changed over time is that nowadays different varieties are used by farmers in comparison with thirty years ago. Plant breeders have introduced new varieties, since they have improved properties compared to their ancestors.

Based on the data coming from the Dutch recommended list of varieties for winter wheat, it can be concluded that new varieties have better resistance against diseases. For example, the variety SW Tataros has been introduced on the list in 2004 and it has been there until now. The relative yield of SW Tataros compared to other, more recently introduced varieties dropped from 101 till 90 over the last 10 years (Figure 1.4 a), while the absolute yield of SW Tataros without crop protection remained constant over this period (data not shown here). The absolute yield with crop protection remained also constant for SW Tataros, while the yield of all varieties together shows an increasing trend. Thus breeding is contributing to higher yields. However, it should be noted that this is not the potential yield. Although the data are coming from experimental stations, where presence of diseases and pests is usually low, the mentioned yields are the water limited yield (Y_w). It is also observed that yields of winter wheat grown with plant protection have increased. This can be explained by two reasons: (i) the recent varieties introduced have a higher water use efficiency and therefore the gap between Y_w and Y_p becomes smaller or, (ii) the recent varieties have a higher yield potential. This process of increasing yields is only shown here for the last 10 years because of lack of information of preceding years. It is unknown which properties of the wheat crop have changed because of breeding.

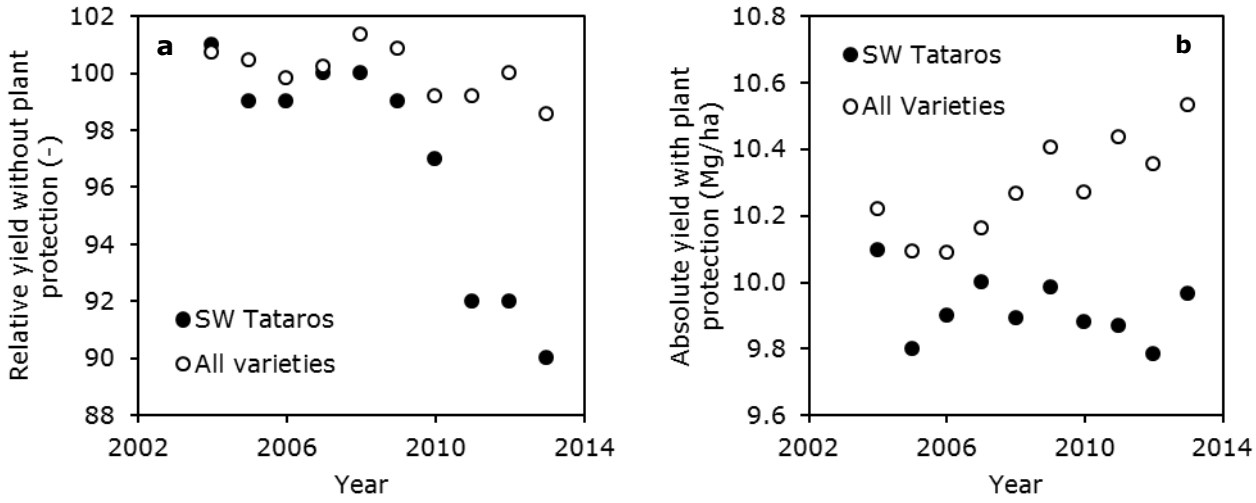

Figure 1.4. (a) The relative yield of SW Tataros and the relative yield of all varieties included at the Dutch recommended list of varieties without any crop protection applied. (b) the absolute yield (including 15% moisture) of SW Tataros and the absolute yield of all varieties at the Dutch recommended list of varieties. All the data is coming from the river clay area of the Netherlands.

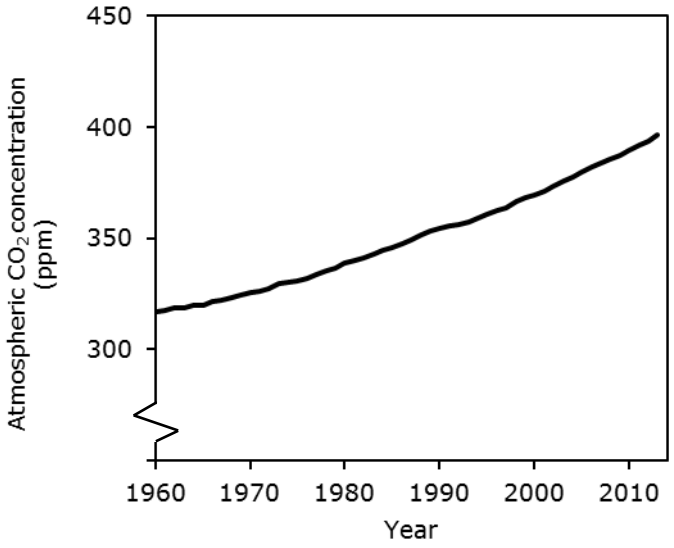

Figure 1.5. Atmospheric CO_2 concentration at Mauna Loa Observatory, Hawai from 1960 till 2013

Climate change

Climate change can have effect on potential crop growth in three ways. It can affect the CO_2 levels of the air, the air temperature and the amount of irradiation.

The atmospheric CO_2 concentration at Hawaii is measured since 1959. Figure 1.5 shows the increase in CO_2 concentration in the air of Hawaii and shows a steady increase of around 1% each year. Nowadays we have reached a CO_2 concentration of circa 400 ppm.

An increased atmospheric CO_2 concentration increases crop growth (Fangmeier *et al.*, 1999, Rogers *et al.*, 1994). A possible increase in growth also depends on the average temperature. As long as the temperature stays below an optimal value, the biomass production will increase (Chen *et al.*, 1994). This optimal temperature depends on the light intensity. At lower light intensities increased CO_2 concentration has less effect then with high light intensities. Furthermore the response of the stomata of the crop on higher temperatures affect the impact of higher CO_2 (Cure & Acock, 1986). Chen *et al.* (1994) mention that CO_2 becomes less soluble in water in plant cells at higher temperatures, which also affects the availability of CO_2 for uptake. However, Chen *et al.* (1994) mention an optimal temperature of 32 °C, which is only reached a few days per year at the warmest moment of the day in the Netherlands. Therefore, it is expected that higher CO_2 levels will have a positive effect on the potential crop growth. This effect is included in the current LINTUL model for winter wheat as a factor that increases the RUE depending on the CO_2 concentration (Het Lam, 2014).

Another part of climate change is the increase in temperature. Figure 1.6 shows the average air temperatures in the Netherlands. There is a trend that temperature increases. The thermal sum will be reached earlier resulting in faster development of the crop. When a crop changes faster from one developmental stage to the other, there is less time to intercept radiation, and to produce dry matter in this stage. In general, the crop growth cycle will be shorter. However, this trend is not observed in harvest dates of farmers. The thermal sum where maturity of a crop is attained is different for each

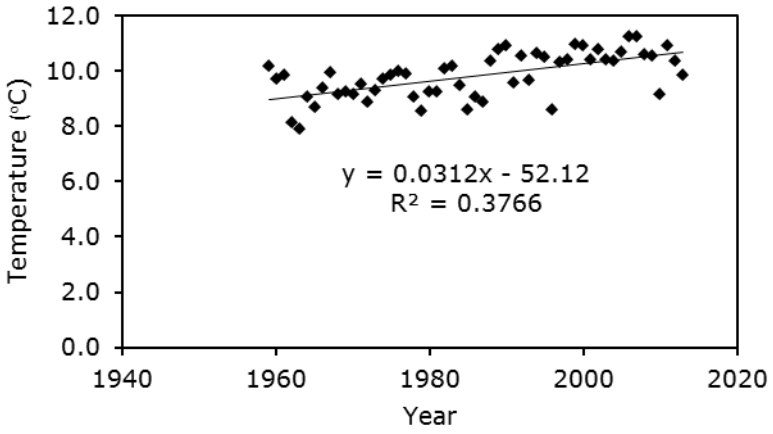

Figure 1.6. Average yearly temperatures in De Bilt (The Netherlands) over the period 1959 till 2013 (Koninklijk Nederlands Meteorologisch Instituut, 2014).

variety and breeding companies are able to breed for varieties that can be harvested late in the season to have as much growth as possible.

Asseng *et al.* (2011) showed that increased temperature can have a drastic effect on grain yield in case the temperature > 34 °C. This effect is included in LINTUL for winter wheat as a linear decrease of the RUE between 30 and 35 °C from 1 to 0 (Het Lam, 2014). In addition, the relative death rate of the leaves increases between 30 and 50 °C from 0.070 to 0.126.

The amount of irradiation is a third climatic factor that affects the potential yield of crops. Wild (2009) wrote a review on the process of global dimming and brightening. It is known that the amount of irradiation reaching the soil surface varies over the years. In Stockholm the annual mean surface solar radiation varied from about 97 W m^{-2} in 1984 till 119 W m^{-2} in 2002. Wild (2009) states that these variations can be explained by aerosols, clouds and aerosol-cloud interactions. Also in the Netherlands the amount of irradiation has increased. Between 1981 and 2013 the global shortwave radiation increased with 9% to a value of about 3600 MJ m^{-2} yr^{-1} (KNMI, 2013). It seems reasonable that these changes have impact on the potential crop growth.

Change in management

Research on the potential yield is often based on crop yields available from experimental fields. In these cases, management is considered to be optimal. Figure 1.4 b shows that the yield of SW Tataros is not clearly increasing or decreasing over time. The variability in the data can theoretically be caused by management, but it is more likely that it is resulting from variability in weather conditions. So, based on these data, there is no reason to assume that management has changed over the last years. Whether crop management is non-optimal and has a reducing effect on the actual yield, and how large this effect then is, cannot be estimated.

1.5 Aim and research questions

The aim of this research is to determine new parameters for winter wheat, to simulate the potential yield of winter wheat in the Netherlands with the model LINTUL1.

In order to achieve this aim, a field experiment of winter wheat was conducted near Wageningen, the Netherlands. From the obtained dataset of this experiment, new crop parameters for LINTUL1 were determined. During this process, the following questions were answered:

- How are crop parameters for LINTUL1 calculated from weather and crop data?
- What are the differences in parameters between varieties?
- What are the differences in parameters between nitrogen levels?
- To what extent have the crop parameters of LINTUL1 changed compared to the current ones?
    - How do these changes relate to changes in climate, genetics and management?

2. Description of LINTUL1

In this chapter the theory of LINTUL1 is explained. The whole model including all equations are described and an overview is given of the parameters that are needed to do a simulation with LINTUL1 for winter wheat. Also a simulation run is presented of the performance of LINTUL1 for winter wheat in the season 2012-2013 to identify aspects of the model that need special attention for improvement.

Input

Since LINTUL1 simulates the potential growth and yield of a crop, only crop parameters and daily data on minimum and maximum temperature (°C) and global shortwave irradiation (kJ m^{-2} d^{-1}) are needed by the model together with the corresponding day of year. The crop parameters are included in the program code and the weather data are provided to the model via an external weather file. Besides this, initial conditions have to be set like day of the year at which modelling starts, initial weight of plant organs, etc..

2.1 Theory

The conversion from crop characteristics and weather data to the growth of different plant organs over the growing season are made by several formulas. Roughly the model can be divided in two parts: one part to calculate the developmental rate and stage of the crop and another part that calculates the growth of the crop.

Development

Developmental stage

The developmental stage (DVS) is expressed as the ratio between the accumulated thermal sum and the required thermal sum to reach the next stage of development.

$$DVS_t = \frac{T_{sum-t}}{T_{sum-growth\ stage}} \tag{2}$$

where $T_{sum\text{-}t}$ (°Cd) denotes the thermal sum over time, $T_{sum\text{-}growth\ stage}$ (°Cd) the thermal sum that separates two distinct stages of development, t is the date for which the DVS is calculated.

LINTUL1 for winter wheat distinguishes three developmental stages: (i) the stage between sowing and emergence; (ii) the stage between emergence and anthesis and, (iii) the stage between anthesis and maturity. For each stage, the thermal sum is calculated differently. The first stage is calculated based on the soil temperature, the second stage is calculated based on the air temperature at 150 cm above the soil, and is affected by vernalization and photoperiod, and the third stage is calculated based only on the air temperature at 150 cm.

Sowing till emergence

The length of the period between sowing and emergence is defined by a thermal sum for emergence ($T_{sum\text{-}emergence}$) and a base temperature for emergence ($T_{b\text{-}emergence}$). Since the seeds are sown in the soil, the soil temperature (T_{soil}) is used to calculate the thermal sum instead of the air temperature. The thermal sum is expressed in °Cd and calculated as follows:

$$T_{sum-emergence} = \int_0^t T_{effective} * dt \tag{3}$$

where t is moment of emergence, 0 is moment of sowing and $T_{effective}$ is:

$$T_{effective} = T_{soil} - T_{b-emergence} \tag{4}$$

where T_{soil} is the soil temperature. Equation 4 is only calculated if $T_{soil} > T_{b\text{-}emergence}$, else is $T_{effective}$ 0. Het Lam (2014) found a value of 0.25 °C for $T_{b\text{-}emergence}$. However Weir *et al.* (1984) for example found a value of 1 °C. The soil temperature is derived from the daily average air temperature (T_{air}) using a formula developed by Zheng *et al.* (1993):

$$T_{soil(t)} = T_{soil(t-1)} + \left(T_{air(t)} - T_{soil(t-1)}\right) * M_{soil} * \Delta t \tag{5}$$

where t is the current time step and M_{soil} is a resistance factor between air and soil with the unit d^{-1}. Het Lam (2014) used a value of 0.25 for M_{soil}. This is the same value as proposed by Zheng *et al.* (1993) to calculate the soil temperature at a depth of 10 cm. The value of M_{soil} will probably depend on soil type, since the heat transfer from a clayey soil probably will be different then from a sandy soil. However, no other values are known for M_{soil} so the value of Zhen *et al.* (1993) is retained in this research.

Emergence till anthesis

The development between emergence and anthesis depends on the air temperature, the photoperiod and vernalization. These three factors are integrated in a single photo-vernal-thermal sum (PVT_{sum}) and expressed in °Cd. The PVT_{sum} is calculated in three steps: (i) the thermal sum is calculated based on T_{air}; (ii) the thermal sum is corrected for the photoperiodic effect; (iii) the thermal sum is corrected for the vernalization effect.

The thermal sum is calculated as:

$$T_{sum-anthesis} = \int_0^t T_{effective} * dt \tag{6}$$

where t is moment of anthesis, 0 is moment of emergence and $T_{effective}$ is:

$$T_{effective} = T_{air} - T_{b-anthesis} \tag{7}$$

where T_{air} is the daily average air temperature at a height of 150 cm. Equation 7 is only calculated if $T_{airl} > T_{b\text{-}anthesis}$, else is $T_{effective}$ 0. Het Lam found a value of 1.5 °C for $T_{b\text{-}anthesis}$. However, Jamieson (1995) reported a value of 0 °C and Weir *et al.* (1984) a value of 1 °C.

The photoperiodic effect is the effect of daylength on crop growth. This is included in the model as a factor between 0 and 1 that affects the accumulation of thermal time. It is assumed that a long daylength is optimal for crop growth. Shorter days slow the accumulation of thermal time linearly with a photoperiodic factor (P_f) and thus increase the time between emergence and anthesis (Van Bussel *et al.*, 2011). P_f is calculated as:

$$P_f = \frac{D_l - P_b}{P_{opt} - P_b} \tag{8}$$

where D_l is daylength (h d^{-1}), P_b is the photoperiodic base or minimum daylength and is set at 9 h d^{-1}, and P_{opt} is the optimal daylength and is set at 16 h d^{-1}. If $D_l < P_b$ then P_f is 0 and if $D_l > P_{opt}$ then P_f is 1 (Het Lam, 2014). The daylength d is calculated based formulas from Goudriaan and van Laar (1994):

$$d = 12 * \left[1 + \frac{2}{\pi} * \sin^{-1}\left(\frac{a}{b}\right)\right] \tag{9}$$

where $a = \sin\lambda \sin\delta$ and $b = \cos\lambda \cos\delta$. λ is the degree of latitude and δ is the declination of the sun with respect to the equator. $\sin\delta$ and $\cos\delta$ are calculated as follows:

$$\sin\delta = -\sin\left(\pi * \frac{23.45}{180}\right) * \cos\left(2\pi * \frac{(t_d + 10)}{365}\right) \tag{10}$$

$$\cos\delta = \sqrt{1 - \sin\delta * \sin\delta} \tag{11}$$

where t_d is the day of year.

Winter wheat has a vernalization requirement before the crop switches from the vegetative to generative developmental stage. This vernalization requirement is included in the model as a vernalization factor (V_f) between 0 and 1 that affects the accumulation of thermal time. Vernalization is only modelled after emergence and as long as the developmental stage is smaller than $DVS_{vernalization}$ (which is set to 0.3 by Het Lam, 2014). When the developmental stage is larger than $DVS_{vernalization}$, no vernalization is taken into account and the accumulation of thermal time is not reduced anymore by vernalization. However, this does not mean that vernalization has completed. Weir *et al.* (1984) report that the progress of vernalization can be lost under high temperatures (30˚C or more). This is not

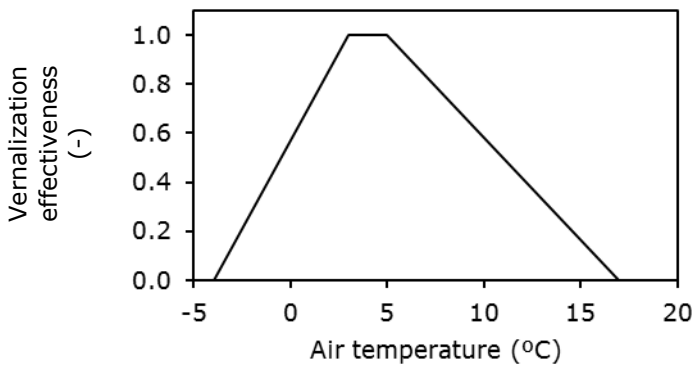

Figure 2.1. The vernalization effectiveness as function of air temperature (Het Lam, 2014).

included in this model since these high temperatures usually do not occur under Dutch circumstances during winter and spring.

The contribution of a day to the total vernalization requirement is defined as the vernalization effectiveness (V_{eff}). V_{eff} depends on the daily average air temperature as shown in Figure 2.1 (Het Lam, 2014). The integral of V_{eff} over time gives the vernal days (VDD). From VDD V_f is calculated using the formula:

$$V_f = \frac{VDD - V_b}{V_{sat} - V_b} \tag{12}$$

where V_b is the vernalization base, a minimum of vernal days that is required before the vernalization factor becomes larger than zero. V_{sat} describes the number of vernal days after which the crop is optimally vernalized. If VDD > V_{sat} than V_f is 1.

PVT_{sum} is calculated as the thermal sum T_{sum} multiplied by the photoperiodic factor P_f and the vernalization factor V_f. Since P_f and V_f are both restricted between 0 and 1, they can only slow down the accumulation of thermal time, but not enhance it.

Anthesis till maturity

In the model of Het Lam (2014) the development between anthesis and maturity depends on the air temperature. The development is calculated in a similar way as the development between sowing and emergence, but with a T_b of 1.5 ˚C. Maturity is reached at a T_{sum} of 590 ˚Cd (Het Lam, 2014).

Crop growth

The increase of dry matter is calculated as the product of intercepted light times the radiation use efficiency. This produced dry matter is distributed over different plant organs. The amount of intercepted light depends on the extinction coefficient and the leaf area index (LAI). All these concepts are explained below, together with the formulas used in LINTUL1 to do the calculations and with the parameters needed for these calculations.

Light interception

The first step in the conversion of the energy of light into assimilates is light interception by leaves. In a homogeneous canopy the intensity of light decreases exponentially from the top of the canopy to the soil surface. This is described by Equation 13:

$$I = I_0 * e^{-k*LAI} \tag{13}$$

where I is the radiation flux of photosynthetic active radiation (PAR) that reaches the soil (MJ m^{-2} d^{-1}), I_0 is the amount of incident PAR and k is the extinction coefficient of the canopy. The amount of intercepted PAR is the difference between the light on top of the canopy and the light that reaches the soil surface. So:

$$I_{int} = I_0\left(1 - e^{-k*LAI}\right) = c_{PAR} * DTR * (1 - e^{-k*LAI}) \quad (14)$$

where *DTR* is the daily total shortwave radiation (MJ m^{-2} d^{-1}). According to Sinclair and Muchow (1999), the amount of PAR is about half the total shortwave radiation (c_{PAR}).

Radiation use efficiency

The production of dry matter in the form of assimilates for each time step is simulated as the product I_{int} times the radiation use efficiency (RUE) in g MJ^{-1} (Equation 15). The total dry matter of the crop is then the integral of Equation 15 which results in Equation 16.

$$\frac{dW}{dt} = RUE * I_{int} \quad (15)$$

$$W = \int_0^t \frac{dW}{dt} * dt \quad (16)$$

Het Lam introduced a correction factor for the effect of sub-optimal day temperatures on RUE ($CF_{RUE\text{-}T}$). The temperature (T_{RUE}) at which $CF_{RUE\text{-}T}$ depends is calculated as:

$$T_{RUE} = T_{max} - 0.25 * (T_{max} - T_{min}) \quad (17)$$

T_{RUE} is on average about 2.3 °C higher than the daily average temperature. Under suboptimal temperatures the RUE is reduced to less than half the original value (Figure VII.1, Appendix VII). The RUE is estimated as a $RUE_{constant}$ (3.15 g MJ^{-1}, Het Lam, 2014) multiplied by the correction factor.

The RUE can be calculated in various ways (Sinclair and Muchow 1999). The RUE mentioned by Het Lam (2014) is based on above-ground dry matter, so the production of dry matter for the roots is not taken into account.

Specific leaf area

The conversion from produced dry weight to leaf area is made with the specific leaf area (SLA), *i.e.* after the exponential development phase. The SLA is the ratio between fresh leaf size and leaf dry weight expressed in $m^2\,g^{-1}$. The SLA is used to calculate the increase in leaf area by multiplying it with the increase of dry matter of the green leaves. According to Hotsonyame and Hunt (1998) SLA is mostly related to temperature during the growing season. A higher air temperature increases the SLA of newly formed leaves. This may have to do with increased plant transpiration at higher temperatures which makes it beneficial to have more surface area per gram of dry matter. It may also have to do with an increased rate of assimilation at higher temperatures. This increases the demand for CO_2 and therefore it would be beneficial to increase the leaf area, thereby increasing the exchange capacity with the air. Hotsonyame and Hunt (1998) did experiments under field conditions, so a higher temperature is then usually related with higher light intensities and therefore with a higher

photosynthesis rate. Ratjen and Kage (2013) state that SLA is mostly linear related to LAI because of mutual shading.

In the current model, SLA is simulated as a constant parameter (SLA_c) which is affected by a correction factor. The SLA_c constant is 0.021 $m^2\ g^{-1}$. The correction factor is derived from an empirical relation between DVS (Equation 2) and SLA (Figure 2.2).

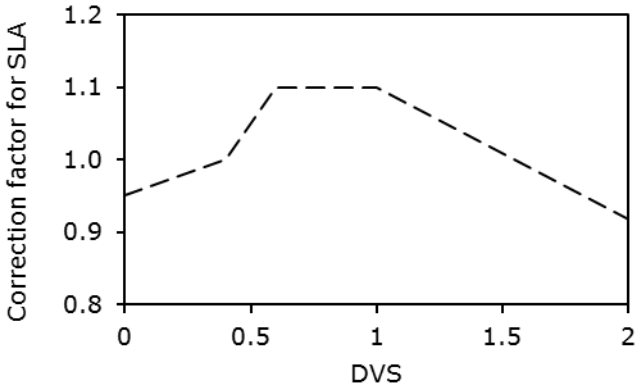

Figure 2.2. The empirical relation between the correction factor for the specific leaf area (SLA) and the developmental stage (DVS) as it is implemented in LINTUL1 for winter wheat (Het Lam, 2014).

Leaf area growth

The calculation of the growth of leaf area depends on several factors. In the first phase of development, it is assumed that leaf area grows exponentially, later on the growth rate decreases because of shading of leaves on each other and because of ageing of the leaves. Senescence of leaves is modelled from anthesis onwards.

The growth of leaf area is calculated as the integral of the growth rate of the leaf area index for each timestep. The total leaf area index at moment t (LAI_t) is the initial LAI together with the grown amount of LAI (Equation 18). The initial leaf area index ($LAI_{initial}$) is calculated as the product of the initial leaf weight ($WLV_{initial}$) and the initial specific leaf area ($SLA_{initial}$). $WLV_{initial}$ is set at 0.10 g DM per square meter soil (Het Lam, 2014), $SLA_{initial}$ is calculated as the product of the SLA value and a correction factor for SLA.

$$LAI_t = LAI_{initial} + \int_0^t \frac{dLAI_{net}}{dt} * dt \tag{18}$$

$$\frac{dLAI_{net}}{dt} = \frac{dLAI_{growth}}{dt} - \frac{dLAI_{senescence}}{dt} - \frac{dLAI_{reallocation}}{dt} \tag{19}$$

The growth rate of the LAI ($dLAI/dt$) depends on the developmental stage and leaf area index. As long as DVS < $DVS_{exp\text{-}leaf\ growth}$ and LAI < $LAI_{exp\text{-}leaf\ growth}$, LAI grows exponentially, and it is assumed that leaves do not shade each other. Het Lam (2014) used a value of 0.2 for $DVS_{exp\text{-}leaf\ growth}$ and 0.6 for $LAI_{exp\text{-}leaf\ growth}$. During this exponential growth phase, $dLAI/dt$ is calculated as follows:

$$\frac{dLAI_{growth}}{dt} = \frac{LAI_t * (e^{r_l * T_{effective} * \Delta t} - 1)}{\Delta t} \quad (20)$$

where r_l times $T_{effective}$ is the relative growth rate with a value of 0.015 (°Cd)$^{-1}$ for r_l. After the exponential growth phase, $dLAI_{growth}/dt$ is calculated as:

$$\frac{dLAI_{growth}}{dt} = SLA * \frac{dW}{dt} * F_{lv} \quad (21)$$

where dW/dt is the increase in dry weight of all above-ground dry matter in one time step and F_{lv} is the fraction of dry matter that is allocated to the green leaves, the so-called leaf weight ratio (LWR) in g leaf DM per g total DM.

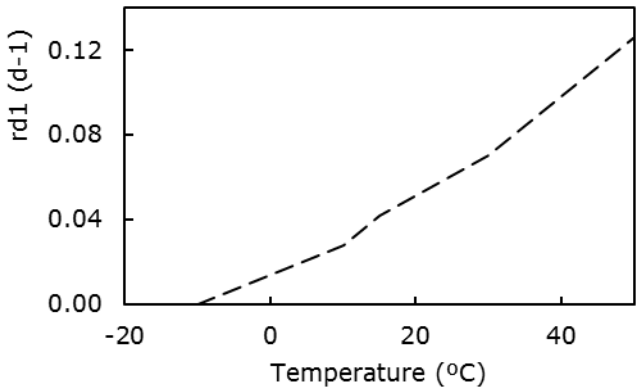

Figure 2.3. The relation between the relative death rate of the leaves (r_{d1}) and the air temperature at 150 cm height if the thermal sum reached is higher than 900 °Cd (Het Lam, 2014).

Leaf area senescence due to ageing, shading and reallocation

The senescence of leaves is a complex process that is dependent on several factors. In LINTUL, senescence of green leaves is dependent on the age of the leaves, the air temperature and the leaf area index. The amount of LAI that senesces is calculated as:

$$\frac{LAI_{senescence}}{dt} = LAI_t * r_d \quad (22)$$

where r_d is the relative death rate of the leaves. r_d can be calculated in two ways: (i) if the thermal sum is larger than a critical value $T_{sum\text{-}senescence}$, then r_d is a function of the daily average temperature at a height of 150 cm above the soil (Figure 2.3) and expresses as r_{d1}. Het Lam (2014) mentions a value of 900 °Cd for $T_{sum\text{-}senescence}$. This number is reached around anthesis. (ii) if the LAI is larger than a critical value $LAI_{senescence}$, then senescence of leaves occurs with a linear increase of $r_{d\text{-}shading}$ for each additional unit of LAI. The relative death rate is then expressed as r_{d2} and is calculated as:

$$r_{d2} = r_{d-shading} * \frac{LAI_t - LAI_{cr}}{LAI_{cr}} \quad (23)$$

where $r_{d\text{-}shading}$ is 0.03 d^{-1} (Van Oijen and Leffelaar, 2008).

The relative death rate (r_d) used in Equation 22 is the maximum of r_{d1}, and r_{d2}.

The growth of the LAI decreases if reallocation of dry matter ($dLAI_{reallocation}/dt$) to the grains occurs. Reallocation from the leaves to the grains means that dry matter is reallocated and that the leaf area senesces. $dLAI_{reallocation}/dt$ is calculated as the fraction of dry weight that is reallocated from the leaves to the grains ($F_{real\text{-}leaves}$ in d^{-1}) multiplied by the dry weight of the leaves (WLV, g m^{-2}) and multiplied by the specific leaf area (SLA, m^2 g^{-1}). $F_{real\text{-}leaves}$ is dependent on the developmental stage (Figure 2.4). In the model of Het Lam (2014), reallocation from the leaves starts already before flowering from a DVS of 0.5 onwards. In reality, this is impossible since no reallocation to grains can occur before flowering since there are no grains by then.

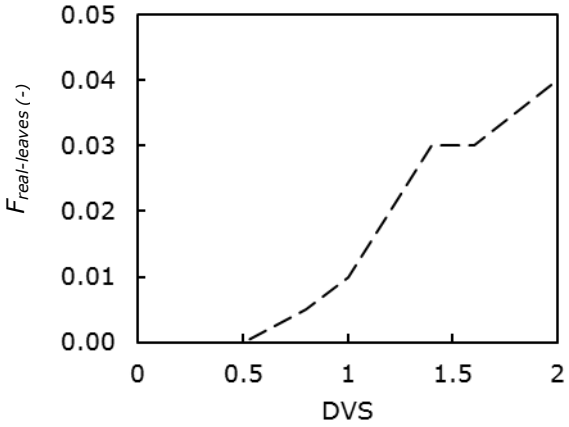

Figure 2.4. The relationship of the fraction of reallocation from the green leaves to the grains ($F_{real\text{-}leaves}$ in g DM reallocated per g DM of green leaves) with the developmental stage (DVS) from Het Lam (2014).

Dry matter allocation

Each time step, the produced assimilates (dW/dt) are distributed over the plant organs. Het Lam (2014) considered the leaves (green and dead), stems and storage organs (or grains). In this study, ears are also introduced as plant organ. Roots are not considered in the model.

The growth rates of individual organs are defined by functions that depend on developmental stage. The increase in dry weight of individual organs is calculated by Equation 24:

$$\frac{dW_i}{dt} = \frac{dW}{dt} * F_i \tag{24}$$

where dW_i/dt is the growth rate of an individual organ i, F_i is the fraction of the total amount of produced assimilates that is assigned to this organ and i is *lvg* for green leaves, *st* for stems, *ear* for ears and *gr* for grains. Roots are in the present study not included in the model because there was no data to calculate allocation functions.

As described in the section about leaf area growth, a part of the leaves senesces due to ageing or shading of the leaves. Dead leaves do not contribute to photosynthesis and therefore the rate of senescence also determines the increase in dry weight of the dead leaves:

$$\frac{dW_{lvd}}{dt} = r_d * W_{lvg} \quad (25)$$

where r_d is the relative death rate of the green leaves and W_{lvg} is the total weight of the green leaves. The total dry weight of the dead leaves is then:

$$W_{lvd} = \int_0^t \frac{dW_{lvd}}{dt} dt \quad (26)$$

During the phase after anthesis reallocation of dry matter takes place from the stems and green leaves to the grains. In the present study, also reallocation from the ears to the grains was introduced in the model. The reallocation is based on a function of DVS and the amount of reallocation is calculated as a reallocation fraction multiplied by the total dry weight of stems, green leaves or ears. This reallocated dry matter is added to the dry weight of the grains.

2.2 Application of LINTUL1 for winter wheat in the Netherlands

The LINTUL models have been parameterized for many different crops and environmental circumstances including winter wheat in the Netherlands (Het Lam, 2014). The current parameters of the model for winter wheat in the Netherlands are based on field experiments performed in the early eighties. Different studies show that the potential yield has increased over the last thirty years (Peltonen-Sainio *et al.*, 2009, Rijk *et al.*, 2013), because of (i) improved genetic properties of the crops, and (ii) climate change (G x E interactions).

De software where in LINTUL1 is programmed is FST (Rappoldt & Van Kraalingen, 2013). With FST the integration method for the simulation can be set. For LINTUL1, the Euler integration method is used with a time step of one day. This one day time step is possible, because the time coefficients in the model are much larger (4-10 days, depending on the growth phase).

Performance of LINTUL1 version of Het Lam (2014) for season 2012-2013

A simulation of the potential yield in the growing season 2012-2013 is done to check the reliability of the parameters obtained by Het Lam (2014). The obtained flowering date and maturity date are compared with those observed in the Netherlands. Also the simulated yield is compared with actual yields of farmers. A weather dataset from 'De Veenkampen' of the growing season 2012-2013 is used as input to test the model of Het Lam (2014). The sowing date was set at the first of October. The estimated day of emergence was October 20, the moment of flowering was estimated at July 9 and maturity at August 12. According to field observations in 2013 winter wheat was flowering in the last week of June (Salomons, 2013, Vlamings, 2013, www.harrysfarm.nl, 2013), which was one and half week earlier than estimated. Harvest was done from the 20st of August onwards (Boerenbusiness, 2013, Rechterveld, 2013, www.harrysfarm.nl, 2013). Harvest was not possible earlier due to changeable weather with some rain in the period between August 7, 2013 and August 19, 2013

(Meteorology and Air Quality Group, 2012-2014). However, it is possible that the wheat was mature some days later than the date simulated by the model. From these observations, it seems that the thermal sum between emergence and anthesis ($T_{sum\text{-}anthesis}$) is too large (926 °Cd was found by Het Lam (2014) while the anthesis date June 26, 2013 could be simulated with a $T_{sum\text{-}anthesis}$ of 750 °Cd) and the thermal sum for maturity ($T_{sum\text{-}maturity}$) was too small (590 °Cd was found by Het Lam (2014) while the maturity date August 18, 2013 could be simulated with a $T_{sum\text{-}maturity}$ of 860 °Cd).

If the values for $T_{sum\text{-}anthesis}$ and $T_{sum\text{-}maturity}$ were retained from Het Lam (2014), then the simulated yield was 10.3 Mg DM ha^{-1}, or 12.1 Mg ha^{-1} with a moisture content of 15%. Based on data presented by (Rijk *et al.*, 2013), this seems a reasonable value. They describe the increase of yields at trial fields between 1978 and 2008 with a linear relationship. Based on this relationship a yield was expected of 11.7 Mg ha^{-1} with a moisture content of 15%.

The grain filling stage starts after flowering, but in the model dry matter is already allocated to the grains from DVS 0.5 onwards. First, reallocation from the leaves takes place and from DVS > 0.8 assimilates produced are also directly allocated to the grains. This is physiologically not possible.

Since the current model is based on data from old varieties, it is questionable whether the light interception has not changed over time. Recent varieties might have a different development of the canopy in time which affects the course of the LAI and therewith the light interception. Also the extinction coefficient is taken as constant over the growing season, but the angle of the leaves with the soil changes during the growing season. First it is more or less horizontal, while later the leaves are standing more in a vertical direction.

3. Material and methods

The material and methods are divided in six parts. First the field experiment is discussed from which data on the growth and development of winter wheat in the Netherlands are derived. Second, the measurements conducted in the field experiment are described. As third, the general analysis of the results is explained. The fourth part is the determination of model parameters for LINTUL1 . Data from the field experiment were used to obtain parameters on the development and growth of winter wheat. The last two parts describe the determination of allocation fractions of dry matter to the different plant organs, and the reallocation fractions from the leaves, stems and ears to the grains.

3.1 Description of the field experiment

In the growing season of 2013-2014 a field experiment in winter wheat was conducted to obtain data for updating the crop parameters of the crop model LINTUL1. Since LINTUL1 simulates the potential growth of a crop, the experiment aimed at reaching Y_p (Van Ittersum *et al.*, 2013). The experiment included three different cultivars grown at three nitrogen levels (180, 240, and 300 kg ha^{-1}) in four blocks in a full factorial split-plot design (Appendix II). The application of 240 kg N ha^{-1} is the Dutch recommended amount of nitrogen fertilizer. One nitrogen application was higher and one application was lower to assess that the application was close to the optimum. The different nitrogen applications were allocated to the whole plots, the varieties to the split-plots.

The observations included crop samplings and observations together with soil and weather measurements.

Cultivars

The cultivars used in the trial are Julius, Tabasco and Ritmo. Julius and Tabasco are two recently released cultivars (2009 and 2008 respectively) which are widely adopted by wheat farmers in the Netherlands at this moment. These two varieties are included in the trial to get insight in the variation of crop specific parameters between modern cultivars. Ritmo is an older variety which was released in 1992, and is not grown by farmers anymore because of the worse characteristics compared to more recently released varieties. It was included in the trial to get insight in the change of crop specific parameters over the last two decades under the current environmental conditions. Table 3.1 shows some characteristics of the winter wheat varieties used.

Table 3.1. Characteristics of the varieties Julius and Tabasco according to the Dutch winter wheat bulletin (PPO, 2013) and of the variety Ritmo according to the recommended list of varieties from 1995 (Ebskamp *et al.*, 1994). Most characteristics are expressed at a scale of 1 to 10 without units, at which a higher number indicates a favourable assessment of the corresponding property.

Characteristic		Julius	Tabasco	Ritmo
Length straw:		105[1]	95[1]	6[2]
Sturdiness[3]:		8.0	7.5	9
Earliness of ear:		6.0	5.5	6
Early ripeness:		5.5	5.5	6
Resistance against	Pre-harvest sprouting:	7.0	6.5	7
	Yellow rust:	8.5	8.5	6
	Brown rust:	7.5	8.5	6
	Powdery mildew:	7.5	8.5	6
	Leaf spot disease	8.5	8.0	6
	Ear fusarium:	6.5	6.0	5

[1] The length of the straw of Julius and Tabasco is expressed relatively. 100 corresponds with 89 cm.

[2] The length of the straw of Ritmo is expressed on a relative scale from 1 to 10. The relation with the absolute length is not given (Ebskamp *et al.*, 1994).

[3] Sturdiness is a measure for the resistance against lodging.

Experimental site

The experiment was located in Wageningen near the Haarweg on a field of the experimental farm of Wageningen University 'Unifarm' (GPS coordinates: N 51 57.737, E 5 38.61, silty clay loam) (Figure 3.1). A report about soil data can be found in Appendix III (in Dutch). This includes a description of the texture and the nutrient status of the soil, together with the methods of the analyses. The first meter of the soil was clayey. Underneath this layer a layer of river sand was situated. There was no artificial drainage present at this field, so the soil drained water via the sand layer.

Figure 3.1. Map of Wageningen. The trial was located at the black dot.

Management

The preceding crop was sugar beet, which was harvested at the end of September. After ploughing and rotary harrowing the winter wheat was sown with field trial equipment at beds of 1.5 meter width at the 23rd of October, 2013. The distance between rows was 12.5 cm, and a bed consisted of 10 rows. The seed was disinfected with Beret Gold (active ingredient is fludioxonil). The nitrogen fertilization of the crop aimed at three different amounts of nitrogen available to the crop: 180, 240 and 300 kg N ha^{-1}

to be able to assess that the optimum nitrogen application was given. A soil sampling was done at the 4th of December to analyse the N availability in the soil. This appeared to be 137 kg N ha^{-1}. It was assumed that of this surplus 100 kg N ha^{-1} would leach away. During the growing season N fertilizer was applied at four different moments. Fertilization of N was always done with calcium ammonium nitrate (27% nitrogen content). Table 3.2 shows the moments of N fertilization. Due to a mistake with the application of fertilizer at the 22nd of May the fields 16, 17 and 18 received 40 kg N ha^{-1} while this was a N1 treatment. Therefore, these fields are left out of the analysis of the results. Besides the nitrogen fertilization, 425 kg/ha of a potassium, sulphur and magnesium containing fertilizer (Patentkali) was applied as fertilizer at the 31st of January. This fertilizer contains 30% K_2O, 42.5% SO_4 and 10% MgO, the remaining 17.5% is not specified by the supplier of the fertilizer.

Table 3.2. Moments of N fertilizer application.

Date	Treatment	Dose (kg N ha^{-1})	DVS* (Feekes)
24-Feb	N1, N2, N3	54	2-3
26-Mar	N1, N2, N3	54	5
16-Apr	N3	40	6
29-Apr	N1	40	7
29-Apr	N2	60	7
29-Apr	N3	80	7
22-May	N2, N3	40	9-10

*DVS: Developmental stage, expressed in the Feekes scale (Large, 1954).

Each week the presence of diseases and pests was checked qualitatively and plant protection was applied, if necessary. The aim of the trial was to obtain the potential yield, so presence of diseases was not tolerated and prevented as much as possible. Table 3.3 gives an overview of the applied crop protection agents with the name of the active ingredient and the dose.

At the first crop sampling at February 18, infection of *Zymoseptoria tritici* was found on the lowest leaves of the crop. Around the end of March a few plants were infected with yellow rust (*Puccinia striiformis*). Cereal leaf beetles (*Oulema melanopus*) were observed at the end of May. The observed diseases were treated curative and preventive, land snails were treated preventive with Coragoal, weeds were treated preventive with Javelin and growth regulators were applied to prevent lodging of the crop.

The water availability to the crop was measured using seven monitoring wells and tensiometers at a depth of 35 and 65 cm in 7 replications. Information on this topic is not published in this report. Based on the measurements on the water availability for the crop, twice 15 mm irrigation (measured with a rain gauge) was applied at July 1 and July 4 respectively using a boom irrigator.

Table 3.3. Overview of the applied crop protection agents.

Date	Product	Active ingredient	Type of chemical	Dose of active ingredient (g ha^{-1})	DVS * (Feekes)
24-Oct	Caragoal	metaldehyde	Pesticide against land snails (*Gastropoda pulmonata)*	448	0
24-Oct	Javelin	diflufenican isoproturon	Soil herbicide against weeds	187 1500	0
4-Apr	Aviator XPRO	prothioconazool bixafen	Fungicide against fungal diseases (stem-base, foliar and ear diseases)	187 93.75	6
22-Apr	Moddus 250EC	trinexapac-ethyl	Growth regulator	100	6 – 7
	Stabilan	chloormequat	Growth regulator	187	
1-May	Corbel	fenpropimorf	Fungicide	375	7 – 8
	Opus	epoxiconazool	Fungicide	187	
30-May	Aviator XPRO	prothioconazool bixafen	Fungicide against fungal diseases (stem-base, foliar and ear diseases)	187 93.75	10.3
	Decis	deltamethrin	Insecticide	6.25	

*DVS: Developmental stage, expressed in the Feekes scale (Large, 1954).

3.2 Description of the measurements

Soil data

In December 2013, soil samples were taken by BLGG AgroXpertus to analyse the initial soil status. Summary results are given in Table 3.4; an extensive report can be found in Appendix III.

From October 28 (5 days after sowing), soil temperature was measured at two depths (5 cm and 10 cm) with three replicates. At the fifth of March a meteorological station was placed close to the field trial. This station measured with a data logger (Campbell CR10X) the soil temperature (°C), soil heat flux (W m^{-2}) and soil volumetric moisture content (–) at three depths (5 cm, 10 cm and 50 cm) with a time interval of 10 minutes.

Table 3.4. Summary of results from the soil analysis before start of the experiment.

Measurement	Unit	Value
pH	-	7.1
SOM[1]	%	3.7
Clay[2]	%	33
Silt[2]	%	50
Sand[2]	%	11
CEC[3]	mmol+/kg	259

[1] SOM: Soil organic matter.

[2] Clay particles have a size smaller than 2 μm, silt between 2 and 50 μm and sand larger than 50 μm.

[3] CEC: Cation exchange capacity.

Weather data

From sowing until the fifth of March, weather data are taken from weather station 'De Veenkampen'. After the fifth of March, weather data were taken from a meteorological station at the trial. The following parameters were measured with ten minute intervals: incoming and reflected short wave radiation (W m^{-2}); incoming and reflected long wave radiation (W m^{-2}); incoming direct PAR (μmol m^{-2} s^{-1}); incoming diffuse PAR (μmol m^{-2} s^{-1}); reflected PAR (μmol m^{-2} s^{-1}); relative humidity (%); air temperature (°C); air pressure (hPa); wind speed (m s^{-1}); wind direction (°); precipitation (mm).

Crop data

From the 25th of February onwards, crop samples were taken each two to three weeks. From each plot, all above ground biomass in 0.5 m^2 was gathered. From this biomass, a subsample was taken to measure the dry weights of the leaf blades, the leaf sheaths + stems, the dead leaf blades and the ears. The distinction between green and dead leaves was made based on visual assessment. From the green leaf blades, the leaf area was measured using a LI-3100C Area Meter (LI-COR, 2004). Subsequently the samples were dried for two days at 70 °C and then the dry weight was determined. The unsplit part of the samples were stored in paper bags for chemical analysis.

Since the size of the samples increased each next sampling, the procedure of making the subsample was not the same for all the samplings. The size of the subsample was chosen in such way that it was between 10 and 15 percent of the original sample. In this way, the leaf area measurements could be finished in one day after the sampling, which was important since the quality of the leaves dropped with time. The exact procedure for each sampling date can be found in Appendix V.

Interception of photosynthetically active radiation

The interception of photosynthetically active radiation (PAR) was measured with the AccuPAR (Decagon Devices, 2013). PAR is the radiation in the 400 to 700 nm waveband. It represents the

portion of the spectrum which plants use for photosynthesis. In order to determine the amount of absorbed radiation, four values should be measured (Figure 3.2): (i) the incident PAR above the canopy (I_0), (ii) the amount of PAR coming from above, below in the canopy (I), (iii) the amount of reflected PAR above the canopy ($I_{ref.canopy}$) and (iv) the amount of PAR reflected by the soil below in the canopy ($I_{ref.soil}$) . The amount of absorbed PAR (I_{abs}) is then:

$$I_{abs} = I_0 - I - I_{ref.canopy} + I_{ref.soil} \quad (27)$$

The intercepted amount of PAR is Equation 27 without $I_{ref.canopy}$ and $I_{ref.soil}$. The AccuPAR has three parts (Figure 3.3): (i) the probe of 86,5 cm; the probe contains 80 independent sensors with 1 cm space in between. The first four cm close to the handle does not contain sensors to avoid the effect of shadow of the handle on the measurements; (ii) the external PAR sensor: this sensor is used to measure the PAR above the canopy while the probe is used to measure the PAR below the canopy. The external PAR sensor can be connected to the AccuPAR with a cable of three meter. During the measurements, the external sensor was placed on a stick so that it was above the canopy; (iii) the handle with display and data logger: here the measurements are displayed and stored. The handle had a spirit level to make sure that all measurements are done parallel to the soil. Furthermore, a cable was provided to connect the data logger with the computer to transfer data from the logger to Excel.

Before starting the measurements, some initial settings had to be set. The location and time, a crop specific leaf distribution parameter χ and a calibration had to be done. The leaf distribution parameter χ refers to the distribution of leaf angles within the canopy. It is the ratio of the length of the horizontal to the vertical axis of the spheroid described by the leaf angle distribution of the canopy. For wheat, this is usually 0.96 (Decagon Devices, 2013). So the wheat leaves are assumed to be a bit more vertical than horizontal. For onions for example, a χ-value of 0.7 is used, and for strawberries a χ-value of 3 is common (Decagon Devices, 2013). It is possible that there are differences between cultivars, and that there are differences during the growing season depending on the developmental stage. However, Goudriaan (1988) stated that the leaf-angle distribution has no strong effect on light extinction and photosynthesis. So highly refined data of the leaf-angle distribution are not required and throughout the season a χ value of 0.96 was used for the light interception measurements.

For calibration of the AccuPAR, the PAR level must be above 600 μmols m^{-2} s^{-1}. On cloudy days, the PAR levels are usually lower. The external sensor is calibrated at the factory and is used in the

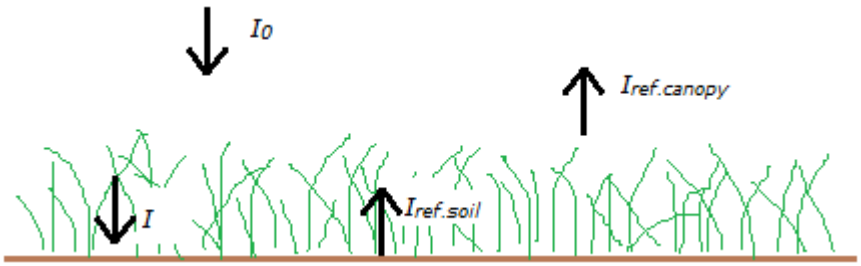

Figure 3.2. Overview of the four radiation fluxes that have been measured to obtain the absorbed PAR by the canopy.

calibration procedure to calibrate the sensors in the probe. During calibration, the external sensor is attached to the probe at the hole next to the spirit level. In this way, the direction towards the sun of the probe and external sensor is always the same.

During the measurements the external sensor was placed at a stick next to the field that was measured. So the external sensor had to be replaced each measurement. Measurements were done within one day from the crop sampling date to correlate the absorption of PAR with the LAI of the crop. Because the sampling had to be done regardless the weather circumstances, some PAR interception measurements were done under direct light and others under diffuse light. The measurements with the AccuPAR took about 2 to 3 hours each time (see Appendix IV for time during the day for each crop sampling when the light interception is measured). At light intensities different than during the calibration, measurements were also done with the probe next to the external sensor. Both values of the external sensor and the probe should be the same, but if there were deviations, than there was corrected for this before other analysis took place. For example, during calibration the PAR level was 1800 μmol m^{-2} s^{-1}, so because of the calibration both the external sensor and the probe measured 1800 μmol m^{-2} s^{-1}. If the PAR level dropped to, for example, 400 μmol m^{-2} s^{-1} during the light interception measurements, then several measurements were done with the probe next to the external sensor in the interval between 1800 and 400 μmol m^{-2} s^{-1}. It was assumed that the value measured by the external sensor was always right since it was calibrated officially at the manufacturer of the AccuPAR. When the values measured with the probe under- or overestimated the actual PAR level, then was corrected for this using the slope of the linear line fitted through a figure with values of

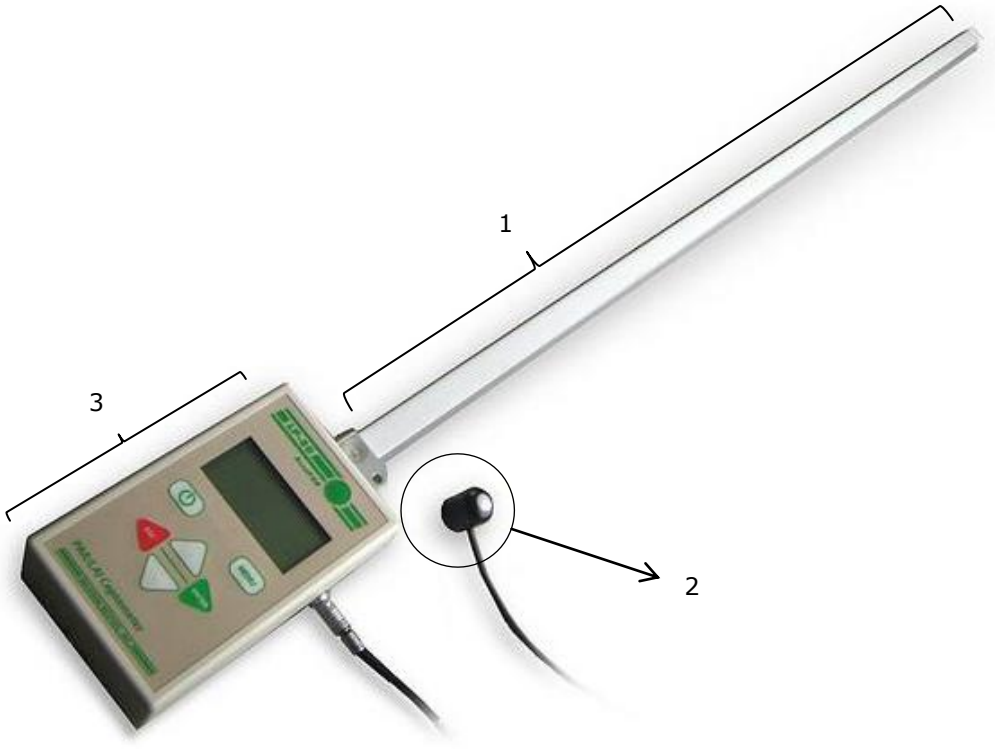

Figure 3.3. The AccuPAR device. 1 is the probe with 80 sensors, 2 is the external PAR sensor and 3 is the handle with display and data logger.

the probe on the Y-axis and values of the external sensor on the X-axis.

For each field, reflection from the canopy ($I_{ref.canopy}$) and the radiation intensity below in the canopy (I) were measured five times. Reflection from the soil ($I_{ref.soil}$) was measured about one time each replication since the variation was circa 10 times lower for these values.

3.3 General analysis of results

Analysis of the results was done with GenStat 16th edition (Payne, 2012). Outliers were identified using XY-scatter from Excel and the boxplot graph from GenStat. If a point lays further away from the whisker of the boxplot than 1.5 times the interquartile range, then it is defined as an outlier. If outliers were identified and excluded from the dataset, then this is mentioned in the results and discussion section.

Since the experimental design was a split-plot design with nitrogen application in the whole plots and varieties in the subplots, it was planned to analyse the data with the ANOVA split-plot option of GenStat. But due to a fertilization mistake, one fertilizer plot had to be omitted from the data and therefore the data were unbalanced. This made use of ANOVA impossible, so the restricted maximum likelihood (REML) procedure of GenStat was used for analysis since this can handle unbalanced data (Payne *et al.*, 2007). The final yield, ears per square meter, kernels per square meter, thousand kernel weights and harvest index were analysed for effects of nitrogen application and variety with the following model:

$$y_{ijk} = \mu + v_r + a_s + va_{rs} + b_i + w_{ij} + \epsilon_{ijk} \quad (28)$$

where y_{ijk} is the final yield, ears per square meter, kernels per square meter or thousand kernel weight at block i, whole-plot j and subplot k (also see Appendix II). According to the REML manual of GenStat (Payne *et al.*, 2007), the fixed part of the model consists of:

μ the overall constant (grand mean),

v_r the main effect of variety r (where r is the variety assigned to unit ijk),

a_s the main effect of nitrogen application at level s (where s is the nitrogen level assigned to subplot ijk), and

va_{rs} their interaction.

The random model terms are

b_i the effect of block i,

w_{ij} the effect of whole-plot j within block i, and

ϵ_{ijk} the random error for unit ijk (which here is the same as the subplot effect).

Weather data

A general overview of the weather data is given in order to place the results in the perspective of the growing season. The total precipitation and total irradiation over the growing season are summed

counting from the date of sowing. From the weather date, two weather files (2013 and 2014) were composed for the LINTUL1 program in FST. The weather files contain data on the location of the meteorological station, year, day of year, daily global incoming shortwave radiation (kJ m^{-2} d^{-1})*, daily minimum air temperature (°C), daily maximum air temperature (°C), daily average vapour pressure (kPa), daily average wind speed (m s^{-1}) and the daily total precipitation (mm d^{-1}). Not all these data is used as input for LINTUL1. Still this information was included in the weather files in order to make a complete weather file that could also be used for other purposes outside the scope of this research. The used weather data originates from the meteorological station at the field trial and from meteorological station 'De Veenkampen' near Wageningen. In first instance, data are used from the station at the trial, but if this was not available, then data were used from 'De Veenkampen'.

3.4 Determination of crop parameters

For parameterization of the crop parameters the variety and nitrogen application with the highest yield is used. In section 1.4 it is shown that newly introduced varieties still obtain higher yields than older varieties. By determining parameters that are best applicable on these recent varieties the model will do the best simulations for the potential yield under current Dutch conditions. The two other varieties with the same nitrogen application that are not used for parameterization can be used for validation of the newly obtained parameters.

The determination of crop parameters was an iterative process. Some parameters were directly calculated based on the obtained dataset. Other parameters were calculated based on data from the dataset, but subsequently adjusted to improve the fit with the observed data. These parameters could not directly be calculated because of the interdependence of these parameters. In the following section the details are described of how each parameter is obtained.

Development parameters

The length of the developmental stages that are distinguished for LINTUL1 are calculated based on the parameters given by Het Lam (2014). It is not possible to calculate base temperatures from data of one growing season (Weir *et al.*, 1984). There were no other recent datasets of winter wheat trials available with information on the development of the crop during the growing season. Therefore, the base temperatures found by Het Lam (2014) are not adjusted and are also used in this thesis. $T_{b\text{-}emergence}$ was 0.25 °C, $T_{b\text{-}anthesis}$ was 1.5 °C and $T_{b\text{-}maturity}$ was 1.5 °C.

* The conversion from μmol m^{-2} s^{-1} is done using the equation (see also the section in the material and methods on the radiation use efficiency):

$$\frac{\mu mol\ PAR}{m^2 \times s} \times \frac{1.986 \times 10^{-16} \times 6.023 \times 10^{23}}{550} \times \frac{60 \times 60 \times 24}{1000 \times 1000000} = \frac{kJ\ PAR}{m^2 \times d}$$

The developmental stage between emergence and anthesis is, besides temperature, also affected by photoperiod and vernalization. Parameters for the response of winter wheat on photoperiod and vernalization are taken from Het Lam (2014) as well. It is known that the vernalization and photoperiod response can differ between varieties. It is also known that there are interactions between the vernalization process and the effect of photoperiod (Evans, 1987). However, no observations were done on these processes because the outline of the experiment was not designed for such measurements. V_{sat} was set at 58 and V_{base} at 10.8 (Het Lam, 2014). The relation between the effectiveness of vernalization and average day temperature is shown in Figure 2.1. According to Het Lam (2014) P_{opt} was 16 h and P_b was 9 h.

During the simulations the developmental stage (DVS) was calculated as the actual temperature sum divided by the determined temperature sum for example between emergence and anthesis, or between anthesis and maturity. In LINTUL1, development starts from emergence onwards (DVS is zero before emergence by definition). Flowering or anthesis is indicated by DVS = 1. After anthesis, the actual DVS is calculated as the actual temperature sum after flowering divided by the determined temperature sum for maturity plus 1. Maturity is indicated by DVS = 2.

Temperature sums

The length of the developmental stages are derived from the temperature sums. The temperature sums are calculated based on 10 minutes data from the meteorological station at the trial field and from 10 minutes data from the meteorological station 'De Veenkampen'. For every 10 minutes, the average temperature during this 10 minutes was known. This is converted to daily data by taking the average temperature of all the 10-minutes data per day. The three temperature sums needed for LINTUL1 for winter wheat were calculated as follows:

- $T_{sum\text{-}emergence}$ was calculated based on soil temperature under bare soil at a depth of 5 cm with Equations 3 and 4. A dept of 5 cm is deeper than the seeds are sown (seeds are sown at a dept of approximately 2 – 3 cm), but it is assumed that the temperature at a depth of 5 cm is representative for the temperature at sowing depth. Data are taken from meteorological station 'De Veenkampen' (Meteorology and Air Quality Group, 2012-2014) near Wageningen (2.5 km from the trial field) because soil temperatures at the trial field were not available immediately from the day of sowing. The crop was sown at the 23rd of October, so October 24 was the first day that counted for the thermal sum. The day of emergence was the last day that contributed to the thermal sum of emergence. The $T_{b\text{-}emergence}$ was taken from Het Lam (2014) since it was not possible to calculate a new value based only data from one growing season.
- $T_{sum\text{-}anthesis}$ depends on daily average air temperature, photoperiod and vernalization. This temperature sum is obtained using the FST program of LINTUL1. The parameters for photoperiod, vernalization and the base temperature are defined in the program code and are taken from Het Lam (2014). The sowing date was set at the October 23 and the weather data of

the growing season was provided to the program with a weather file. The temperature sum for anthesis was obtained by adjusting it for several runs in the program until the flowering date in the output corresponded with the observed flowering date.

- $T_{sum\text{-}maturity}$ was calculated based on the daily average air temperature and $T_{b\text{-}maturity}$.

Leaf area parameters

Specific leaf area

Box-plots were made from the SLA for each sampling date using GenStat. Values indicated as outliers were excluded from further analysis. If a point lays further away from the whisker of the boxplot than 1.5 times the interquartile range, then it is defined as an outlier. The data of SLA were analysed with the REML procedure of GenStat as a split-split-plot design. If SLA was significantly different between sampling dates, then the correction factor for SLA was adjusted to the new situation. If the SLA did not change significantly over the growing season, then the average SLA was taken as the new SLA constant, and the correction factor for the SLA was removed from the model.

In addition, a regression analysis was performed on the SLA data with the Linear Mixed Models function of GenStat 16th edition. SLA was the response variate and LAI or LAI * variety * nitrogen the explanatory variate.

Relative growth rate of leaves and initial LAI

The relative growth rate of the leaves (r_l) was calculated based on the observations at February 18 and March 10. During these observations the LAI values of Julius and Ritmo were smaller than 0.6 $m^2\ m^{-2}$ and the assumption for exponential growth was still valid. Tabasco had a LAI of 0.71 at March 10, but also for Tabasco r_l is calculated in order to do a comparison with the r_l values of Julius and Ritmo. In addition, in LINTUL1 for spring wheat it was assumed that the exponential phase of leaf area growth occurs until LAI is larger than 0.75 (Van Oijen and Leffelaar, 2008).

With the trendline option of a XY-scatter graph in Excel an exponential curve was fitted through the two observations. From two observations it is impossible to determine if there is an exponential relation between two variables or, for example, a linear relation. However, an exponential relation was assumed for the first growth stage based on Van Oijen and Leffelaar (2008). The fitted equation had the following form:

$$y = a * e^{b*x} \tag{29}$$

where y is the LAI_{t+1}, a is LAI_t, b is $r_l * T_{effective}$ and x is Δt. The effective temperature was known for all the days of the growing season, so an average $T_{effective}$ was calculated for the period between the first and the second crop sampling. Dividing b from Equation 29 by this average $T_{effective}$ gave an estimate of

the relative growth rate. From the r_l between February 18 and March 10 the LAI was calculated for all days between sowing and February 18 to obtain $LAI_{initial}$ using Equation 29.

Relative death rate of leaf sheaths

The relative death rate of leaves depended amongst others on $T_{sum\text{-}ageing}$. The parameter $T_{sum\text{-}ageing}$ indicates the moment during development from which the leaves can start to senesce because of ageing of the leaves. Het Lam (2014) set this parameter at 900 °Cd while flowering occurred at 926 °Cd. So senescence could start already before flowering. After parameterization, this constraint was removed from the model. The relative death rate is now accounted for in another way.

The relative death rate of leaves depends furthermore on the parameters LAI_{cr}, $T_{sum\text{-}senescence}$, $r_{d\text{-}shading}$, and a function between average daily air temperature and the relative death rate. These parameters are interrelated and changing the value of one parameter affects the influence of the other parameters on the total senescence as well. Therefore, an Excel-file was created with the same equations for leaf area senescence as in LINTUL1 where each row represented one timestep. The parameters were adjusted until the senescence because of shading showed a good fit with the observations. The examination of a good fit was done visually with a XY-scatter graph.

The senescence because of ageing of the crop was changed. The relative death rate was made dependent on the developmental stage instead of the daily average air temperature. In this way all the green leaves could have senesced at maturity. By definition, this was not possible in the model of Het Lam (2014). The relative death rate never exceeded 0.126 (highest r_d in the temperature function) and therefore at least 87.4% of the green leaves present at the previous timestep were still present at the current timestep.

The method for obtaining parameters for leave senescence is described in more detail in Appendix VI.

Dry matter production

Extinction coefficient

The amount of light intercepted depends on de extinction coefficient (k) of the crop. From Equation 13 the following equation can be derived:

$$-\ln\left(\frac{I}{I_0}\right) = k \times LAI \tag{30}$$

where k is the slope of the linear relation between the LAI and the negative natural logarithm of the amount of radiation reaching soil level (I) divided by the incident amount of radiation (I_0). Both I and I_0 are obtained from the AccuPAR measurements and the LAI is derived from the crop samplings. The extinction coefficient is derived using the linear trendline function of Excel. This trendline was forced to go through the origin (0,0) since no light can be intercepted if no leaf area is present.

Radiation use efficiency

The radiation use efficiency (RUE) determines the effectiveness of the utilization of PAR to produce dry matter, and is expressed in g above-ground dry matter per MJ PAR. The RUE is calculated as the slope of the linear relation between the total amount of intercepted PAR (in MJ m^{-2}) by the crop in the period between March 31 and June 12 2014, and the accumulated amount of above ground dry matter. The RUE is calculated over this period since the AccuPAR measurements started at March 31 and the LAI decreased from June 12 onwards. For the calculation of RUE, only interception by green leaves is relevant. Interception of light by dead leaves gives an underestimation of the RUE. From the AccuPAR measurements, the percentage of light interception was calculated as the total incoming PAR above the canopy minus the PAR reaching the probe of the AccuPAR at soil level. The light interception between two measurements was linearly interpolated using the equation:

$$y_t = y_{t-1} + \frac{y_{obs2} - y_{obs1}}{t_{obs2} - t_{obs1}} \tag{31}$$

where y is the percentage of intercepted PAR, t is a certain day between observation date 1 (*obs1*) and observation date 2 (*obs2*). The increasing percentage of intercepted light over time results from increasing LAI. The daily amount of intercepted radiation is calculated by multiplying the percentage of intercepted PAR with the total incoming PAR. Data on the PAR from the meteorological station at the trial field was available every 10 minutes as µmol PAR m^{-2} s^{-1}. Daily values were calculated by taking the average of these 10 minutes values. Conversion from µmol PAR m^{-2} s^{-1} to MJ m^{-2} d^{-1} is done as follows (Van Oijen and Leffelaar, 2008):

$$\frac{\mu mol\ PAR}{m^2 \times s} \times \frac{1.986 \times 10^{-16} \times 6.023 \times 10^{23}}{550} \times \frac{60 \times 60 \times 24}{1000000 \times 1000000} = \frac{MJ\ PAR}{m^2 \times d} \tag{32}$$

where 1.986×10^{-16} is the product of Planck's constant (unit: J×s) and the speed of light (nm s^{-1}), 6.023×10^{23} is the Avogadro constant (unit: number of particles mol^{-1}), 550 is the average wavelength for photosynthetic active radiation (unit: nm), 60×60×24 is the conversion from s^{-1} to d^{-1}, and the denominator with 1000000 × 1000000 is to convert from µmol to mol and from J to MJ.

Above-ground dry matter data is taken from the field with the N3 application. These fields had green leaves for the longest time. Sinclair and Muchow (1999) describe that lower nitrogen availability decreases the maximum photosynthetic capacity of the leaves and therefore also affects the RUE. That is why only data from the highest nitrogen application is taken. This also holds for the AccuPAR data. This is only taken from the fields with the highest N application. This was also done because it was aimed to monitor the potential production situation. The total amount of above ground dry matter was known since this was determined every crop sampling.

The linear trendline function of Excel was used to obtain the RUE from the equation:

$$y = a * x + b \tag{33}$$

where a is the RUE (g DM MJ^{-1} PAR), y is the total above-ground dry matter (g m^{-2}), x is the total amount of intercepted PAR (MJ m^{-2}) and b represents the amount of dry matter present at March 31.

3.5 Dry matter allocation fractions

Data of the variety Julius from the highest nitrogen application were used for parameterization of the allocation fractions since this treatment gave the highest yield in the experiment. Therefore, the parameters obtained can be compared with the observations of Ritmo and Tabasco for validation.

The total daily dry matter increment is partitioned to the plant organs according to fractions that are a function of DVS. The calculation of these allocation fractions is done based on the description of Kropff *et al.* (1994). They give a method to derive allocation fractions based on the increase of dry matter of plant organs between two subsequent crop samplings. In the present model reallocation is included which is not present in the model of Kropff *et al.* (1994). This makes it necessary to start allocation to grains after flowering (and not before, as in their method). Therefore, some adjustments are done on their method. The allocation fractions are calculated as follows:

1. The DVS for each crop sampling date is obtained from the FST program of LINTUL1 (Het Lam, 2014). The temperature sums are adjusted by trial and error in order to have the same date for flowering and maturity as observed in the field. Other developmental parameters such as base temperatures and parameters for vernalization and photoperiod are not changed and taken from Het Lam (2014).
2. A table is made with the dry weights of the above-ground organs (stems, ears, grains and leaves; dead and green leaves must be taken together in this calculation, because they have been produced up to that moment of harvesting) for each sampling date and the corresponding DVS. The difference in weight between two harvests is also included (ΔGrowth). When the weight of an organ decreased, the maximum weight is retained because the decrease in weight is accounted for by reallocation, and not indirectly with the allocation functions.

   The measured increase in dry weight of grains is a result of allocation of newly formed assimilates and of reallocated dry matter that originates from the ears, stems and leaves. Since reallocation is accounted for in another way, the increase of dry matter of grains due to reallocation is subtracted from the total increase of dry matter of the grains. So the weight of the grains is decreased before the allocation fractions are calculated. By calculating the amount of reallocation as the sum of the decrease in weight of the ears, stems and leaves, it is assumed that the decrease in dry matter of organs is completely reallocated to the grains (Table IX.2).

Table 3.5. Dry weights of various organs at subsequent crop samplings.

Sampling date d	DVS -	Leaves kg ha^{-1}	Stems kg ha^{-1}	Panicle kg ha^{-1}	Total kg ha^{-1}	ΔGrowth kg ha^{-1}
100	0.8	2000	4000	0	6000	
						3500
120	1.0	2500	6000	1000	9500	
						2000
140	1.2	2500*	6000*	3000	11500	
						2000
160	1.4	2500*	6000*	5000	13500	

* The maximum value is retained

Table 3.6. Partitioning table with allocation fractions and mean DVS based on dry weights of Table 3.5.

DVS	F_{leaves}	F_{stems}	$F_{panicle}$
-	d^{-1}	d^{-1}	d^{-1}
0.9	500/3500 = 0.14	2000/3500 = 0.57	1000/3500 = 0.29
1.1	0/2000 = 0.0	0/2000 = 0.0	2000/2000 = 1.0
1.3	0/2000 = 0.0	0/2000 = 0.0	2000/2000 = 1.0

3. The allocation fraction is calculated for each period between two subsequent crop samplings. The increase in dry weight of an organ is divided by the total increase of dry weight in the same period. The corresponding DVS is the mean DVS over the same period. Table 3.5 gives an example of the calculation of allocation fractions from Kropff *et al.* (1994).
4. Table 3.6 shows that allocation to the panicle starts already before DVS = 0.9. This is a way to overcome the lack of reallocation in the model of Kropff *et al.* (1994). Since reallocation is present in the version of LINTUL1 in this study, allocation to the grains should start from DVS = 1 onwards. To attain this, an additional row with DVS = 1 is added to the partitioning table. The calculation of the allocation fractions for this row with DVS = 1 could not be based directly on crop samplings but is derived from the crop samplings directly before and after flowering. The calculation of this row is done in three steps:
    a. Values for the row with DVS = 1 are calculated by linearly interpolating between the row directly before flowering (DVS<1) and the row directly after flowering (DVS>1). This is done with equation:

$$F_{i,DVS=1} = \frac{DVS_{=1} - DVS_{<1}}{DVS_{>1} - DVS_{<1}} \times \left(F_{i,DVS>1} - F_{i,DVS<1}\right) + F_{i,DVS<1} \tag{34}$$

    where F is allocation fraction, DVS is developmental stage and i is leaves, stems or ears.
    b. The allocation fraction for grain (F_{grains}) is set at zero, since until flowering no dry matter is partitioned to the grains.
    c. The sum of the allocation fractions has to be 1. Since F_{grains} is set at zero, this is not the case. To make sure that the sum of F_{leaves}, F_{stems} and F_{ears} is 1, the following equation is used:

$$F_{i,new} = \frac{F_{i,step\ a}}{F_{leaves} + F_{stems} + F_{ears}} \tag{35}$$

    where i is leaves, stems or ears and F is the allocation fraction calculated in step a.

3.6 Dry matter reallocation

Reallocation is modelled as a fraction of the total biomass of an organ:

$$\frac{dW_{reallocation,i}}{dt} = W_i \times f_{reallocation,i} \tag{36}$$

where $f_{reallocation}$ is the reallocation fraction (d^{-1}), i is ears, stems or green leaves. The reallocation fraction is a function of DVS and is calculated similar to the allocation factors. For each period between two crop samplings that a plant organ showed a decrease in dry weight, a reallocation fraction is calculated. These fractions together define the reallocation. Each individual fraction is calculated as:

$$f_{reallocation,i} = \frac{\frac{W_{t,i} - W_{t+j,i}}{t_{t+j} - t_t}}{\frac{W_{t,i} + W_{t+j,i}}{2}} \tag{37}$$

where W is the dry weight of organ i in g m^{-2}, t is the number of days after emergence of one crop sampling, and $t+j$ is the days after emergence of the subsequent crop sampling. Equation 37 can be rewritten as:

$$f_{reallocation,i} = \frac{W_{t,i} - W_{t+j,i}}{W_{t,i} + W_{t+j,i}} \times \frac{2}{t_{t+j} - t_t} \tag{38}$$

This equation clearly shows that $f_{reallocation}$ is expressed as d^{-1}.

It is assumed that the reallocation starts from flowering (DVS=1) onwards. Therefore, a row with DVS is added in the reallocation fractions table at DVS=1 with 0 for all reallocation fractions. Furthermore, it is assumed that the reallocation fractions obtained from the last two crop samplings (3 days before final harvest) did not change anymore.

Initial conditions

The initial weight of the green leaves had a value of 0.07 g m^{-2} (Het Lam, 2014). Since SLA and $LAI_{initial}$ are calculated from the dataset obtained, $W_{lvg\text{-}initial}$ will be derived from this as:

$$W_{lvg-inital} = \frac{LAI_{initial}}{SLA_{inital}} \tag{39}$$

The initial weight of the stems ($W_{st\text{-}initial}$) was set at a value of 0.04 g m^{-2} (Het Lam, 2014). This weight is lower than the weight of the initial green leaves since there are hardly any stems at the start of the growing season. No observations are available on the initial weight of the stems. However, if the proportion of the dry weights of leaves compared to the stem is unrealistic, then $W_{st\text{-}initial}$ was adjusted.

4. Results and Discussion

4.1 General results

Environmental conditions

The potential yield is defined by crop characteristics, CO_2 level in the air, the amount of irradiation and by the temperature. Since the aim of the research was to obtain crop parameters for the growth of winter wheat in the Netherlands under potential conditions, figures are shown of the irradiance and temperature during the growing season. The CO_2 level is not measured and assumed to be at a constant level during the growing season of 397.1 ppm (ESRL NOAA, 1960-2014). However, it is known that the CO_2 concentration also fluctuates within a year with about 9 ppm at Hawaii (392 – 401 ppm). The effect of this fluctuation is only small. According to the correction function for the RUE by Het Lam (2014) the RUE would increase with 0.9% for an increase in CO_2 concentration from 394 to 403 ppm. In addition, it is unknown if this fluctuation also occurs in the Netherlands, and how large this fluctuation then would be.

The precipitation is also shown since the plant water availability is an important factor for the realization of a potential yield. Not only because water is directly needed by the plant for growth and transpiration, but also because nutrients are only available to the crop in a dissolved status. So under dry circumstances, the crop growth is not necessarily water limited, but it might also be nutrient limited.

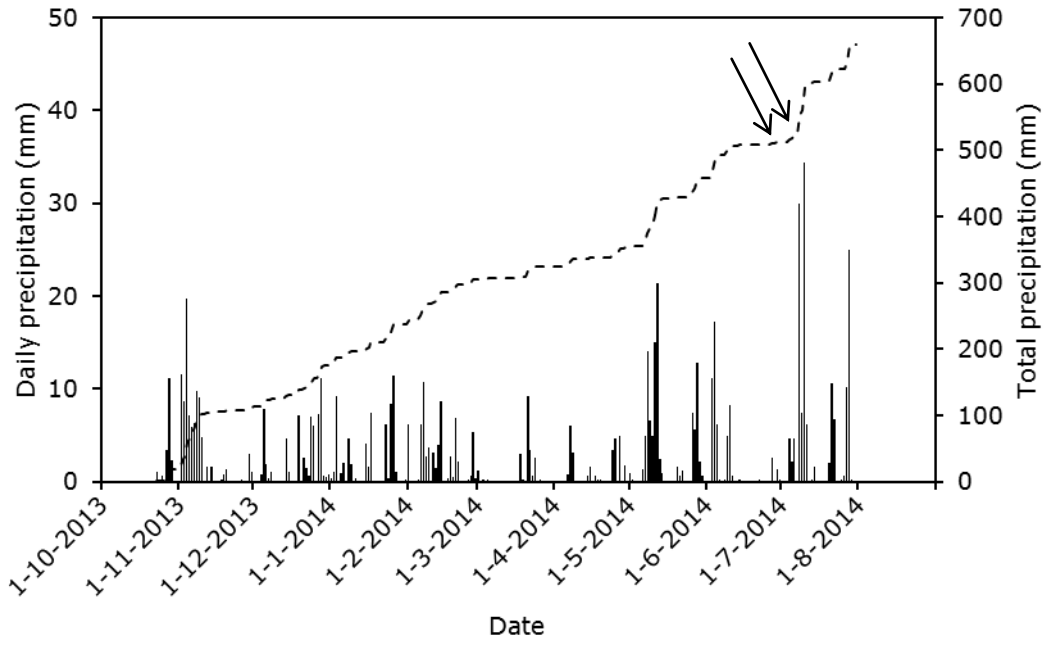

Figure 4.1. Daily and accumulated precipitation during the growing season. On the first of July irrigation was applied because of drought in June (arrow). The amount of irrigation was 15 mm but is not shown in this figure.

Precipitation

The trial was sown at October 23, 2013 after a rainy period. Also the period after sowing some precipitation occurred. At the first of December about 110 mm of rain had fallen after seeding the trial. However, the germination was not reduced or even improved by this large amount and enough plants per square meter survived this period. March until May was a relatively dry period, but measurements of the soil water status during this period did not denote a water deficiency of the crop (Sprangers, 2014 personal communication).

A hailstorm occurred at May 9, resulting in some damage at the second leaves below the flag leaf (the flag leaf and the leaf below the flag leaf still had to appear at that time). It is not probable that the hailstorm reduced the crop growth because no leaves died after the event. Some leaves were only ruptured in the middle of the leaf in the direction of the nerves.

June was a dry month leading to a critically low water availability that was assessed by tensiometers (see also BSc thesis of Sprangers. Therefore, 15 mm of water was irrigated at the first of July and secondly 15 mm on July 4.

At July 10, a storm caused lodging of field 29 and 30, also field 7 and 8 were partly lodged. These fields had the highest nitrogen treatment and the varieties Tabasco and Ritmo were grown there. At July 28 there was another rain shower, but without a lot of wind, so this caused no damage. At July 31 the trial was harvested under optimal conditions.

Irradiation

Between October 23, 2013 and July 31, 2014 the global shortwave irradiation was 2827 MJ m^{-2}. In this period, about 75% of the annual irradiation reaches the Dutch earth surface (Velds *et al.*, 1992), so if this amount of irradiation is extrapolated for a whole year, the annual global shortwave irradiation would be around 3800 MJ m^{-2}. This is circa 200 MJ m^{-2} above the average of the last ten years (KNMI, 2013). This above average amount of irradiation can have a positive effect on the obtained yield.

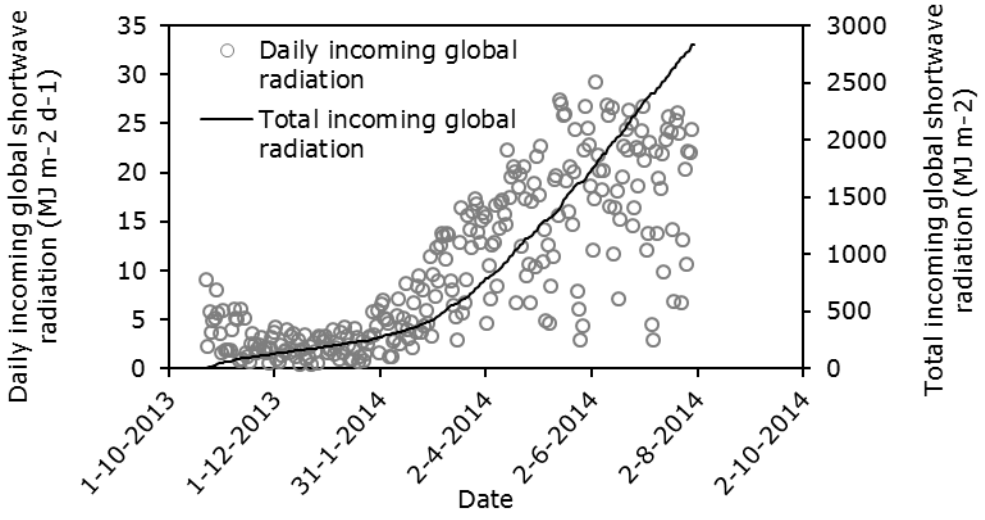

Figure 4.2. Incoming global shortwave radiation per day (left y-axis: MJ m^{-2} d^{-1}) and integrated over the growing season (right y-axis: MJ m^{-2}). Measurements originate from the Veenkampen until March 5, afterwards, data were taken from the meteorological station at the field trial.

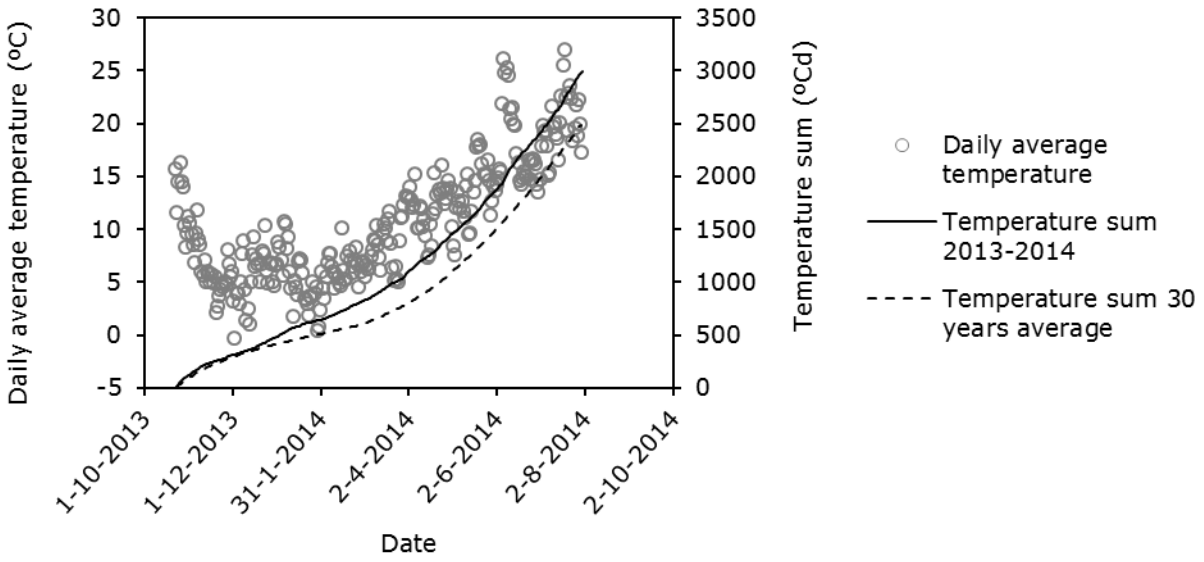

Figure 4.3. The daily average air temperature (at 150 cm above the soil, °C), the temperature sum over the growing season 2013-2014 (°Cd) and the average temperature sum for the last 30 years (1983-2013, De Bilt, KNMI).

Temperature

The daily average temperatures were higher than in an average year (Figure 4.3). During winter only one day had an average temperature below zero. This implies that there was hardly any frost and that possibly present diseases were not reduced due to a harsh winter. The relative high temperatures resulted in faster development of the crop than in an average year. A faster development means that there are less days within a certain developmental stage to intercept PAR. Therefore, it is possible that the dry matter production would have been higher in a 'colder' growing season. However, the relatively high amount of irradiation could compensate for the shorter developmental stages to some extent.

Crop measurements

During the growing season crop samplings were done 10 times. Beforehand, a protocol for the sampling was made based on personal communication with colleagues who had some experience with similar field work. However, during the first sampling it appeared that the time required to split all the plant material from 0.5 m^2 from all 36 plots in dead leaves, green leaves and stems took more time than available. Therefore, during the first sampling date 12 plots were processed instead of all 36. For the subsequent crop samplings the protocol was adjusted to be able to process samples of all plots within 24 hours to prevent leaves from wilting despite cold storage after sampling.

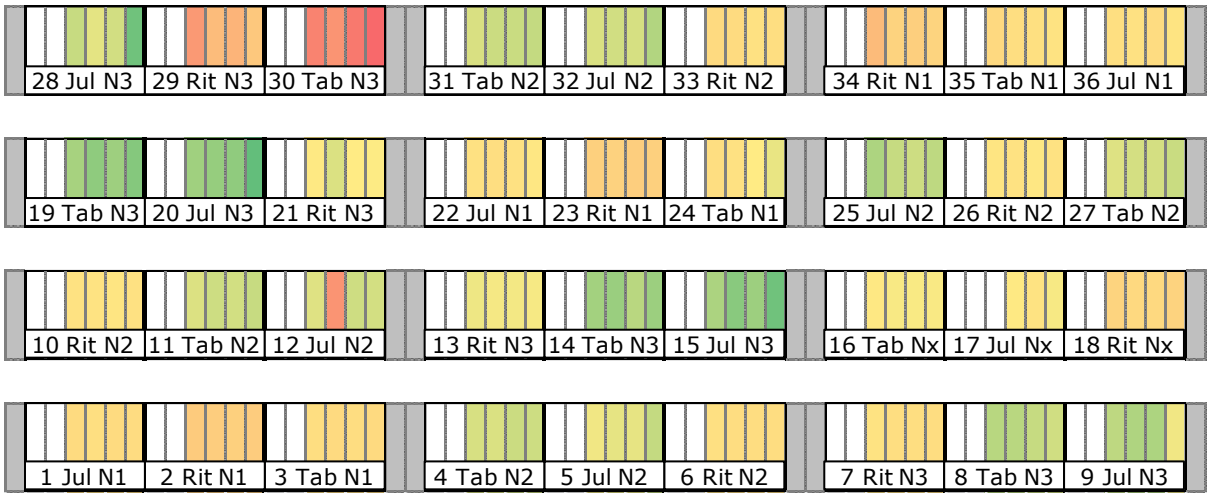

Figure 4.4. An overview of the net grain yield of each plot. Within each plot, four observations of the net grain yield were done, one for each bed. A higher intensity of the green colour indicates a higher yield, a higher intensity of the red colour indicates a lower yield. The minimum and maximum yields are 5.7 Mg ha^{-1} and 13.1 Mg ha^{-1} respectively.

Figure 4.4 shows the trial field with the obtained grain yields. Based on this map, plot 29 and 30 were completely excluded and one bed of plot 9 was excluded from further analysis, because of lodging during the storm of July 10. This explains the low yield for these fields. One bed of plot 12 was excluded because of an adversity during harvest. The excluded fields were not taken into account in the analysis of the grain yield, thousand kernel weight, kernels per square meter, ears per square meter and harvest index.

Grain yield

The effect of N application and the effect of variety on the yield were both strongly significant ($P < 0.001$). No interaction between N application and variety on the yield was observed. The data show that the yield increases with a higher nitrogen application. The highest nitrogen application (300 kg N ha^{-1}) still increased the yield significantly (Table 4.1) but goes actually beyond the Dutch legal nitrogen limitation for wheat. The variety effect shows that the two recently widely distributed varieties Julius and Tabasco have a higher yield than the older variety Ritmo. This is in agreement with the observations of the data from the Dutch recommended list of varieties for winter wheat in Section 1.3.

The estimated variance components for the yield were 0.01785 for the blocks and 0.00504 for the nitrogen whole plots. So the blocks are more variable than the nitrogen whole plots (Figure 4.5). This supports the design of the experiment (Payne *et al.*, 2007).

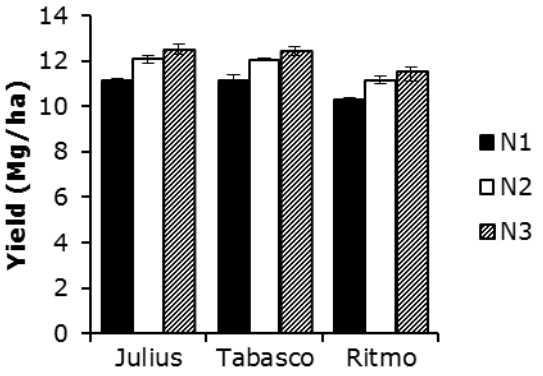

Figure 4.5. The final yield with 15% moisture for all the different treatments. The error bars indicate the maximum and minimum values.

Harvest index

The harvest index with respect to the above ground dry matter was significantly affected by the type of variety (P = 0.039). Tabasco had a significantly higher HI (0.492) then Julius and Ritmo (0.470 and 0.463, respectively). In the field it was observed that Julius had a higher amount of straw than Ritmo and Tabasco. This explains why Julius had a lower HI than Tabasco.

Ears per square meter

Julius had 649.2, Ritmo 618.8 and Tabasco 576.5 ears m^{-2}. This difference between varieties was significant (P<0.001). Neither the relation of the number of ears with the nitrogen treatment nor the interaction between nitrogen and variety was significant (P=0.127 and P=0.987, respectively). However, there was a tendency of an increasing number of ears per square meter with increasing nitrogen application. (N1 had 594.1, N2 601.6 and N3 643.7 ears m^{-2}).

The number of ears per square meter were counted once during the growing season, close before maturity. Maybe that more observations of the number of ears would increase the significance of the relationship between nitrogen application and number of ears. More observations increase the number of degrees of freedom of the residual in the statistical analysis. This usually increases the significance of the outcome of the statistical analysis.

Kernels per ear

The kernels per ear were significantly related to variety (P<0.001). Tabasco was significantly different from Julius and Ritmo with 46.5 kernels ear^{-1} compared to 36.5 and 37.4 kernels ear^{-1}, respectively. The number of kernels per ear was not significantly affected by the nitrogen application nor by the interaction between nitrogen application and variety.

Thousand kernel weight

The weight of 1000 kernels (with 15% moisture) was significantly affected by the variety. All varieties differed significantly from each other with a TKW of 51.3 g for Julius, 48.5 g for Ritmo and 46.6 for Tabasco (P < 0.001).

Kernels per square meter

The number of kernels per square meter was significantly affected by the main effects of nitrogen and variety (P = 0.003 and P < 0.001 respectively). Nitrogen application increased the kernel number from 22445 at N1 to 25218 at N3 (Table 4.1). Ritmo had the lowest number of kernels per square meter (22595) and Tabasco the highest (25545). Julius had 10% less kernels per square meter than Tabasco, but in return a TKW of 10% higher.

Table 4.1. Overview of the results of the final harvest of the trial at July 31. Different letters next to the values indicate significant differences between the values with a least significant difference (LSD) of 5%. If no letters are shown behind the value, then no significant differences were present.

		Grain yield[1] Mg ha^{-1}	Harvest index -	Ears m^{-2}	Kernels m^{-2}	TKW[2] g
Main effects	N1	10.87 a	0.463	594.3 a	22445 a	48.12
	N2	11.75 b	0.484	601.6 a	23603 b	49.87
	N3	12.13 c	0.479	643.7 b	25218 c	48.44
	Julius	11.90 b	0.470 a	647.2 b	23127 b	51.28 c
	Tabasco	11.87 b	0.492 b	574.6 a	25545 c	46.61 a
	Ritmo	10.98 a	0.463 a	617.7 b	22595 a	48.54 b
Interaction effects	N1 × Julius	11.13	0.461	624.4	22139	49.79
	N1 × Tabasco	11.12	0.478	553.6	24062	46.04
	N1 × Ritmo	10.32	0.445	604.8	21136	48.54
	N2 × Julius	12.06	0.470	640.9	22976	52.49
	N2 × Tabasco	12.04	0.499	579.0	25230	47.79
	N2 × Ritmo	11.15	0.485	584.8	22603	49.32
	N3 × Julius	12.51	0.481	676.3	24266	51.56
	N3 × Tabasco	12.41	0.499	591.2	27343	46.01
	N3 × Ritmo	11.47	0.456	663.5	24047	47.76

[1] The grain yield includes 15% moisture.

[2] TKW: Thousand kernel weight including 15% moisture.

4.2 Crop parameters

Data used for the parameterization of LINTUL1 are taken from the highest yielding variety and nitrogen treatment. Julius with nitrogen treatment N3 had the highest yield. Despite the fact that this yield was not significant different from Tabasco under N3 this treatment was not included in the data for parameterization. In this way, the data from Tabasco and N3 could be used as validation dataset.

Development parameters

Thermal sums

Julius and Tabasco emerged at November 4th, Ritmo at November 6th. The calculated thermal sum for emergence was 127 °Cd for Julius and Tabasco and for Ritmo it was 141 °Cd based on a $T_{b\text{-}emergence}$ of 0.25 °C and based on the soil temperature at 'De Veenkampen' at a depth of 5 cm under bare soil.

For all varieties and nitrogen levels anthesis was at June 3, therefore the PVT_{sum} between emergence and anthesis was equal for all treatments and found to be 680 °Cd. The period between anthesis and maturity was also equally long for all treatments, so again the thermal sum was the same for all treatments and found to be 1030 °Cd.

Leaf area parameters

Specific leaf area

Figure 4.6 shows the observed SLA during the growing season. Plot 6, 7, 8, 11, 17, 28, 30 and 32 at March 10 and plot 3 and 13 at July 16 were excluded from statistical analysis based boxplots which indicated these values as outliers. At March 10, the leaves were cut with a scissors from the roots in the field in order to avoid that clay would stick to the leaves and affect the dry matter measurements.

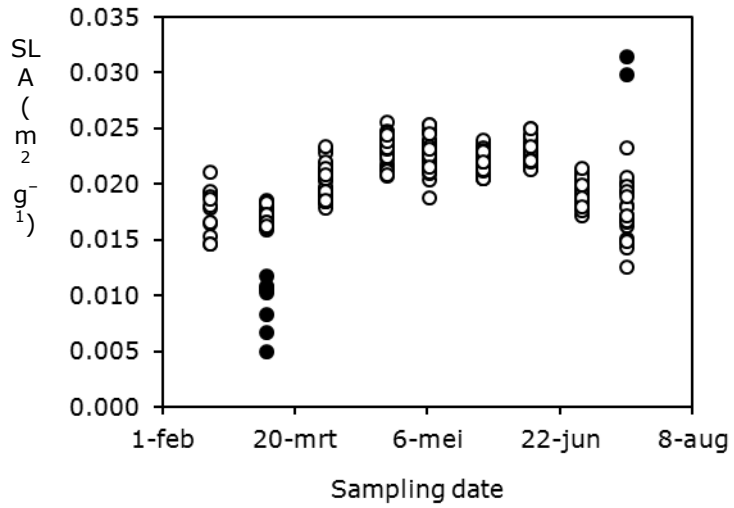

Figure 4.6. The observed specific leaf area (SLA) at each sampling date. The observations with the full black circles are excluded from the statistical analysis because they are outliers.

Since the leaves were still very small, moisture was lost rapidly from the leaves so the leaves were flabby during the leaf area measurements. In addition, the leaves were rolling up in the length direction of the leaves in the form of a needle. This made leaf area measurement difficult and caused probably underestimation of the leaf area for some samples, resulting in a lower SLA. From July 16, 2 of 28 observations were excluded from further statistical analysis because of their high SLA values. From 8 plots no SLA was determined because all the leaves had already senesced. The distinction between green leaves and dead leaves was difficult to make at the end of the growing season. In addition, the size of the samples on which the SLA was based at July 16 was relatively small compared to earlier samplings. The two outliers had a dry weight of 0.09 and 0.05 g in the subsample and a leaf area of 27 and 17 cm^2. These small numbers increase the risk of measurement errors.

A split-split-plot analysis with the REML procedure of GenStat on the SLA showed a significant effect of the sampling date on the SLA. Therefore, SLA was not taken constant over the growing season but was represented as a function of the developmental stage. The function defined by Het Lam (2014) was adjusted to obtain a better fit with the observations from the field trial (Figure 4.7).

The SLA is an input variable in LINTUL1. This means that the SLA is given for each developmental stage. The SLA is used as conversion factor of dry matter of the green leaves to the LAI of the crop in the linear growth phase. However, if the simulated LAI is divided by the simulated dry weight of the green leaves, then the SLA is not returned. This results in a worse fit of the simulation of the SLA with the observed SLA. This is a problem that cannot easily be solved because in the exponential growth phase the LAI is not related to SLA or dry weight of green leaves in LINTUL1.

The regression of the SLA with the LAI showed a strongly significant relation ($P<0.001$). The regression analysis did not show any effect of amount of nitrogen application, type of variety or the interaction between both. The estimated parameters by the regression were an intercept with the SLA-axis (LAI = 0) of 0.0170 $m^2 g^{-1}$ and an increase of the SLA of 0.0010 $m^2 g^{-1}$ * LAI.

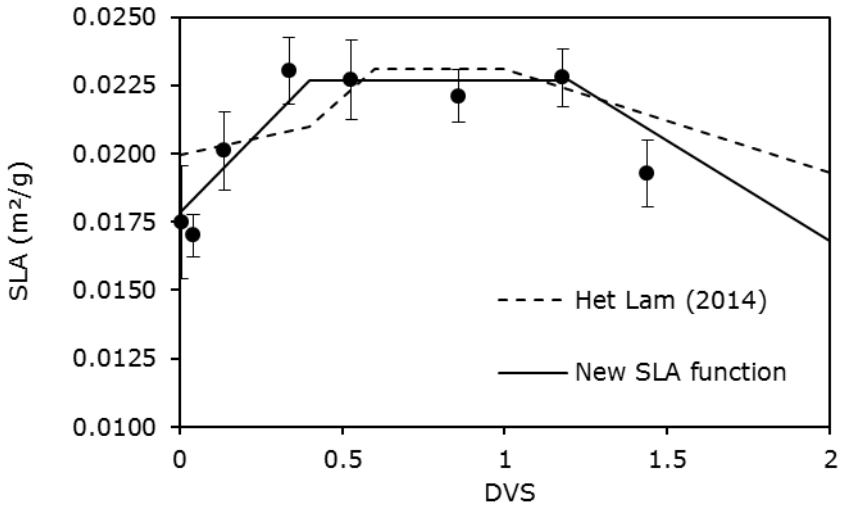

Figure 4.7. The new function for the specific leaf area (SLA) in $m^2 g^{-1}$ in LINTUL1 (full line) is obtained by multiplying the SLA constant (0.021) with the correction factor (see the model code). The dots are observations from all the varieties and from all nitrogen levels; the dashed line was used in Het Lam (2014).

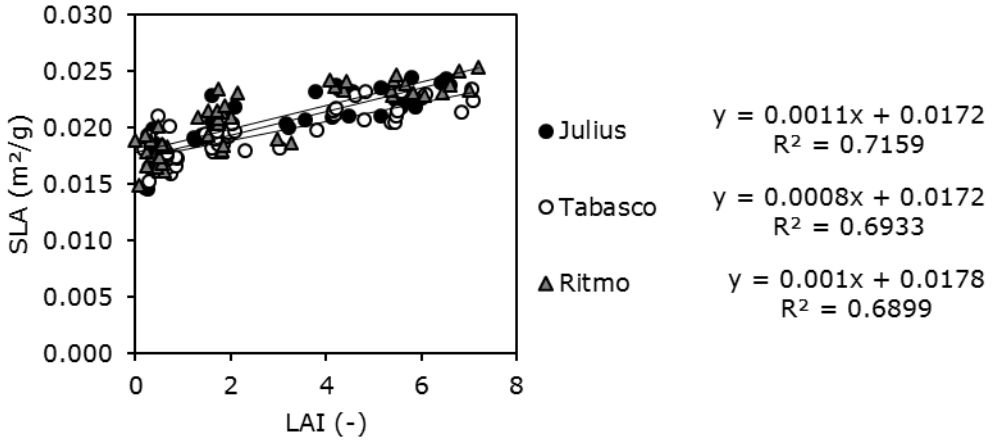

Figure 4.8. The specific leaf area (SLA) as function of the leaf area index (LAI). The trendlines next to the legend correspond with the adjacent variety.

This result supports the theory of Ratjen and Kage (2013) that SLA is related to the LAI. It should be mentioned that this relation is valid for the SLA of the whole crop, but not necessarily for the SLA of individual leaves. It is expected that SLA of individual leaves can increase because of reallocation of dry matter. This does not concur with the observation that SLA of green leaves drops at the end of the growing season when reallocation starts to occur. Research on SLA of individual leaves might improve the insight in the dynamics of SLA over the season.

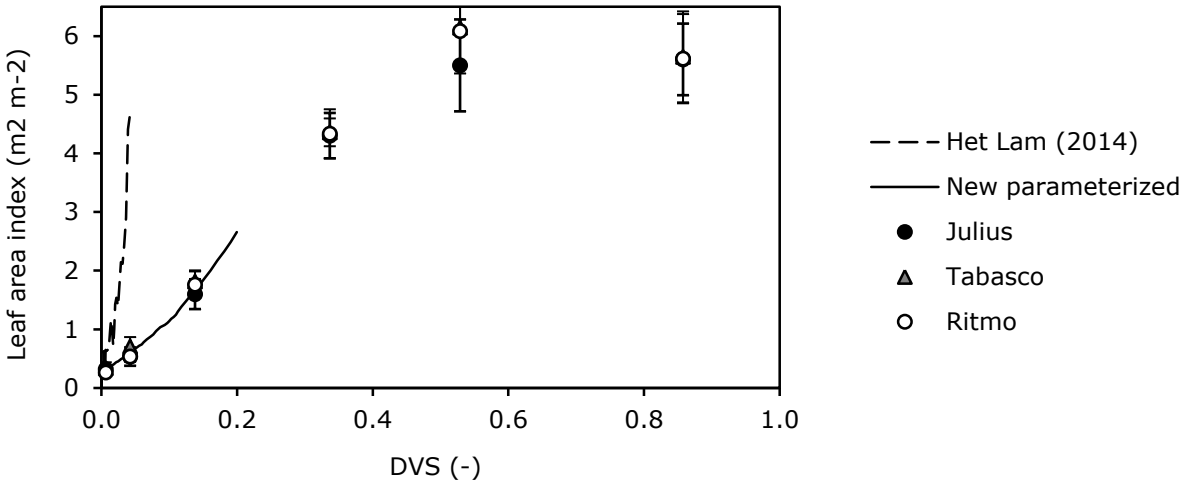

Figure 4.9. The points show the observed leaf area index for the three varieties. The three observations with DVS < 0.2 have all the same N application, the three observations with DVS > 0.2 are average values of all N applications. The dotted line shows the increase of LAI as it was calculated with the relative growth rate of the leaves (r_l = 0.015) of Het Lam (2014). The full line shows the calibrated relative growth rate for Julius, Tabasco and Ritmo (r_l = 0.0061). From the three observations with DVS < 0.2 can be seen that the exponential phase is only valid in the beginning of the growth (until DVS = 0.2), since the full line would overestimate the LAI at DVS > 0.2.

Relative growth rate of leaves

Figure 4.9 shows that the original r_l overestimated the observed LAI. Furthermore it can be seen from the figure that the error bars of the observations overlap. So there was no significant difference between varieties at these observation dates. Het Lam (2014) assumed exponential growth as long as DVS < $DVS_{exp\text{-}leaf\ growth}$ and the LAI < $LAI_{exp\text{-}leaf\ growth}$. From Figure 4.9 can be seen that the exponential growth phase was valid until LAI = 2.0 and DVS = 0.2. So $DVS_{exp\text{-}leaf\ growth}$ = 0.2 (also found by Het Lam (2014) and $LAI_{exp\text{-}leaf\ growth}$ = 2.0 (Het Lam (2014) found a value of 0.6). This means that exponential growth occurs for the first three observation dates.

The higher value for $LAI_{exp\text{-}leaf\ growth}$ found in this study cannot be explained by genetic improvement of varieties. Ritmo is not significantly different from Julius and Tabasco. If the higher value for $LAI_{exp\text{-}leaf\ growth}$ results from change of climate or change of management is unknown.

Table 4.2 shows the relative growth rates for the three varieties. The calculation of the relative growth rate is based on the LAI at February 18 (t1) and the LAI at March 10 (t2). The first three columns show the relative growth rate for Julius, Ritmo and Tabasco when the average LAI is taken. The middle three columns show the relative growth rates when the lowest observed LAI at February 18 and the highest LAI at March 10 is taken, and the right three columns show the relative growth rates when the highest observed LAI at February 18 and the lowest LAI at March 10 is taken. These columns give an indication of the spread in the data, and how r_l is affected by this.

Based on the calculated relative growth rates from Table 4.2, and visual optimization with an XY scatter in Excel, a relative growth rate is obtained of 0.0061 d^{-1}. The LAI_{ini} is parameterized as 0.026 $m^2\ m^{-2}$.

Leaf area index and shading

The leaf area index is affecting the shading of higher leaves on lower leaves. The critical value (LAI_{cr}) above which leaves start to senesce was originally 4 $m^2\ m^{-2}$. From the new dataset there was no evidence that this value was not correct, so this value is retained.

Table 4.2. Relative growth rates for Julius, Ritmo and Tabasco. The columns with LAI_{t1} min – LAI_{t2} max, and LAI_{t1} max – LAI_{t2} min give an indication of the variance of the relative growth rates. *a* and *b* are parameters of the exponential trendline (see Equation 29).

	Average			LAI_{t1} min – LAI_{t2} max			LAI_{t1} max – LAI_{t2} min		
	Julius	Ritmo	Tabasco	Julius	Ritmo	Tabasco	Julius	Ritmo	Tabasco
LAI_{t1}	0.32	0.26	0.33	0.25	0.27	0.22	0.48	0.41	0.34
LAI_{t2}	0.53	0.53	0.71	0.89	0.74	0.68	0.38	0.11	0.36
a	0.3092	0.2526	0.3213	0.2389	0.2582	0.2082	0.4887	0.4337	0.3378
b	0.0259	0.0356	0.0375	0.0625	0.0501	0.0563	-0.0123	-0.0640	0.0024
r_l	0.0043	0.0059	0.0062	0.0103	0.0082	0.0093	-0.0020	-0.0105	0.0004

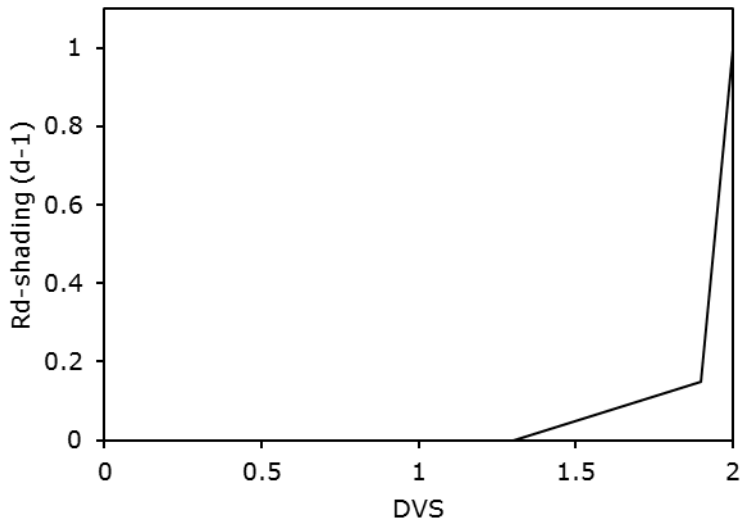

Figure 4.11. The relative death rate due to ageing of the crop ($r_{d\text{-}ageing}$) in relation with the developmental stage (DVS).

Relative death rate of leaf sheaths

The relative death rate of leaves (r_d) was based on either the effect of shading of the leaves on each other or the effect of ageing of the crop (i.e. a temperature larger than $T_{sum\text{-}ageing}$). From the simulation with the parameters of Het Lam (2014), it appeared that senescence of green leaves happened too fast in the growing season. So $r_{d\text{-}ageing}$ was reduced from 0.030 to 0.0009 d^{-1}. This is the death rate for the part of the LAI that is larger than LAI_{cr} (Equation 23).

The senescence of green leaves due to ageing also did not match the observations. In LINTUL1 ageing of leaves is determined by a relative death rate related to the daily average temperature. Based on this relation, it was not possible to do simulations where all the leaves died off (LAI = 0), while this is usually observed in field situations. Therefore, the relative death rate has been defined in a new way based on the developmental stage of the crop instead of the daily average temperature. From DVS = 1.3 onwards senescence of leaves starts due to ageing until DVS = 1.9. At DVS = 1.9, $r_{d\text{-}ageing}$ = 0.15 d^{-1}, at DVS = 2.0, $r_{d\text{-}ageing}$ = 1.0 d^{-1} (Figure 4.11).

With this new function, it is made sure that all the leaves have died at the end of the growing season. Therefore, also the production of new dry matter stops at the end of the growing season. This gave an improved fit with the observations.

Dry matter production

Extinction coefficient

The extinction coefficients found ranged between 0.54 and 0.60 (Figure 4.12). On average this was lower than the *k* value found by Het Lam (2014). Especially for the observations in Figure 4.12 with

LAI > 5 a large variance is present. This is because the ratio between light reaching the soil surface and the incident radiation at LAI > 5 differed about 4%. The relatively high values for the R^2 suggest a good fit of the trendline with the observations, but if the data from the last two observation dates are left out of the fit of the trendline (May 26 and June 12), then the *k* values lie in the range of 0.47 till 0.54. The variance in the observations for LAI > 5 may result from the presence of dead leaves during the measurements with the AccuPAR. This increases the $-\ln(I/I_0)$ while the LAI is based only on the green leaves. This results in an overestimation of the extinction coefficient.

For a next study it is recommended to do more measurements on light interception, especially when LAI < 5 in order to estimate *k* based on more observations over a wider range of LAI. Therefore, it is also recommended to do more crop samplings when LAI < 5, since the LAI is needed together with the light interception data to estimate *k*.

For the simulations in this study, an extinction coefficient of 0.6 is used. For Julius, this value was also obtained (Figure 4.12) and it corresponds with earlier findings of Het Lam (2014).

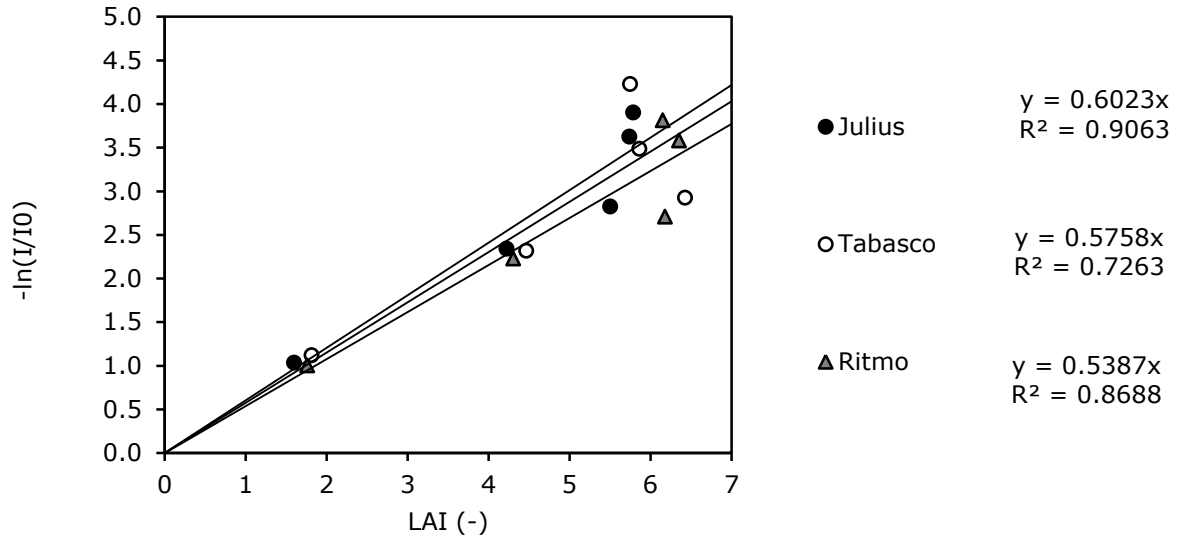

Figure 4.12. Determination of the extinction coefficient for the 3 varieties with the highest nitrogen application.

Amount of PAR in global radiation

Based on the measurement of incoming PAR and incoming global shortwave radiation for the period of March 1 till June 15, a value for c_{PAR} was calculated as 0.446. After June 15, no valid data on incoming PAR was available. Also the obtained data in the period between March 1 and June 15 had some errors. Some birds used the radiation sensors of the meteorological station to leave their droppings, which probably led to an underestimation of the incoming radiation. The sensors were cleaned frequently, but part of the variance in Figure 4.13 may be explained by the bird droppings. The crosses in Figure 4.13 are not included in the fit of the trendline. In that case, the ratio between PAR and global shortwave radiation was 0.4594. Therefore c_{PAR} is estimated as 0.46. This value is used in the simulations.

The usually used value of 0.50 is overestimating the amount of PAR in this study with about 10%. The effect of this on a simulation with the model is not quantified, but it is clear that a too high value for c_{PAR} results in an overestimation of crop growth. It was observed that the amount of radiation in the growing season 2013-2014 was higher than in an average season. It was also visually observed that there were more days than average with direct sunlight. It is known that the amount of PAR is lower in direct sunlight than in diffuse sunlight (Sinclair and Muchow, 1999). This can explain the lower value for c_{PAR}. It is recommended to be cautious when using global shortwave radiation to estimate the amount of incoming PAR.

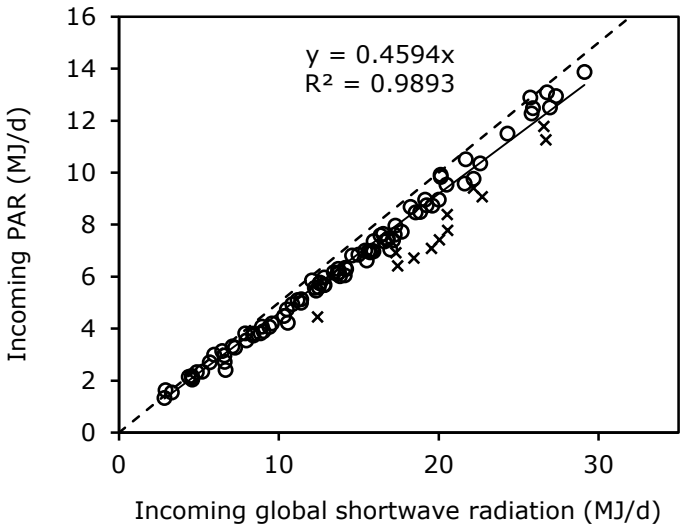

Figure 4.13. The incoming global shortwave radiation and the incoming PAR at the trial field measured with the meteorological station in the period from March 1 till June 15. The full line is the trendline through the data, the dashed line is the line if the conversion from incoming global shortwave radiation (DTR) to photosynthetic active radiation (PAR) was exactly 0.5 MJ PAR per MJ DTR.

Radiation use efficiency

The radiation use efficiency was calculated for the above-ground dry matter. Based on the intercepted PAR and only the above-ground dry matter produced, the RUE was estimated as 3.20 g DM MJ^{-1} for Julius with the highest nitrogen application (Figure 4.14). This was slightly lower than the RUE of Ritmo, but this difference was not significant. Despite this higher RUE, the lower yield of Ritmo can be explained by the smaller LAI with as consequence a lower total amount of intercepted PAR.

The trendlines in Figure 4.14 do not go through the origin because the observations shown are from March 31 till June 12. At March 31, there was of course already some dry matter. Since no observations were done on light interception before March 31, it was not possible to calculate a RUE before this date. The obtained RUE might deviate from the real RUE before March 31. Different studies show that the RUE can be lower during early growth stages because of suboptimal temperatures (Garcia *et al.*, 1988; Sinclair and Muchow, 1999). It is likely that this is also the case for winter wheat in the Netherlands. Het Lam (2014) also included a correction function in the model where the RUE was

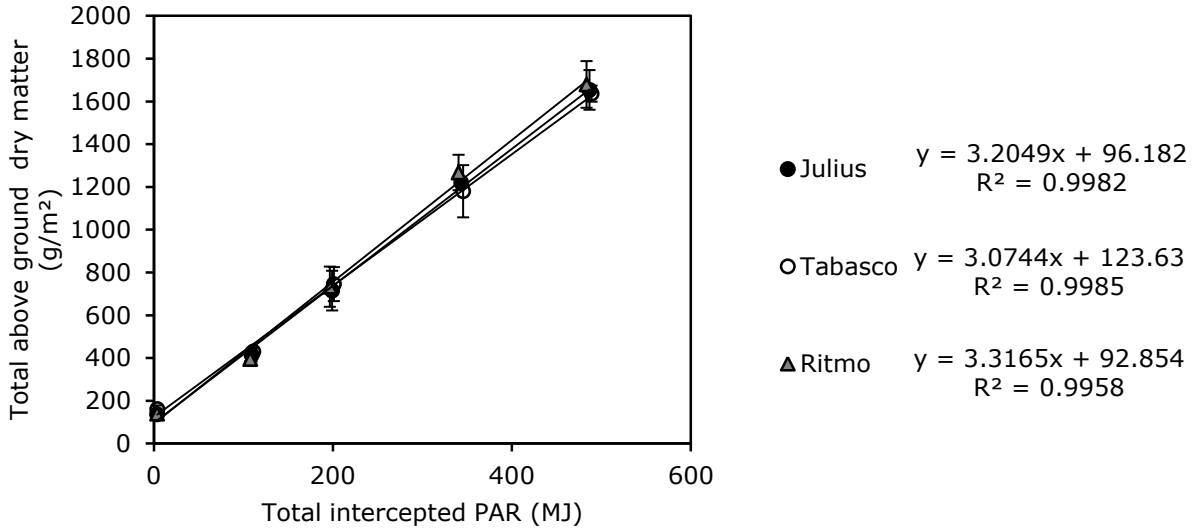

Figure 4.14. The total above-ground dry matter as function of the accumulated intercepted photosynthetic radiation (PAR) for the period from March 31 till June 12. The observations shown concern the highest nitrogen application (N3, 300 kg N ha^{-1}).

multiplied with 1 at a day temperature of 12 degrees Celsius and with 0 at a day temperature of 0 degrees Celsius. The day temperature (T_{day}) is calculated as:

$$T_{day} = T_{max} - 0.25 \times (T_{max} - T_{min}) \quad (40)$$

where T_{max} is the daily maximum temperature and T_{min} is the daily minimum temperature.

This correction function was slightly changed. For the period between emergence and March 31, the RUE was estimated. This is done as follows: the amount of total above ground dry matter at March 31 is known. The total amount of PAR intercepted is calculated by the model and depends on the LAI and the incident PAR. The increase of LAI of the crop was simulated exponentially until April 7. Therefore, the amount of LAI present was not related to the amount of dry matter produced in the simulation. The RUE for the period between emergence and March 31 was calculated as the observed amount of above ground dry matter divided by the simulated amount of intercepted PAR. This gave a RUE of 1.66 g DM per MJ PAR.

In order to obtain this RUE in the model, the temperature correction function was changed. The RUE is multiplied with 0 at 1.5 degrees Celsius. The correction factor is linearly interpolated between the temperatures 1.5 and 8.11 degrees Celsius. 8.11 degrees Celsius was the average day temperature in the period between emergence and March 31. At a temperature of 8.11 degrees Celsius, the RUE is multiplied with a correction factor of 0.52. With this correction factor, the RUE is 1.66 at a day temperature of 8.11 degrees Celsius.

4.3 Dry matter (re)allocation functions

Initial conditions

The initial conditions apply to the first time step after emergence of the crop. The initial dry weight of the green leaves has been adapted from 0.10 g m^{-2} to 0.55 g m^{-2}. This adaptation was a consequence of the changed LAI_{ini} (section 4.2 – Relative growth rate of leaves) to retain a reasonable initial SLA value (SLA = LAI / W_{lvg}). Other initial values have not been changed and are set as follows: $W_{stems\text{-}ini}$ = 0.05 g m^{-2}, $W_{ears\text{-}ini}$ = 0.00 g m^{-2}, and $W_{grains\text{-}ini}$ = 0.00 g m^{-2}.

No measurements were done on the dry weights of the different plant organs immediately after emergence. All the observations at the first sampling at February 18 together had an average dry weight of the green leaves of 12.4 g m^{-2} and of the stems of 8.0 g m^{-2}. This was already about 20 and 160 times higher, respectively than the initial conditions. Actually, the initial conditions are chosen in such way that the model performs good estimations for the later growth. It is difficult to parameterize the initial conditions based on observations because of the very small amount of dry matter.

Dry matter allocation

The partitioning table obtained for the variety Julius with highest nitrogen application is shown in Appendix IX. Figure 4.15 shows the allocation factors graphically. The first crop sampling was at February 18 with DVS = 0.01. The second crop sampling was at March 10 with DVS = 0.04. The calculated allocation fractions between these two dates are assumed to be representative for the allocation of assimilates in the period between sowing and February 18.

Between July 16 and July 28 a decrease of 15.6 g m^{-2} was observed. This decrease was neglected and set at 0. So it was assumed that the dry weight of the organs did not change anymore after July 16, and therefore also the allocation fractions did not change anymore. This assumption was done because the standard deviation of the crop sampling at July 28 was larger than the decrease in weight compared to July 16. So the decrease in weight was not significant.

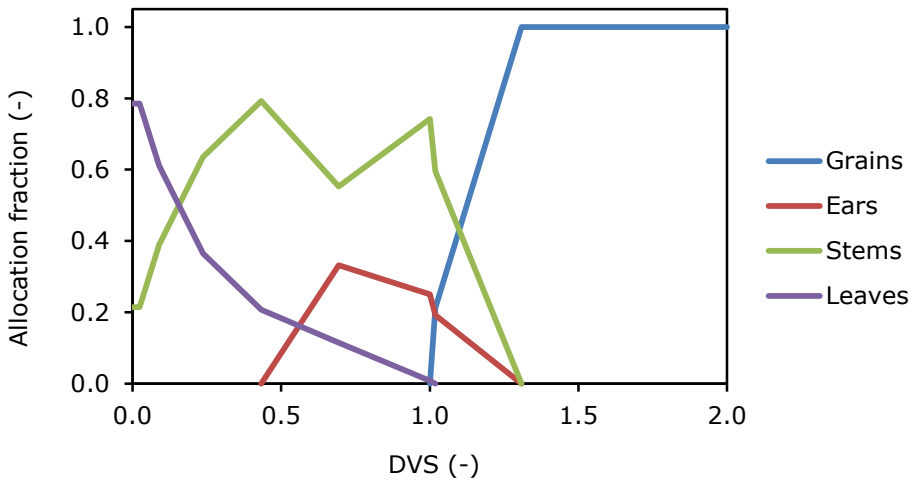

Figure 4.15. The allocation fractions based on data from Julius with the highest nitrogen application.

Figure 4.15 shows the allocation factors to the different above-ground plant organs. Roots are not included because no observations have been done on the roots. The sum of all the allocation factors are 1 for each DVS. From the figure it can be seen that allocation to the grains starts after anthesis (DVS = 1) with the new allocation factors. Furthermore the ears are added as plant organ.

The amount of dead leaves was very small until the developmental stage of 0.5 (Figure VIII.4). Therefore, it was considered to be zero, because of the relatively large fluctuations in the data, Especially in the first samplings, the amount of dead leaves was very difficult to assess, since the dead leaves were laying on the soil surface and were hard to collect. This soil surface was moist and clayey, so it is likely that clay sticked to the dead leaves and influenced the weight significantly. In addition, the amounts of dead leaves were very small and it was hardly possible to do good measurements on the weight, because of this small weight. The assumption that there were no dead leaves until DVS 0.5 is made only for the determination of the allocation fractions. The amount of dead leaves was used for the determination of the radiation use efficiency for the production of above ground dry matter.

The amount of grains was not measured at June 12 because the grains could not be separated from the ear. However, the DVS was already 1.18 at this date, so the amount of grains present at this moment was estimated at 120 g m^{-2}. This was based on the weight of the ear including the grains at June 12 and on the weight of only the ear at June 30. It was assumed that the weight of the ear had decreased a bit because of reallocation between June 12 and June 30. The value for the grain weight was used to obtain the allocation fraction to the grains.

Dry matter reallocation

For Julius with the highest nitrogen application, the reallocation fractions are shown in Table 4.3. These reallocation functions are implemented in the model. Reallocation from the ears to the grains has been introduced because a decrease in dry weight of the ear was observed. Furthermore, reallocation to the grains starts after flowering (DVS = 1), so the simulation of reallocation is now more in agreement with reality.

Table 4.3. Reallocation fractions for different plant organs of Julius with the highest nitrogen application.

DVS	Ears	Stems	Leaves
-	d^{-1}	d^{-1}	d^{-1}
0.00	0	0	0
0.69	0	0	0
1.00	0	0	0
1.02	0	0	0.00543
1.31	0.00448	0.00781	0.00352
1.57	0.00419	0.01042	0.01808
1.81	0.00508	0.00325	0.01411
2.00	0.00508	0.00325	0.01411

4.4 Model performance

Fit with dataset for parameterization

The following figures with the progress of the dry matter of each separate plant organ are obtained by the simulation with the allocation factors from Figure 4.15, for the model as parameterized in this work. The simulation is based on parameters described in section 4.2 (See Table VII.1 for the values of each parameter). Also, the fit of the observations used for parameterization (Julius, N3) with the newly parameterized model (Simulation) is shown.

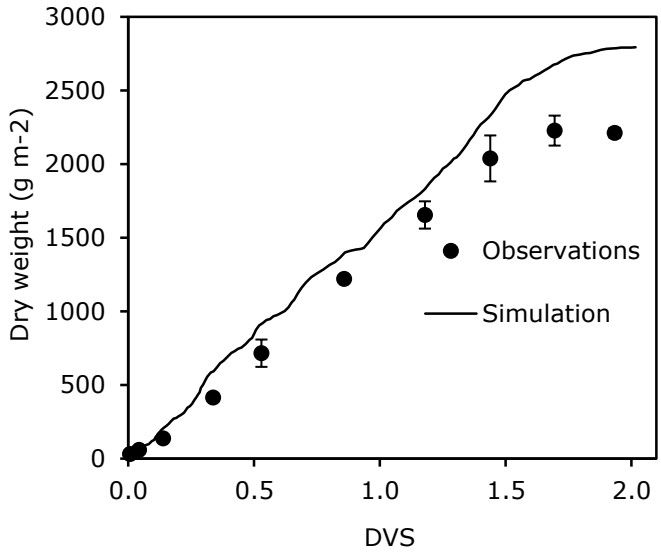

Figure 4.16. The simulated and observed total above ground dry matter based on Julius with the highest nitrogen application.

The simulated amount of total above ground dry matter is larger than the observed amount. The total amount of dry matter results in de simulation from several parameters. The utilization of light for dry matter is described by the RUE. The amount of intercepted light depends on the LAI and the extinction coefficient, the development of LAI depends on the parameters until which exponential growth of leaves occurs, the relative growth rate during exponential conditions and specific leaf area after the exponential growth phase.

Since the overestimation of the total amount of dry matter by the model already occurs before DVS = 0.2, at least one of these parameters is not totally correct. This suggest that the RUE or the r_l are too high during this exponential growth phase. According to me, a too high RUE is the reason of the overestimation of dry matter in the period of DVS < 0.2.

When DVS > 0.2, the increase in LAI is calculated as the SLA multiplied with the amount of dry matter that is allocated to the leaves. Figure 4.17 shows that the LAI is overestimated during the entire growth period. This results in an overestimation of the amount of intercepted PAR, and therefore also of the amount of dry matter produced. An overestimation of produced dry matter leads to too much allocation of dry matter to various organs. In other words, there is a vicious circle.

This vicious circle is a result of the too high LAI after the exponential growth phase. Forcing the model to simulate with a RUE of 1.66 when DVS < 0.2 gave an underestimation of the total dry matter produced of about 35 to 40% (data not shown here). This proofs that the model is very sensitive for changes in the RUE during early growth stages, while the absolute amounts of produced dry matter when DVS < 0.2 is relatively small (about 10% of the total produced above ground dry matter).

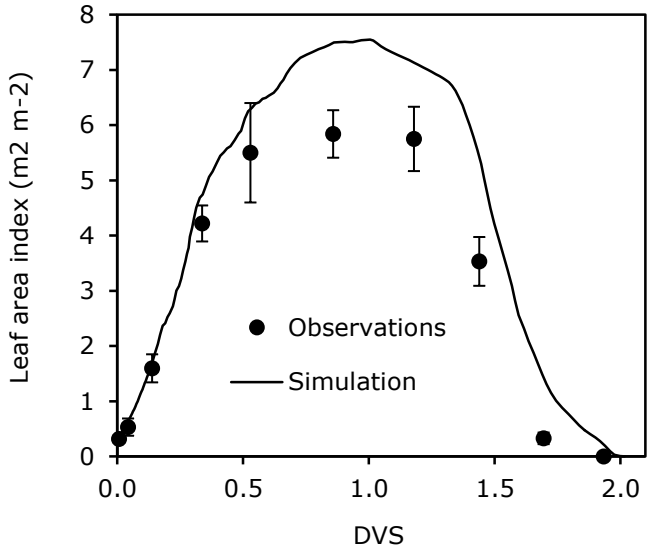

Figure 4.17. The simulated and observed leaf area index based on Julius with the highest nitrogen application.

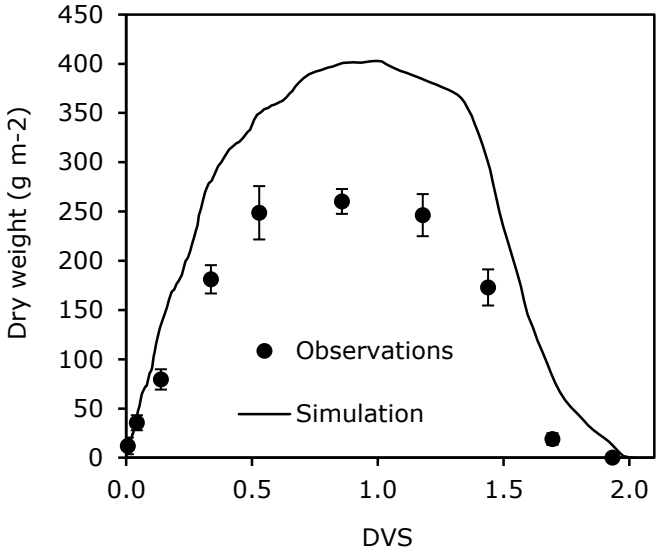

Figure 4.18. The simulated and observed dry matter of green leaves based on Julius with the highest nitrogen application.

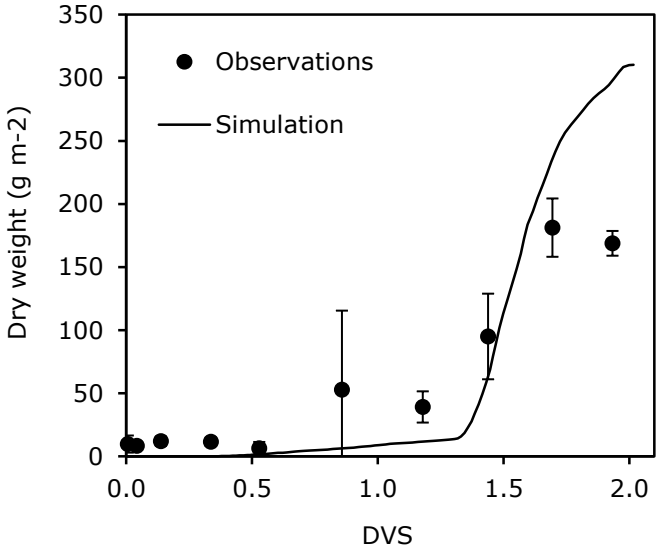

Figure 4.19. The simulated and observed dry matter of dead leaves based on Julius with the highest nitrogen application.

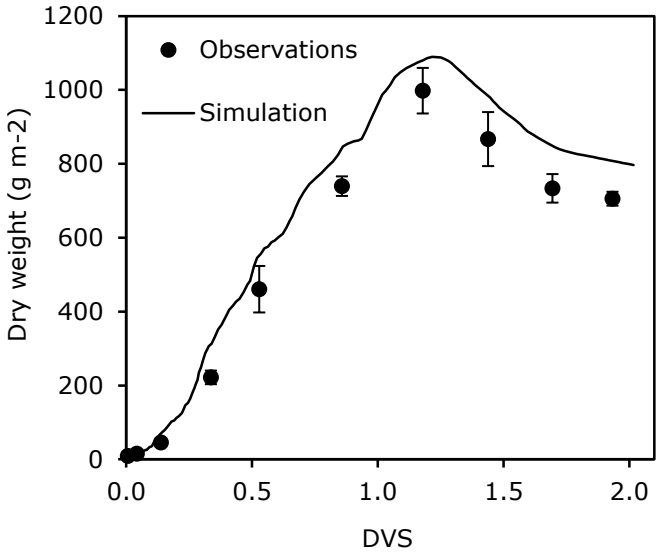

Figure 4.20. The simulated and observed dry matter of stems based on Julius with the highest nitrogen application.

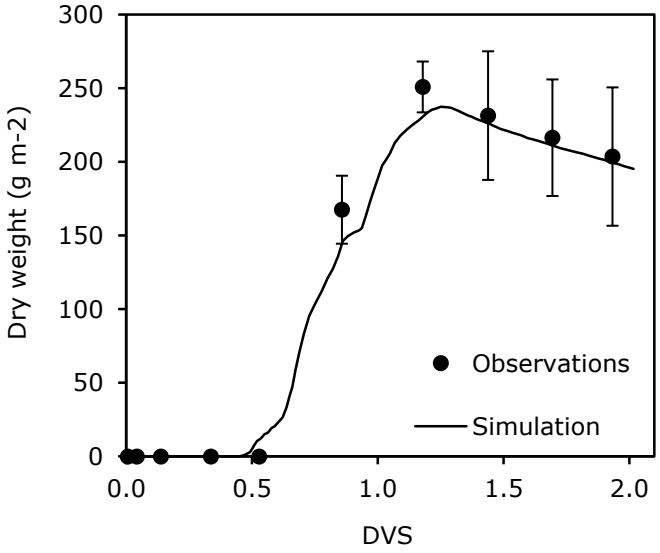

Figure 4.21. The simulated and observed dry matter of ears based on Julius with the highest nitrogen application.

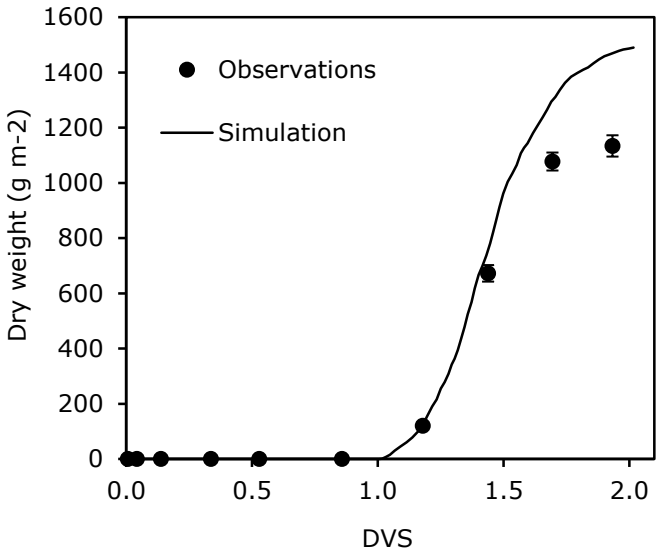

Figure 4.22. The simulated and observed dry matter of grains based on Julius with the highest nitrogen application.

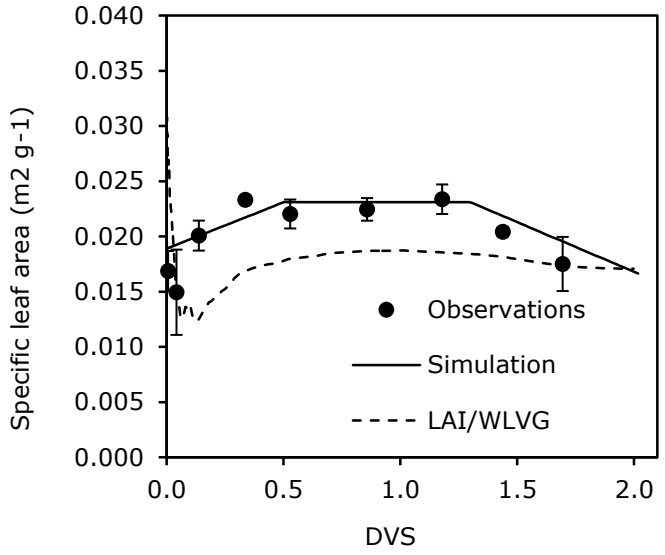

Figure 4.23. The simulated and observed dry specific leaf area based on Julius with the highest nitrogen application.

In the model, the specific leaf area is handled as a forced function. It is given as an input to the model. From Figure 4.23 can be seen that the SLA given as input (indicated by the full line, simulation) differs significantly from the 'true' SLA of the model, namely the LAI divided by the weight of the green leaves (the dashed line). This results from the exponential growth phase of the leaves where growth of LAI is unrelated with the leaf dry matter. In the presented simulation, the green leaf dry matter is higher than observed, while the LAI matches the observed LAI quite good. Therefore, the SLA (LAI/WLVG) is lower than observed. The simulation would improve if the RUE in the exponential growth phase is better described.

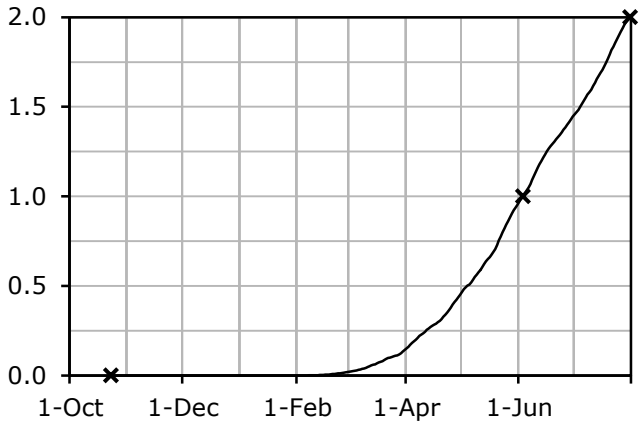

Figure 4.24. The development of the crop over time. The first cross at October 23 indicates the day of sowing, the second cross at June 3 indicates flowering and the third cross at July 31 indicates maturity of the crop.

Soil temperature module

The soil temperature is calculated as a function of the daily average air temperature. This relation is estimated by Zheng *et al.* (1993). Figure 4.25 shows that the correlation between the observed and calculated soil temperature is very low. Therefore, it was tried to improve the soil temperature module. After sowing, the first soil temperature is taken 0.8 times the average air temperature instead of 0 ºC. This improved the correlation between observed and calculated soil temperature (data not shown), but there is still room for improvement. It is recommended to validate the soil temperature module with observations for different soil types if LINTUL1 will be used under different conditions than those from this study.

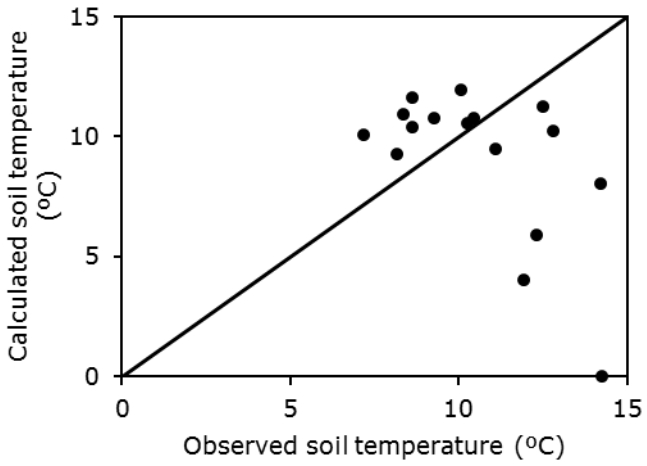

Figure 4.25. The observed soil temperature in the period of October 23, 2013 till November 7, 2013 (data from 'De Veenkampen') against the calculated soil temperature in the same period with the model. The black line is the 1:1 line.

4.5 Interpretation of results

Daily growth of dry matter

The daily growth of dry matter is usually estimated by a rule of thumb of 200 kg dry matter per day per hectare (Sibma, 1968). Whether this rule still holds is checked with the data of the field experiment. Figure 4.28 shows the development of dry matter over the growing season for the highest nitrogen application. The trendlines in Figure 4.28 are plotted through three data points where the LAI was larger than 4. The equations show that the increase of dry matter per day was around 26 g m^{-2} d^{-1}, or 260 kg ha^{-1} d^{-1}. This increase compared to the 200 kg ha^{-1} d^{-1} mentioned earlier could be caused by increase in atmospheric CO_2.

If the effect of the increase of the CO_2 level over the last 30 years on the RUE is evaluated with the CO_2 correction function of Het Lam (2014), then an increase of 11% of the RUE is estimated. This is less than the 30% increase found in this research (200 to 260 is 30% increase). One reason can be the uncertainty of the value of 200 kg DM ha^{-1} d^{-1}.

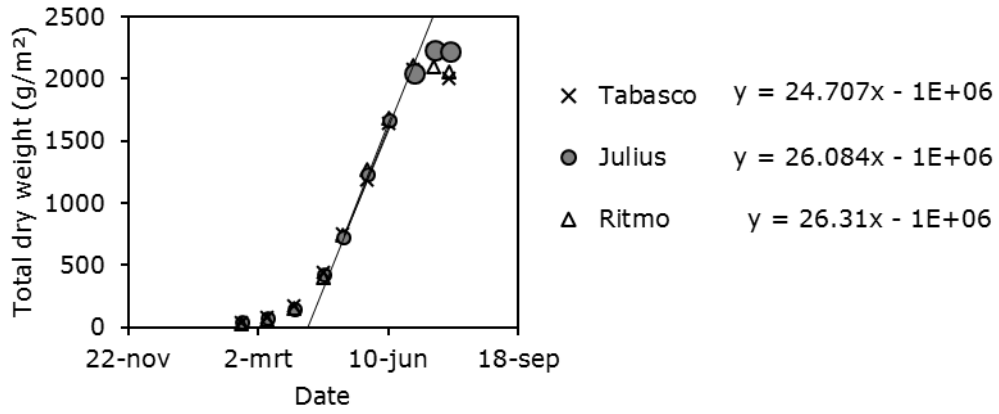

Figure 4.28. The increase of total above-ground dry matter for the three varieties Julius, Tabasco and Ritmo at the highest nitrogen application. The equations next to the variety name in the legend correspond with the adjacent variety. The equations are from the trendlines which are plotted through the observations at May 7, May 26 and June 12 when the LAI was larger than 4. The coefficient besides x in the equation indicate the increase of dry matter in g per square meter per day.

5. Conclusions

The aim of the research was to determine new parameters for LINTUL1 to simulate the potential yield of winter wheat under Dutch conditions. For most of the parameters, this aim has been achieved.

The parameters are based on data from a field trial in 2013-2014, in Wageningen, the Netherlands. The maximum yield was 12.5 Mg ha^{-1} (15% moisture, or 10.6 Mg ha^{-1} dry weight) and was obtained with the variety Julius and a nitrogen level of 300 kg ha^{-1}. The older variety Ritmo had a yield of 11.5 Mg ha^{-1}, and Tabasco had a yield of 12.4 Mg ha^{-1} with a nitrogen gift of 300 kg ha^{-1}. There was a significant difference between the number of ears per square meter, the number of kernel per ear, and the thousand kernel weight. However, these differences did not result in a significant difference between the grain yield of Julius and Tabasco. There might be a trade-off between these crop characteristics.

The length of the temperature sums for development are adjusted to the growing season of 2013-2014. The parameters on vernalization and photoperiod could not be updated since no specific measurements were done on these parameters.

The relative growth rate of the leaves was found to be 0.0061 d^{-1}. No significant difference between varieties was found for this parameter. The RUE was calculated as 3.20 g dry matter per MJ PAR for the whole growing season for Julius with nitrogen application N3. There was no significant difference of the RUE with other varieties.

The SLA was variable over the season but no significant differences between varieties was found. The relative death rate of the leaves has been defined in a new function depending on DVS. At DVS is 2, is the relative death rate 1 d^{-1}, what implies that all leaves have senesced at the end of the growing season. This new function for r_d improved the fit of the observations with the simulation of the model.

The allocation factors appear to be variety dependent, especially for the green leaves. The new varieties (Julius and Tabasco) had a higher LAI than Ritmo and for a longer period, resulting in more light interception and a higher dry weight grain yield.

The aim of this research was to determine new parameters for winter wheat, to simulate the potential yield of winter wheat in the Netherlands with the model LINTUL1. This goals has been achieved in this study. Most parameters are obtained from the variety Julius with a nitrogen application of 300 kg ha^{-1}.

Most of the parameters have not been calculated for the nitrogen applications of 180 and 240 kg ha^{-1}. In addition, most calculations have not been done for the varieties Tabasco and Ritmo because this was not possible in the planning of this thesis research. However, for most parameters methods to describe their calculation are now described. These descriptions themselves can also be regarded as a result of this study. Especially the method to calculate allocation and reallocation fractions for winter wheat.

6. Recommendations

Based on the results, some recommendations are done. The aim was to achieve new parameters for LINTUL1 to simulate the potential yield of winter wheat in the Netherlands. For many developmental parameters, this aim could not be achieved because the design of the experiment did not allow to do observations on these developmental parameters. It was not possible with the obtained dataset to determine parameters for vernalization or the effect of photoperiod on crop development. The difference between varieties on these properties is not considered in this research and parameters are taken from previous research that dates back till the nineteen eighties (Weir *et al.*, 1984). It is unknown how current varieties respond at vernalization and if they are still photoperiod sensitive. Due to a changing climate, temperatures during might increase with certainly some effect on vernalization. Therefore, it is recommended to conduct research on these processes in order to obtain renewed quantitative insight in these processes.

For the parameters that have been determined, are also some recommendations done. The RUE seemed to be changing over the growing season. These changes are not explained in this report and further research on the fluctuations of RUE of modern varieties is needed. Sinclair and Muchow (1999) report that seasonal variations of RUE might occur due to differences in photosynthetic capacity between leaves. Especially during winter the RUE values seemed to be lower than during spring and summer. It seems likely that this reduced RUE results from lower temperatures, but more research is needed to quantify this relationship between RUE and temperature. RUE is temperature dependent since the utilization of light is a process regulated by enzymes, diffusion, and many other biochemical mechanisms. All these mechanisms have their own ideal optimal circumstances. It would be good to obtain more insight in the quantitative contribution of these processes for the RUE, since the RUE is a very important parameter for the model. More fundamental research on these individual processes is also useful, but not directly implementable in LINTUL1 since no parameters are determined by such individual processes.

During the execution of the trial in 2013-2014, there was drought in spring. The measurements on water availability did not indicate water limitation, but it might have been that nutrients were not available to the crop because of a dry nutrient rich top layer (first 30 cm), while water was available in deeper layers. Regular chemical analyses or the use of signal plants could decrease the risk for nutrient deficiencies in the crop.

The specific leaf area varied over the growing season. The driving factors behind this variation are not clearly understood. One factor might be transpiration. With little transpiration less leaf area is needed, then under hot conditions with a lot of transpiration. This can explain the increase in SLA from winter till the start of June. However, this does not explain the drop of SLA at the end of the growing season. The relationship of SLA with LAI was empirically shown, but if there is a causal relation is

unclear. More research on SLA is useful since it is an important parameters as conversion factor from dry weight to leaf area.

Pay attention to the measurements of the light interception. The extinction coefficient is difficult to determine when too few measurements are done for the light interception. In this research, only measurements were done around the date of crop sampling, while it would be useful to have more observations. The observations are now to less distributed over the X-axis, especially for LAIs in between the observation dates when the LAI is still increasing, so for LAI < 4.

For crop growth simulations, weather data is necessary. If PAR data is not directly available from a meteorological station, then it is recommended to be cautious in the conversion of global shortwave radiation to PAR. LINTUL is very sensitive to over- or underestimations of the PAR level. This will lead to deviations between the observations and simulations. In this study, the conversion of global shortwave radiation to PAR was a factor 0.46 and not 0.50, which is usually assumed.

The developmental parameters related to the thermal sums, vernalization and photoperiod could not be parameterized based on the obtained dataset. Developmental data from several seasons is needed to make good estimates of the thermal sums. To obtain parameters related to vernalization and photoperiod, different experimental set-ups are needed than the one used in this research. For example day length or air temperature cannot be varied in an outdoor experiment. To obtain developmental parameters, growth chamber experiments are better suited.

Since the parameters are not calculated for Tabasco and Ritmo and for N1 and N2, it is not possible to make a comparison between these parameters. Nevertheless, it is recommended that these calculations are done in order to obtain even more information from the conducted experiment.

It is recommended that a sensitivity analysis is done on the obtained parameters in this study. This will give insight in the reliability of the obtained values. Furthermore, one can decide on which measurements should be focused during the experimental work if a similar field experiment is conducted again.

7. References

Andersen MN, Munkholm LJ, Nielsen AL. 2013. Soil compaction limits root development, radiation-use efficiency and yield of three winter wheat (triticum aestivum l.) cultivars. *Acta Agriculturae Scandinavica, Section B - Soil & Plant Science* **63**: 409-419.

Asseng S, Foster IAN, Turner NC. 2011. The impact of temperature variability on wheat yields. *Global Change Biology* **17**: 997-1012.

Boerenbusiness (2013). "Combines oogsten nog vochtige tarwe." Retrieved August 24, 2014, from http://www.boerenbusiness.nl/artikel/item/10832731/Combines-oogsten-nog-vochtige-tarwe.

Centraal Bureau voor de Statistiek. Landbouw; vanaf 1851. Den Haag, 2014.

Chen DX, Coughenour MB, Eberts D, Thullen JS. 1994. Interactive effects of co2 enrichment and temperature on the growth of dioecious *hydrilla verticillata*. *Environmental and Experimental Botany* **34**: 345-353.

Cure JD, Acock B. 1986. Crop responses to carbon dioxide doubling: A literature survey. *Agricultural and Forest Meteorology* **38**: 127-145.

Decagon Devices I. Accupar par/lai ceptometer model lp-80. Pullman, 2013.

Ebskamp AGM, Bonthuis H, Van Huet SM. 1994. *70e rassenlijst voor landbouwgewassen 1995*. Wageningen: Centrum voor Plantenveredelings- en Reproducktieonderzoek (CPRO-DLO).

ESRL NOAA. Atmospheric co_2 at mauna loa observatory, 1960-2014.

Evans LT. 1987. Short day induction of inflorescence initiation in some winter wheat varieties. *Functional Plant Biology* **14**: 277-286.

Fangmeier A, De Temmerman L, Mortensen L, Kemp K, Burke J, Mitchell R, Van Oijen M, Weigel HJ. 1999. Effects on nutrients and on grain quality in spring wheat crops grown under elevated co2 concentrations and stress conditions in the european, multiple-site experiment 'espace-wheat'. *European Journal of Agronomy* **10**: 215-229.

Garcia, R., Kanemasu, E. T., Blad, B. L., Bauer, A., Hatfield, J. L., Major, D. J., Reginato, R.J. & Hubbard, K. G. 1988. Interception and use efficiency of light in winter wheat under different nitrogen regimes. *Agricultural and Forest Meteorology*, **44(2)**: 175-186.

González JA, Calbó J. 2002. Modelled and measured ratio of par to global radiation under cloudless skies. *Agricultural and Forest Meteorology* **110**: 319-325.

Goudriaan J. 1988. The bare bones of leaf-angle distribution in radiation models for canopy photosynthesis and energy exchange. *Agricultural and Forest Meteorology* **43**: 155-169.

Goudriaan J, van Laar HH. 1994. *Modelling potential crop growth processes : Textbook with exercises*. Dordrecht [etc.]: Kluwer.

Groot JJR, Verberne ELJ. 1991. Response of wheat to nitrogen-fertilization, a data set to validate simulation-models for nitrogen dynamics in crop and soil. *Fertilizer Research* **27**: 349-383.

Het Lam A. 2014. *The impact of climate and co_2 on potential winter wheat yields in the netherlands from 1981 to 2010*: Wageningen University.

Hotsonyame GK, Hunt LA. 1998. Seeding date, photoperiod and nitrogen effects on specific leaf area of field-grown wheat. *Canadian journal of plant science* **78**: 51-61.

KNMI (2013). "Klimaatverandering: De feiten op een rij." Retrieved 15-10, 2014, from http://www.knmi.nl/klimaat/klimaatverandering/deel11.html#wolken.

Koninklijk Nederlands Meteorologisch Instituut. Average daily temperature in the nederlands (in degree celsius). De Bilt, 2014.

Kropff MJ, Van Laar HH. Oryza1: An ecophysiological model for irrigated rice production. In: *SARP Research Proceedings*, edited by Matthews RB. Wageningen, 1994.

Large EC. 1954. Growth stages in cereals: Illustrations of the feekes scale. *Plant Pathology* **3**: 128-129.

LI-COR i. Li-3100c area meter: Instruction manual. Lincoln, 2004.

Meteorology and Air Quality Group. Weather data 'de veenkampen'. Wageningen, 2012-2014.

Monteith JL. 1977. Climate and the efficiency of crop production in britain. *Philosophical Transactions of the Royal Society of Londen B, Biological Sciences* **281**: 277-294.

Payne RW. A guide to anova and design in genstat (15^{th} edition). Hemel Hempstead: VSN International, 2012.

Payne RW, Welham S, Harding S. A guide to reml in genstat. Hertfordshire: VSN International, 2007.

Peltonen-Sainio P, Jauhiainen L, Laurila IP. 2009. Cereal yield trends in northern european conditions: Changes in yield potential and its realisation. *Field Crops Research* **110**: 85-90.

PPO. Praktijkonderzoek plant & omgeving: Rassenbulletin Wintertarwe 2013, 2013.

Rabbinge R. 1993. The ecological background of food production. *Ciba Foundation Symposia* **177**: 2-29.

Rappoldt C, Van Kraalingen DWG. The fortran simulation translator 4.12. Plotting, sensitivity analysis, events and measured variables. In: *EcoCurves rapport 16*. Wageningen: EcoCurves BV, 2013.

Ratjen AM, Kage H. 2013. Is mutual shading a decisive factor for differences in overall canopy specific leaf area of winter wheat crops? *Field Crops Research* **149**: 338-346.

Rechterveld t (2013). "Tarweoogst 22/08/2013." Retrieved September 24, 2014, from http://www.boerderijwinkelrechterveld.nl/fotoboek/category/11-tarweoogst.html.

Rijk HCA, Van Ittersum MK, Withagen J. 2013. Genetic progress in dutch crop yields. *Field Crops Research* **149**: 262-268.

Rogers HH, Runion GB, Krupa SV. 1994. Plant responses to atmospheric co2 enrichment with emphasis on roots and the rhizosphere. *Environmental Pollution* **83**: 155-189.

Salomons J (2013). "Aarfusarium wintertarwe. ." Retrieved September 24, 2014, from http://www.kennisakker.nl/actueel/kennistekst/aarfusarium-wintertarwe

Sibma, L. 1968. Growth of closed green crop surfaces in the Netherlands (No. 368). [sn].

Sinclair TR, Muchow RC. 1999. Radiation use efficiency. *Advances in agronomy* **65**: 215-265.
Spitters CJT, Schapendonk AHCM. 1990. Evaluation of breeding strategies for drought tolerance in potato by means of crop growth simulation. *Plant and Soil* **123**: 193-203.
Van Bussel LGJ, Ewert F, Leffelaar PA. 2011. Effects of data aggregation on simulations of crop phenology. *Agriculture, Ecosystems & Environment* **142**: 75-84.
Van Ittersum MK, Cassman KG, Grassini P, Wolf J, Tittonell PA, Hochman Z. 2013. Yield gap analysis with local to global relevance—a review. *Field Crops Research* **143**: 4-17.
Van Oijen M., Leffelaar, P.A., 2008. Chapter 10(a): Lintul-1: Potential crop growth. In: *Crop ecology 2010*, edited by Leffelaar PA. Wageningen.
Van Oijen M. , Leffelaar, P.A., 2011. Chapter 10(b): Lintul-2: Water limited crop growth. In: *Crop ecology 2011*, edited by Leffelaar PA. Wageningen: Wageningen University.
Velds CA, Van der Hoeven PCT, Koopstra JM, Raaff WR, Slob WH. Zonnestraling in nederland: Koninklijk Nederlands Meteorologisch Instituut, 1992.
Vlamings (2013). "Elke week een nieuwe actuele tip voor akkerbouw/vollogrond/veehouderij." Retrieved September 24, 2014, from http://vlamings.nl/Admin/Nieuws/tabid/229/articleType/ArticleView/articleId/352/Elke-week-een-nieuwe-actuele-tip-voor-akkerbouwvollegrondveehouderij.aspx.
Weir AH, Bragg PL, Porter JR, Rayner JH. 1984. A winter wheat crop simulation model without water or nutrient limitations. *The Journal of Agricultural Science* **102**: 371-382
M373 - 310.1017/S0021859600042702.
Wild M. 2009. Global dimming and brightening: A review. *Journal of Geophysical Research: Atmospheres* **114**: D00D16.
www.harrysfarm.nl (2013). "Verloop gewasgroei wintertarwe 2013." Retrieved September 24, 2014, from http://www.harrysfarm.nl/index.php/groei/wintertarwe-2013.
Zheng D, Hunt Jr ER, Running SW. 1993. A daily soil temperature model based on air temperature and precipitation for continental applications. *Climate Research* **2**: 183-191.

Appendix I – Potential yield of winter wheat

Based on winter wheat LAI data of Groot and Verberne (1991) and photosynthetic active radiation (PAR) data from De Veenkampen in 2014 a first estimate of the potential winter wheat yield in the Netherlands is performed. The aim was to show how leaf area development was in the eighties, and what the potential yield of winter wheat would be under the climatic conditions of 2014.

The LAI is interpolated between the data given by Groot and Verberne (1991) as shown in Table I.1. ΔLAI is calculated as:

$$\Delta LAI = \frac{LAI_t - LAI_{t-1}}{DOY_t - DOY_{t-1}} \quad \text{(I.1)}$$

Table I.1. Calculation of the leaf area index (LAI) for each day of the year (DOY) based on data of Groot and Verberne (1984).

Date	DOY	LAI	ΔLAI
		$m^2\ m^{-2}$	d^{-1}
01-01-1984	1	0.0	
13-02-1984	44	0.1	0.002
12-03-1984	72	0.1	0.000
02-04-1984	93	0.1	0.000
24-04-1984	115	0.8	0.032
07-05-1984	128	2.2	0.108
28-05-1984	149	3.5	0.062
18-06-1984	170	4.0	0.024
02-07-1984	184	3.2	– 0.057
16-07-1984	198	3.0	– 0.014
06-08-1984	219	1.7	– 0.062
21-08-1984	234	0.0	– 0.113

Appendix II – Trial Plan

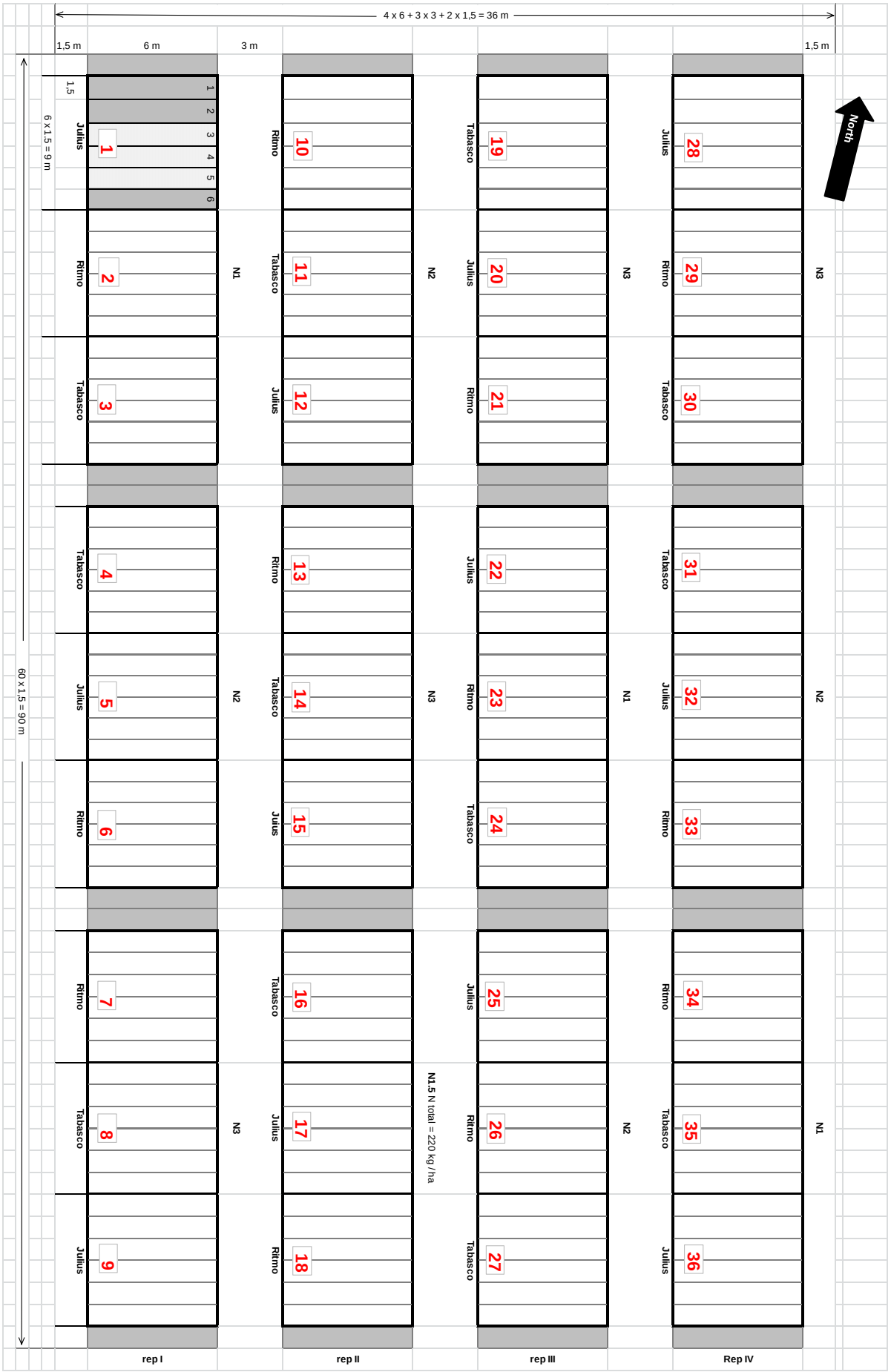

Appendix III – Soil Report

BEMESTINGSWIJZER
Akker-/tuinbouw
HW 06

BLGG AGROXPERTUS

Postbus 170
NL - 6700 AD Wageningen

T monstername: Herman Dorresteijn: 0652002114
T klantenservice: +31 (0)88 876 1010
E klantenservice@blgg.agroxpertus.nl
I blgg.agroxpertus.nl

Uw klantnummer: 2211378

Unifarm De Haaff
Vollegrond
Bornsestg 48
6708 PE WAGENINGEN

Onderzoek	Onderzoek-/ordernr:	Datum monstername:	Datum verslag:	Subsidieverlener:
	611081/003245611	04-12-2013	12-12-2013	BLGG AgroXpertus, Kortingsregeling
	WUR 702260			Postbus 170, 6700 AD WAGENINGEN

Resultaat		Eenheid	Resultaat	Gem.*	Streeftraject	laag	vrij laag	goed	vrij hoog	hoog
hoofdelement										
	N-totale bodemvoorraad	mg N/kg	2360							
	C/N-ratio		8	10	13 - 17					
	N-leverend vermogen	kg N/ha	137	138	93 - 147					
	S-totale bodemvoorraad	mg S/kg	340							
	C/S-ratio		55		50 - 75					
	S-leverend vermogen	kg S/ha	17	22	20 - 30					
	P plant beschikbaar	mg P/kg	1,6	1,9	1,1 - 2,1					
	P-bodemvoorraad (P-Al)	mg P_2O_5/100 g	68	40	24 - 37					
	P-buffering		43		17 - 27					
	Pw	mg P_2O_5/l	60							
	K plant beschikbaar	mg K/kg	61		70 - 110					
	K-getal		19	19						
	K-bodemvoorraad	mmol+/kg	6,1		4,9 - 6,4					
	Ca plant beschikbaar	kg Ca/ha	239		215 - 502					
	Ca-bodemvoorraad	kg Ca/ha	13560		10300 - 15450					
	Mg plant beschikbaar	mg Mg/kg	123	234	49 - 82					
	Na plant beschikbaar	mg Na/kg	14	33	37 - 60					
fysisch										
	Zuurgraad (pH)		7,1							
	C-organisch	%	1,9							
	Organische stof	%	3,7	5,5						
	C-anorganisch	%	0,35							
	Koolzure kalk	%	2,3	0,3						
	Klei	%	33	34						
	Silt	%	50							
	Zand	%	11							
	Klei-humus (CEC)	mmol+/kg	259	272	> 207					
	CEC-bezetting	%	100	84	> 95					
biologisch										
	Bodemleven	mg N/kg	32		60 - 80					

* Dit zijn regiogemiddelden. Meer informatie staat bij onderdeel Gemiddelde.

HW 06

Advies in kg per ha per jaar		Frequentie	Gewas	Adviesgift				Afvoer
	N-correctie	per jaar		0				
			Deze gift kunt u als correctie op de basisgift toepassen. Zie voor meer info de toelichting.					
	Sulfaat (SO_3)	per jaar	Zetmeelaardappelen	0				60
			Consumptie-aardappelen	0				58
			Suikerbieten	0				100
			Graszaad	0				43
			Koolzaad	48				150
			Snijmais	19				73
	Fosfaat (P_2O_5)	per jaar	Zetmeelaardappelen	35				40
			Consumptie-aardappelen	35				55
			Suikerbieten	25				55
			Graszaad	0				30
			Koolzaad	0				50
			Snijmais	35				80
			Wilt u de fosfaattoestand handhaven dan adviseren wij u minimaal de afvoer te geven.					
	Kali (K_2O)	per jaar	Zetmeelaardappelen	90				-
			Consumptie-aardappelen	255				255
			Suikerbieten	150				150
			Graszaad	125				125
			Koolzaad	35				35
			Snijmais	300				300
	Calcium (CaO)	per jaar	Zetmeelaardappelen	125				
			Consumptie-aardappelen	125				
			Suikerbieten	90				
			Graszaad	70				
			Koolzaad	70				
			Snijmais	70				
				2014	**2015**	**2016**	**2017**	
	Magnesium (MgO)	per jaar	Zetmeelaardappelen	0	0	0	60	
			Consumptie-aardappelen	0	0	0	60	
			Suikerbieten	0	0	0	60	
			Graszaad	0	0	0	60	
			Koolzaad	0	0	0	60	
			Snijmais	0	0	0	60	
	Kalk (nw)	eenmalig		0				
			De kalkgift is gebaseerd op een optimale pH van 6,4					

BLGG AGROXPERTUS

Toelichting

De resultaten en/of het advies van dit bemestingsonderzoek kunt u t/m 2017 gebruiken. Laat het perceel daarna opnieuw bemonsteren. Dan krijgt u een betrouwbaar bemestingsadvies gebaseerd op de actuele bodemtoestand.

gebruiksnorm

De adviezen die vermeld worden, zijn gebaseerd op het halen van een landbouwkundig optimale opbrengst op perceelsniveau. Vanuit de wetgeving zijn er gebruiksnormen. Gebruiksnormen gelden op bedrijfsniveau. Als de som van de landbouwkundige adviesgiften hoger is dan de gebruiksnorm, verlaag dan de gift bij de minst behoeftige gewassen. Overleg dit met uw adviseur.
De adviesgift voor fosfaat en kali is als volgt opgebouwd:
- Is de gevonden toestand lager dan het streefniveau, dan geldt: adviesgift = reparatiegift + economische gift of afvoer indien deze hoger is.
- Is de gevonden toestand gelijk aan het streefniveau, dan geldt: adviesgift = economische gift of afvoer indien deze hoger is.
- Is de gevonden toestand hoger dan het streefniveau, dan geldt: adviesgift = economische gift.

De aangegeven afvoer is gebaseerd op de hieronder vermelde gemiddelde opbrengst die is geoogst. Is de werkelijke opbrengst bijvoorbeeld 10% hoger of lager, dan ligt de afvoer ook 10% hoger of lager. Indien achter een gewas geen afvoer staat vermeld, dan zijn gemiddelde afvoerwaarden niet voorhanden.

Gewas	Opbrengst (ton/ha)	Afvoer van oogstrest
Zetmeelaardappelen	45,0	Nee
Consumptie-aardappelen	50,0	Nee
Suikerbieten	75,0	Nee
Graszaad	1,3	Ja
Koolzaad	3,2	Nee
Snijmais	50,0	Nee

Stikstof:
Op basis van de N-levering is geen aanpassing nodig van de basisgift.
Neem voor een toegespitst stikstofadvies een N-mineraalmonster!

Zwavel:
Bij de adviesgift voor zwavel is rekening gehouden met capillaire opstijging, depositie, S-leverend vermogen (SLV) en onttrekking door het gewas.

Fosfaat:
Op pagina 1 van dit verslag staat de berekende Pw vermeld. Dit getal kunt u gebruiken bij het aanvragen van Flexibele Gebruiksnormen Fosfaat.
Het advies is gebaseerd op de direct beschikbare fosfaat (P-PAE) en op de voorraad fosfaat (P-Al).

Kali:
Let op: een hogere kaligift dan geadviseerd is niet zinvol voor een hoger zetmeelgehalte in zetmeelaardappelen. De afvoer van kali bij zetmeelaardappelen bedraagt 235 kg/ha.

Calcium:
Het calciumadvies is gebaseerd op de hoeveelheid calcium aan het klei-humuscomplex (CEC), voor de plant beschikbare calcium in de bodem (Ca-beschikbaar) en op gewaseigenschappen (o.a. type gewas en gevoeligheid voor Ca-gebrek).
Om de bodemtoestand te handhaven en/of omdat voor bepaalde gewassen de gevoeligheid voor Ca dusdanig is, kan er - ondanks een grote hoeveelheid Ca-beschikbaar - toch nog een Ca-advies gegeven zijn.
De adviesgift moet u nog corrigeren voor de hoeveelheid calcium in meststoffen zoals KAS, (tripel)superfosfaat en kalkmeststoffen.

Textuur:
Naast klei (lutum), worden ook de silt- en zandfracties weergegeven. Klei is kleiner dan 2 micrometer (µm), siltdeeltjes zijn 2-50 µm en zanddeeltjes groter dan 50 µm. De onderlinge verdeling van bodemdeeltjes wordt onder andere gebruikt om het verslempingsrisico van een bodem in te schatten. Bij verslemping wordt de bodem dichtgesmeerd met kleinere deeltjes (klei en silt). Een heel eenzijdige verdeling (bijvoorbeeld hoofdzakelijk zand- of kleideeltjes) levert het minste risico van slemp op. Bij een bepaalde verhouding aan bodemdeeltjes met 10-20% klei is het risico op slemp het grootst.
Indicatie van % afslibbaar = % klei plus 0,3 * % silt.

GIS-info

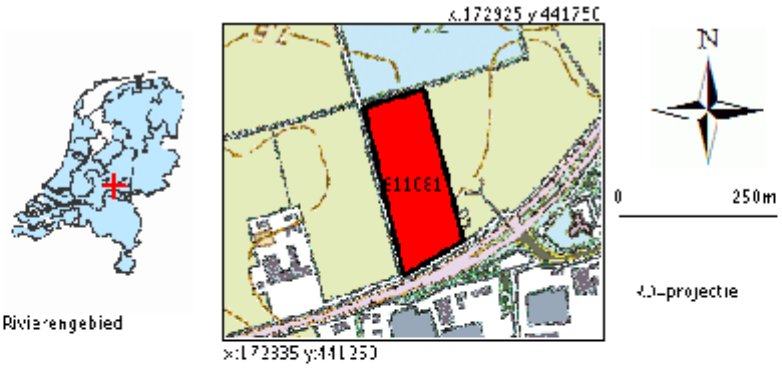

Hoekpunten perceel: 172613 441359, 172708 441412, 172646 441649, 172551 441622, 172613 441359

611081, 12-12-2013

HW 06

Org.stofbalans In de gekleurde balk staat de informatie over organische stof (kg/ha) die u moet weten om het organische stofgehalte niet te laten dalen.

Jaarlijks afbraakpercentage van de totale voorraad organische stof: 3,0

- Voorraad organische stof die over 1 jaar in de bemonsterde laag nog aanwezig zal zijn als er geen (effectieve) organische stof wordt aangevoerd.
- Totaal benodigde aanvoer van effectieve organische stof om percentage organische stof op peil te houden.
- Aanvoer via gewasresten (gemiddeld binnen opgegeven bouwplan of gewassen).
- Nog aan te vullen via bijv. dierlijke mest, groenbemesters en/of compost.

Gewas(rest)	Aanvoer effectieve organische stof
Zetmeelaardappelen	875
Consumptie-aardappelen	875
Suikerbieten	1275
Graszaad	2300
Koolzaad	975
Snijmais	660
Gemiddelde aanvoer/jaar	1160

Om het organische stofgehalte met 0,1% te verhogen dient u een hoeveelheid effectieve organische stof aan te voeren van: 2985 kg per ha.

Fysisch

De beoordeling van de structuur wordt gedaan op basis van de gemeten verhouding tussen calcium, magnesium en kali als bezetting aan het klei-humuscomplex. Uiteraard is de werkelijke structuur ook afhankelijk van weersomstandigheden en vochttoestand van de bodem tijdens berijden en bewerken en de zwaarte van transportmiddelen en machines. De beoordeling is een basis voor de realisatie van een goede structuurvoorwaarde.

Weergave onderlinge verhouding van de CEC-bezetting.

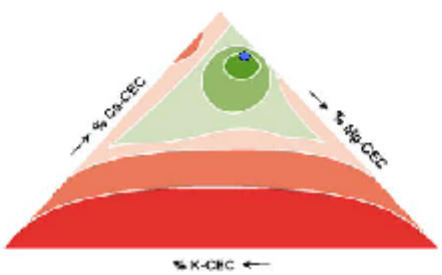

- optimale structuur
- goede structuur
- matige structuur
- zeer matige structuur
- slechte structuur
- zeer slechte structuur
- huidige situatie van dit perceel

	Eenheid	Resultaat	Streeftraject	laag	vrij laag	goed	vrij hoog	hoog
Klei-humus (CEC)	mmol+/kg	259	> 207					
Ca-bezetting	%	88	65 - 85					
Mg-bezetting	%	9,8	6,0 - 12					
K-bezetting	%	2,4	2,0 - 5,0					
Na-bezetting	%	0,3						
H-bezetting	%	< 0,1						
Al-bezetting	%	< 0,1						

In kg per ha per jaar

	Frequentie	Adviesgift
Calcium (CaO)	eenmalig	0

Een calciumgift op basis van de verhoudingen aan het complex is niet nodig. Het is mogelijk dat u wel een calciumadvies voor uw gewas geadviseerd krijgt. Dit kunt u gewoon opvolgen zonder dat dit nadelige gevolgen heeft voor de structuur.

	Eenheid	Waardering	Streeftraject	laag	vrij laag	goed	zeer goed
Verkruimelbaarheid	rapportcijfer	5,1	6,0 - 8,0				
Verslemping	rapportcijfer	6,6	6,0 - 8,0				

De verkruimelbaarheid - onderlinge binding tussen de bodemdeeltjes - is niet optimaal. De maatregelen om de verkruimelbaarheid te verbeteren zijn divers.

Gezien het resultaat is de kans op verslemping klein.

611081, 12-12-2013

HW 06

Fosfaat

Op de voorkant van het verslag staan de resultaten voor fosfaat op de gebruikelijke manier gepresenteerd: een getal en een waarderingsbalkje. De cijfers zijn ook verwerkt in een 'bodemprofiel' (zie figuur). Hierin geven we de fosfaatvoorraad en de beschikbare hoeveelheid P met kleuren aan. De pijl symboliseert de nalevering vanuit de voorraad. De dikte van de pijl toont hoeveel nalevering van fosfaat per groeiseizoen mogelijk is.

Gemiddelde

Op de voorzijde van dit verslag zijn regiogemiddelden weergegeven. Hiermee kunt u uw resultaten vergelijken met overeenkomstige percelen uit uw regio. Indien we onvoldoende gegevens hebben - als gevolg van te weinig geanalyseerde grondmonsters - zijn landelijke gemiddelden berekend.

Het gemiddelde is berekend voor de situatie:

Regio:	Rivierengebied
Grondsoort:	Rivierklei
Teeltgroep:	Akker-/tuinbouw

De meest opvallende afwijkende resultaten (max. 5) ten opzichte van het gemiddelde én streeftraject zijn weergegeven in onderstaande tabel:

	Resultaat	Gem.	Streeftraject
C/N-ratio	8	10	13 - 17
P-bodemvoorraad (P-Al)	68	40	24 - 37
Mg plant beschikbaar	123	234	49 - 82
Na plant beschikbaar	14	33	37 - 60
Koolzure kalk	2,3	0,3	

Contact & info

Bemonsterde laag:	0 - 25 cm
Grondsoort:	Rivierklei
Monster genomen door:	BLGG AgroXpertus, Herman Dorresteijn
Contactpersoon monstername:	Herman Dorresteijn: 0652002114
Bemonsteringsmethode:	W-patroon, min. 40 steken; volgens BLGG AgroXpertus standaard MIN 1000 Q
Specificatie oppervlakte:	Normaal

Na verzending van dit verslag wordt, indien de aard en de onderzoeksmethode van het monster dit toelaat, het monster nog twee weken bij BLGG AgroXpertus voor u bewaard. Binnen deze tijd kunt u eventueel reclameren en/of aanvullend onderzoek aanvragen.

Methode

N-totale bodemvoorraad	Q	Em: NIRS (TSO®)	C-organisch	Q	Em: NIRS (TSO®)
C/N-ratio		afgeleide waarde	Organische stof		afgeleide waarde
N-leverend vermogen		afgeleide waarde	C-anorganisch		Em: NIRS (TSO®)
S-totale bodemvoorraad	Q	Em: NIRS (TSO®)	Kooizure kalk		afgeleide waarde
C/S-ratio		afgeleide waarde	Klei		Em: NIRS (TSO®)
S-leverend vermogen		afgeleide waarde	Slit		Em: NIRS (TSO®)
P plant beschikbaar	Q	Em: CCL3(PAE®)	Zand		Em: NIRS (TSO®)
P-bodemvoorraad (P-Al)	Q	PAL1: Gw NEN 5793	Klei-humus (CEC)		Em: NIRS (TSO®)
Pw		afgeleide waarde	Ca-bezetting		Em: NIRS (TSO®)
K-getal		afgeleide waarde	Mg-bezetting		Em: NIRS (TSO®)
K plant beschikbaar	Q	Em: CCL3(PAE®)	K-bezetting		Em: NIRS (TSO®)
K-bodemvoorraad		Em: NIRS (TSO®)	Na-bezetting		Em: NIRS (TSO®)
Ca plant beschikbaar		Em: NIRS (TSO®)	H-bezetting		afgeleide waarde
Ca-bodemvoorraad		afgeleide waarde	Al-bezetting		afgeleide waarde
Mg plant beschikbaar	Q	Em: CCL3(PAE®)	CEC-bezetting		afgeleide waarde
Na plant beschikbaar	Q	Em: CCL3(PAE®)	Bodemleven		Em: NIRS (TSO®)
Zuurgraad (pH)		Em: NIRS (TSO®)			

Q Methode geaccrediteerd door RvA
Em: Eigen methode, Gw: Gelijkwaardig aan, Cf: Conform

P plant beschikbaar	Deze analyse is in duplo uitgevoerd.
P-bodemvoorraad (P-Al)	Deze analyse is in duplo uitgevoerd.

De resultaten zijn weergegeven in droge grond.
Alle verrichtingen zijn binnen de gestelde houdbaarheidstermijn tussen monstername en analyse uitgevoerd.

Pagina: 6
Totaal aantal pagina's: 6

611081, 12-12-2013

Appendix IV – Moments of light interception measurements

Table IV.1. Moments during the day at which the light interception measurements are done.

Crop sampling	AccuPAR measurements			
	From		Till	
31-Mar	2-Apr	9:25	2- Apr	12:05
22-Apr	24-Apr	13:45	24-Apr	15:15
7-May	6-May	13:50	6-May	15:55
26-May	25-May	15:15	25-May	18:15
12-Jun*	11-Jun	10:50	11-Jun	12:00
	13-Jun	15:40	13-Jun	16:00

* AccuPAR measurements are done at two days due to circumstances. Light interception of field 1 – 7 and 10 – 17 are measured at June 11, light interception of field 8 & 9 and 18 – 36 are measured at June 13.

Appendix V – Crop sampling procedure for different sampling dates

Table V.1. Relative sizes of the subsamples for each sampling date and the time required to process all the samples.

Sampling date	*Plant parts distinguished*[*]	*Average size of split subsample*	*Size of dried sample*	*Part of fresh weight sample not used*	*Time required for processing fresh product*[**]
		%	%	%	hours
18 Feb	GL, DL, ST	16	84	0	72
10 Mar	GL, DL, ST	28	72	0	72
31 Mar	GL, DL, ST	14	86	0	48
22 Apr	GL, DL, ST	10	90	0	48
7 May	GL, DL, ST	12	88	0	40
26 May	GL, DL, ST, EA	8	20	72	36
12 Jun	GL, DL, ST, EA	11	24	65	36
30 Jun	GL, DL, ST, EA, GR	9	30	61	36
16 Jul	GL, DL, ST, EA, GR	13	32	55	36
28 Jul	GL, DL, ST, EA, GR	14	32	54	30

[*] GL: green leaves; DL: dead leaves; ST: stems; EA: ears (including grains); GR: grains.

[**] The time required is the total number of hours of all helping persons together.

During the first sampling (February 18, 2014) it appeared that it was necessary to make subsamples from the plant material that was collected from 0.5 m^2 because of the time needed to process the samples. This was done during the processing, so part of the samples have completely been separated (plots 5, 7, 12, 16) and of others have been made first a subsample and then this was split in green leaves, dead leaves and stems.

The harvest of the first sampling took more time than expected because the clayey soil made it difficult to harvest fast. Big clods were on top of the small plants what made the distinction between above-ground and below-ground plant parts difficult. In addition the measurement of the leaf area took a lot of time (about 30 minutes per sample) since the leaves were still very small. The leaves rolled up in the length direction of the leaves. So the leaves were rolled up like needles. It took a lot of effort to unroll these leaves again and to do a good measurement of the leaf area. Therefore, only samples from 12 plots were analysed instead of all the 36 plots.

During the second harvest (March 10) subsamples were made of about 25% of the total fresh weight. This sample size was based on a guess of the time needed for processing these samples. The processing had to be done as fast as possible since the leaves started to roll up in the length direction of the leaf after some time. This process can be delayed by storing the samples in the fridge but especially when the green leaves are separated from the rest of the plant, the quality of the leaves drops rapidly.

Because the absolute size of the samples from 0.5 m^2 increased, the relative size of the subsample decreased in order to maintain a feasible amount of work during the crop samplings. Each crop sampling was aimed to have a subsample with a size of at least 10% of the original sample. This was done by weighing all the samples before the subsamples were made. Then the size of the subsample could be estimated. However, this was not possible at all sampling dates. A few times the subsamples were already made before all the total weights of the samples were known. Therefore, it was possible that the size of the subsamples was estimated too small, resulting in a relatively low average subsample size.

Appendix VI – Calculations of relative death rate

The calculations for the relative death rate are performed in Excel. The parameters $T_{sum\text{-}senescence}$, $r_{d\text{-}shading}$ and LAI_{cr} are set as constants in three cells. The relative death rate is calculated for each day from February 18 till July 28 in 161 rows (one row for each day). The observed T_{air} (°C), LAI ($m^2\ m^{-2}$), W_{lvd} (g m^{-2}) and W_{lvg} (g m^{-2}) are used as input. The LAI, W_{lvd} and W_{lvg} are linearly interpolated between the observation dates in order to have a value for all the days from February 18 till July 28. The equation used for linearly interpolation was:

$$y_t = y_{t-1} + \frac{y_{obs2} - y_{obs1}}{t_{obs2} - t_{obs1}} \quad \text{(VI.1)}$$

where y_t is LAI or W_{lvd} or W_{lvg} at day t; y_{t-1} indicates the LAI or W_{lvd} or W_{lvg} at the previous day; the subscript *obs1* indicates the most recent the observation before the currently simulated day and *obs2* indicates the observation ahead of the currently simulated day. For example, if February 25 is the currently simulated day, then *obs1* is February 18 and *obs2* is March 10 and; t_{obs2}–t_{obs1} indicates the number of days between two observations. In addition, also the daily calculated developmental stage and daily calculated $T_{sum\text{-}anthesis}$ + $T_{sum\text{-}maturity}$ are used as input (see Section 3.5).

For each timestep the amount of LAI that senesces is calculated as in Equation 22. r_d is calculated as the maximum of r_{d1} and r_{d2}.

r_{d1} has been made a function of developmental stage instead of daily average air temperature. The function consisted of three parts: (i) DVS < $DVS_{start\text{-}senescence}$, as long as the developmental stage of the crop has not reached a certain value $DVS_{start\text{-}senescence}$, then no senescence can occur because of ageing of the crop. r_{d1} is at this stage zero; (ii) $DVS_{start\text{-}senescence}$ < DVS < $DVS_{rapid\text{-}senescence}$, Until a certain developmental stage ($DVS_{rapid\text{-}senescence}$) senescence of green leaves occurs relatively slow. The value for r_{d1} at $DVS_{rapid\text{-}senescence}$ is parameterized using the Excel file. (iii) DVS > $DVS_{rapid\text{-}senescence}$, from a certain developmental stage onwards, the senescence of the crop happens fast until r_{d1} is 1 at DVS is 2.

r_{d2} is parameterized together with the LAI_{cr}. These parameters appeared to be very dependent on each other.

From the calculated r_d, $LAI_{senescence}$ was calculated for each timestep. This was integrated for each timestep and plotted together with the observed W_{lvd}, with the developmental stage on the X-axis and the dry weight per square meter on the Y-axis. The goodness of fit of the simulated W_{lvd} with the observed W_{lvd} was done visually.

Appendix VII – Parameters and functions for LINTUL1 for winter wheat

The following table gives an overview of all the parameters that are needed for LINTUL1 for the crop winter wheat. Two abbreviations are given, one that is used in the report and one that is used in the model. Furthermore a description of the parameter and the method that is used to determine the value of the parameter in this research is given.

Table VII.1. An overview of the necessary parameters for LINTUL1 for winter wheat.

Abbreviation		Unit	Original value	New value
Report	LINTUL		(Het Lam, 2014)	
$T_{b\text{-}emergence}$	TBASEM	°C	0.25	0.25
$T_{sum\text{-}emergence}$	TSUMEM	°Cd	122	127
M_{soil}	MSOIL	d^{-1}	0.25	0.25
$T_{sum\text{-}anthesis}$	TSUMAN	°Cd	926	680
$T_{b\text{-}anthesis}$	TBASE	°C	1.5	1.5
$DVS_{vernalization}$	DVSVER	-	0.3	0.3
V_b	VBASE	-	$0.2 \times V_{sat}$	$0.2 \times V_{sat}$
V_{sat}	VERSAT	-	58	58
P_b*		h	9	9
P_{opt}*		h	16	16
$T_{sum\text{-}maturity}$	TSUMMT	°Cd	590	1030
$T_{b\text{-}maturity}$	TBASE	°C	1.5	1.5
k	K	-	0.6	0.6
c_{PAR}	CONPAR	MJ PAR / (MJ DTR)	0.5	0.46
RUE**	LUE	g above-ground DM MJ^{-1} PAR	3.15	3.20
SLA_c	SLAC	$m^2\ g^{-1}$	0.021	0.021
SLA_{ini}	ISLA	$m^2\ g^{-1}$	-	-
$WLVI_{ini}$	WLVGI	$g\ m^{-2}$	0.10	0.55
	WSTI	$g\ m^{-2}$	0.05	0.05
	WEAI	$g\ m^{-2}$		0
	WSOI	$g\ m^{-2}$	0.0	0
	LAII	$m^2\ m^{-2}$	-	0.026
$DVS_{exp\text{-}lea\ growth}$	DVSEXP	-	0.2	0.2
$LAI_{exp\text{-}growth}$	LAIEXP	$m^2\ m^{-2}$	0.6	2.0
r_l	RGRL	$(°Cd)^{-1}$	0.015	0.0061
$T_{sum\text{-}ageing}$	TSUMAG	°Cd	900	-
LAI_{cr}	LAICR	$m^2\ m^{-2}$	4	4
$r_{d\text{-}shading}$	RDRSHM	d^{-1}	0.03	0.0009
$r_{d\text{-}ageing}$	RDRDV	d^{-1}	-	-

* These values are not explicitly mentioned in the program code in FST but are included in a function between developmental stage and photoperiod.

** The RUE used by Het Lam (2014) is used for as well above-ground as below-ground dry matter, while the new value for RUE is calculated based only at above-ground dry matter.

The functions that are included in the model and that are not described in the text of the report are shown here.

Correction factor for RUE as function of T_{RUE}

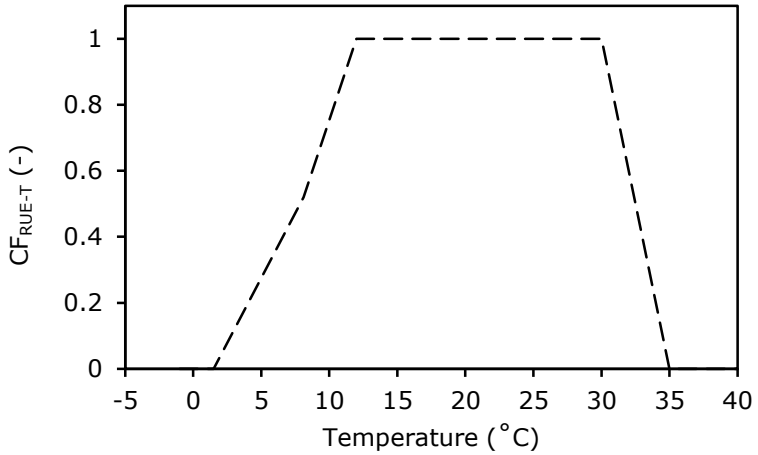

Figure VII.1. The correction factor for the RUE as function of T_{RUE}.

Appendix VIII – Progress of measured dry matter and LAI over the growing season

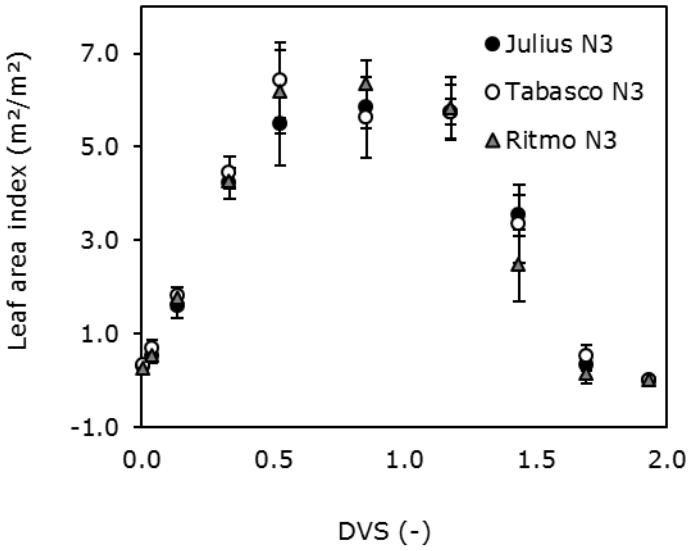

Figure VIII.1. The leaf area index in relation to the developmental stage (DVS) of the crop. The three varieties used in the trial are shown for the highest nitrogen application (300 kg ha^{-1}).

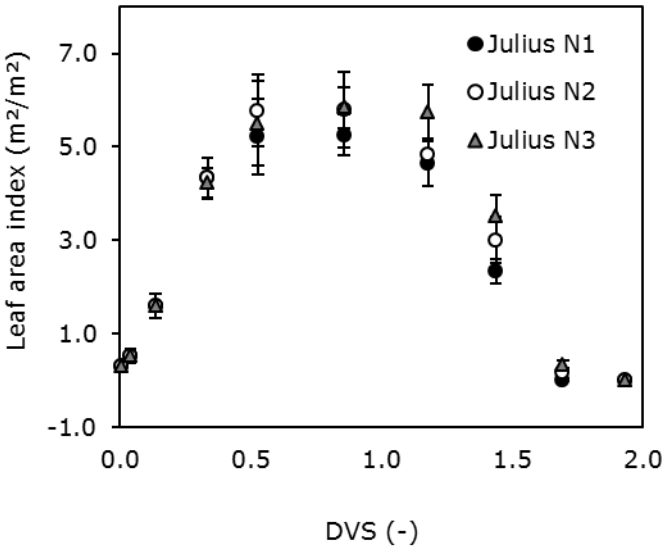

Figure VIII.2. The leaf area index in relation to the developmental stage (DVS) of the crop. Julius is selected as variety and the three nitrogen applications are shown.

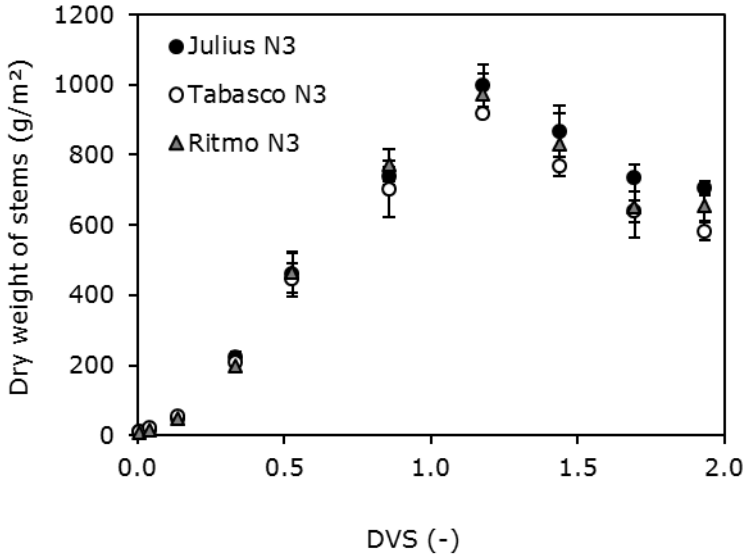

Figure VIII.3. Development of the dry weight of the stems in relation with the developmental stage (DVS) of the crop. No significant differences are found between the three varieties. However, Julius tend to have a higher stem weight. This is in accordance with the observation of taller straw of this variety.

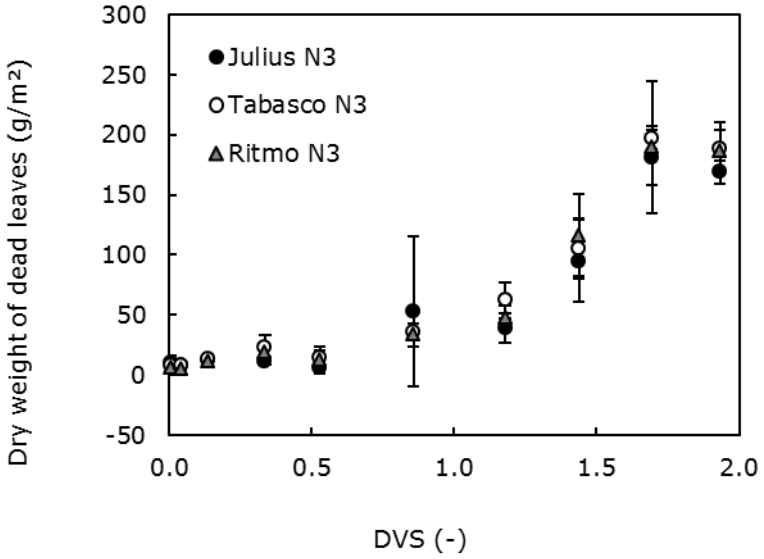

Figure VIII.4. The dry weight of dead leaves in relation to the developmental stage (DVS) of the crop. The three varieties used in the trial are shown for the highest nitrogen application (300 kg ha^{-1}).

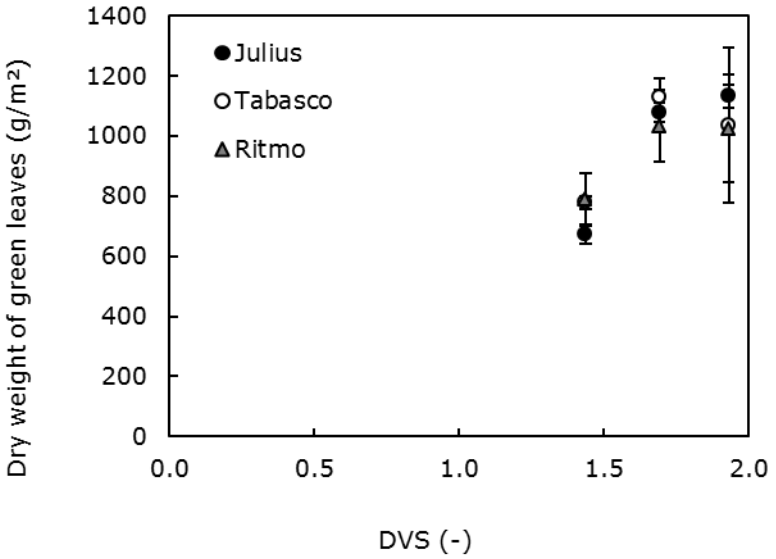

Figure VIII.5. Development of the dry weight of the grains in relation with the developmental stage (DVS) of the crop.

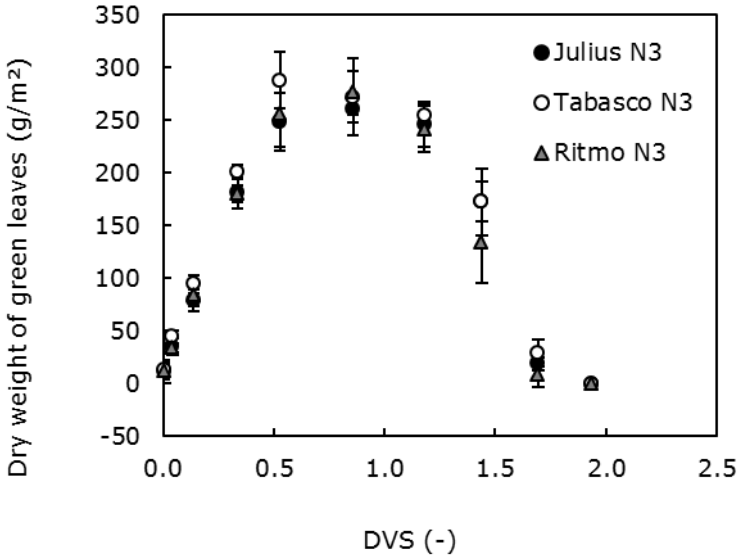

Figure VIII.6. The dry weight of green leaves in relation to the developmental stage (DVS) of the crop. The three varieties used in the trial are shown for the highest nitrogen application (300 kg ha^{-1}).

Appendix IX – Calculation of allocation fractions

The red values in Table VIII.1 show the values when the weight decreased compared to the previous crop sampling. This decrease is assumed to be caused by reallocation. In Table VIII.2, the highest observed values for DWEA, DWST and DWL are retained. The observed decrease in dry weight for DWL, DWEA and DWST is subtracted from DWGR in Table VIII.2. So, the dry weight of the grains in Table VIII.2 results only from allocation, and not from reallocation.

The final harvest was at July 31, but then no crop sampling is done, so the dry weights of various plant organs for this date is unknown.

Table IX.1. Observed dry weights of grains (DWGR), ears (DWEA), stems (DWST) and leaves (as well dead as green leaves, DWL) from Julius with highest N application. The total dry weight (DWT) and the difference between two subsequent crop samplings (ΔGrowth). DAE: days after emergence, DVS: developmental stage.

Date	**DAE**	**DVS**	**DWT**	**DWGR**	**DWEA**	**DWST**	**DWL**	**ΔGrowth**
	d	-	g/m2	g/m2	g/m2	g/m2	g/m2	g/m2
2/18/2014	106	0.01	31.0			9.2	21.8	
								28.2
3/10/2014	126	0.04	59.1			15.2	43.9	
								78.0
3/31/2014	147	0.14	137.1			45.6	91.6	
								277.4
4/22/2014	169	0.34	414.5			221.7	192.7	
								301.0
5/7/2014	184	0.53	715.5			460.4	255.1	
								504.6
5/26/2014	203	0.86	1220.1		167.6	739.4	313.1	
								434.2
6/12/2014	220	1.18	1654.2	120.0	251.0	997.8	285.5	
								384.0
6/30/2014	238	1.44	2038.2	672.0	231.5	866.8	267.9	
								188.9
7/16/2014	254	1.69	2227.2	1077.0	216.5	733.4	200.2	
								0.0
7/28/2014	266	1.93	2211.5	1133.5	203.7	705.4	169.0	
7/31/2014	269	2.00	-	-	-	-	-	

Table IX.2. The dry weight of different plant organs from Julius with highest N application, corrected for reallocation.

Date	**DAE**	**DVS**	**DWT**	**DWGR**	**DWEA**	**DWST**	**DWL**	**dGrowth**
	d	-	g/m2	g/m2	g/m2	g/m2	g/m2	g/m2
2/18/2014	106	0.01	31.0			9.2	21.8	
								28.2
3/10/2014	126	0.04	59.1			15.2	43.9	
								78.0
3/31/2014	147	0.14	137.1			45.6	91.6	
								277.4
4/22/2014	169	0.34	414.5			221.7	192.7	
								301.0
5/7/2014	184	0.53	715.5			460.4	255.1	
								504.6
5/26/2014	203	0.86	1220.1		167.6	739.4	313.1	
								434.2
6/12/2014	220	1.18	1654.2	92.4	251.0	997.8	313.1	
								384.0
6/30/2014	238	1.44	2038.2	476.4	251.0	997.8	313.1	
								188.9
7/16/2014	254	1.69	2227.2	665.3	251.0	997.8	313.1	
								0.0
7/28/2014	266	1.93	2211.5					
7/31/2014	269	2.00	-	-	-	-	-	